

ANNALS OF THE NEW YORK ACADEMY OF SCIENCES

VOLUME 89, ART. 4      PAGES 573-714

THERMODYNAMICS AND MECHANICS OF POLYMER SYSTEMS

*Conference Editor:* F. R. EIRICH

LIST OF AUTHORS

F. R. EIRICH (*Conference Chairman*), B. D. COLEMAN, E. W. FISCHER, M. FIXMAN,  
M. KURATA, J. MAZUR, W. NOLL, A. PETERLIN, F. T. WALL, AND B. H. ZIMM

*Editor*

FRANKLIN N. FURNESS

*Managing Editor*

EDGAR W. WHITE

*Associate Editor*

ANNA SYARSE



NEW YORK

PUBLISHED BY THE ACADEMY

January 16, 1961



ANNALS OF THE NEW YORK ACADEMY OF SCIENCES

VOLUME 89, ART. 4      PAGES 573-714

January 16, 1961

THERMODYNAMICS AND MECHANICS OF  
POLYMER SYSTEMS\*

*Conference Chairman and Conference Editor*

F. R. EIRICH

---

*Editor*

FRANKLIN N. FURNESS

*Managing Editor*

EDGAR W. WHITE

*Associate Editor*

ANNA SYARSE

---

CONTENTS

Introductory Remarks. <i>By</i> F. R. EIRICH.....	575
Short- and Long-range Interaction in the Isolated Macromolecule. <i>By</i> ANTON PETERLIN.....	578
Statistical Thermodynamics of Coiling-type Polymers. <i>By</i> FREDERICK T. WALL AND JACOB MAZUR.....	608
Thermodynamical Explanation of Large Periods in High Polymer Crystals and Drawn Fibers. <i>By</i> E. W. FISCHER.....	620
Lattice Theory of Chain Polymer Solutions. <i>By</i> MICHIO KURATA.....	635
Concentration Dependence of Polymer Dimensions. <i>By</i> MARSHALL FIXMAN....	657
Theory of the Non-Newtonian Viscosity of High Polymer Solutions <i>By</i> BRUNO H. ZIMM.....	670
Recent Results in the Continuum Theory of Viscoelastic Fluids. <i>By</i> BERNARD D. COLEMAN AND WALTER NOLL.....	672

\* This series of papers is the result of a conference on *Thermodynamics and Mechanics of Polymer Systems* held by The New York Academy of Sciences on May 27, 1960.

*Copyright, 1961, by The New York Academy of Sciences*



## INTRODUCTORY REMARKS

F. R. Eirich

*Institute of Polymer Research, Polytechnic Institute of Brooklyn, Brooklyn, N. Y.*

The performance of high polymers in all forms of usage and their behavior during measurements is intimately linked to their structure. Solutions of long-chain molecules, in particular, show very unusual solubility patterns and a readiness to exhibit non-Newtonian viscosity. The papers presented in this monograph deal with some new developments in our views of these phenomena.

The first advances in an understanding of polymer solutions were made by P. Flory and M. Huggins, in conjunction with the model of the random flight chain molecule treated by W. Kuhn and H. Eyring, by considering the configurations of chain molecules in solution and calculating the corresponding entropy of mixing. Notwithstanding the great progress represented by this approach, the limits of some of the basic assumptions and of the agreement with the experiments remained as a stimulus for further work. Various refinements were required, especially with respect to the lattice model, to the specific rotational characteristics of the chains as influencing coil dimensions, and to the energetic interactions of the polymer molecules with the solvent and one another.

Much progress has been made subsequently by Flory and his school by the ingenious analysis of long- and short-range polymer interaction in terms of the expansion factor  $\alpha$  and of the ideal random flight dimensions in theta ( $\theta$ ) solvents. A survey of the most recent advances is given in the paper by Peterlin with special reference to chain structure and to the effect and the nature of the coil expansion. The paper by Wall and Mazur, then, makes an important contribution to the problem of coil dimensions by computer analysis of the configurations as a function of lattice type and of bond angle of chains with three levels of energy interaction. The influence of the presence of other polymer molecules, that is, the concentration effect on coil dimensions, is then discussed by Fixman on the basis of a Gaussian model for the distribution of chain segments. The paper by Kurata makes an important contribution to the application of the lattice theory to polymer solutions. While recognizing the general validity of Flory's derivation of the entropy of mixing, the theory is extended to take account of the inevitable close connection of coil segments, due to their chemical linkages, and the concomitant solvent clustering. Extensive use is made of experimental data from the  $\theta$  state to derive functional forms and values for the interaction constants.

It might be added parenthetically that the formulation of the  $\theta$  state is not without conceptual difficulties because of the fact that the "ideality" of  $\theta$  solutions (as at the Boyle point) is operational and not real. It is

true that the validity of van't Hoff's limiting law shows the existence of ideal additivity, or of proportionality, between chemical potential and log mole fraction, and therefore indicates an ideal entropy. However, as in other regular solutions, the  $\Delta H$  term is not zero but positive, so that random mixing at temperatures close to precipitation in any but the most dilute solutions is most unlikely. In other words, with lowering temperatures the distribution of the solute must pass a state of clustering on the way from complete randomness to the critical point. Although the temperature range of such clustering is probably narrow, as Debye<sup>1</sup> has recently found, with increasing molecular weight this range must move upward toward the  $\theta$  temperature and eventually extend above it. In the latter cases, the absence of bias in the segment-solvent or solute distribution at the  $\theta$  point can be only an apparent one. More likely, the "ideality" will be produced by some state of order that also leads to a cancellation of the factors contributing to the virial coefficients; to the extent that this happens deductions from  $\theta$ -point data may have to be revised. Reported discrepancies in the entropy and interaction parameters from different methods or between calculated and experimental values, or abnormally large values of the ratio  $\bar{M}_w : \bar{M}_n$  may be due to this inadequacy of our picture of the polymer distribution.

A most unexpected behavior of polymer chains that has recently come to light and that may well be related to the state of coiling at the critical point is the crystallization in thin platelets by way of uniformly folded chains. There are many puzzling features to this phenomenon, not the least being its widespread occurrence and the apparent disregard for acquiring a large surface energy. Fischer's paper presents a thermodynamic theory that has found wide support in Europe. A different, kinetic, hypothesis discussed by F. P. Price is to be published elsewhere.<sup>2,3</sup>

The dimensions, density, and rigidity of the polymer coils express themselves in their contributions to the solution viscosity. The second part of Peterlin's paper reviews the recent status of our knowledge in this area. In particular he shows that we have now a much better understanding of the gradient dependence of the viscosity of dilute solutions based on intramolecular hydrodynamic interaction and coil deformation, but a generally satisfactory theory has not been proposed. Zimm, in a brief report, outlines a new approach that seems promising.

Generally, the papers in this monograph are concerned with the discontinuous nature of polymer solutions and the interaction of chains with the surrounding medium. With increasing concentration the separation of the particles disappears more and more, until at high concentrations or in the melt a practically continuous medium occurs. At this stage it becomes fruitful to inquire into the general properties of media that exhibit the characteristics of polymer systems, especially their viscoelasticity.



The mathematical-mechanical analysis of such fluids has made great progress under the impetus of work by A. E. Green, R. S. Rivlin, J. E. Erickson, and others, a development that has not received as wide an attention as it deserves. The concluding paper by Coleman and Noll affords an excellent acquaintance with the basic approach and results in this field.

### *References*

1. DEBYE, P., H. COLL & D. WOERMANN. 1960. J. Chem. Phys. **32**: 939.
2. PRICE, F. P. 1960. J. Polymer Sci. **42**: 49.
3. LAVRITZEN, J. I. & J. D. HOFFMAN. 1960. J. Research Nat. Bur. Standards. **A64**: 73.

# SHORT- AND LONG-RANGE INTERACTION IN THE ISOLATED MACROMOLECULE\*

Anton Peterlin†

*Department of Chemistry, Wayne State University, Detroit, Mich.‡*

## *Preface*

Extensive hydrodynamic and optical studies on dilute solutions have revealed a great many data on size and other physical properties of isolated linear macromolecule. The dependence on molecular weight, temperature, solvent, and rate of shear has shown the inadequacy of the original concept of the Gaussian coil, which did not take into proper account either the fine structure of the chain or the steric, energetic, hydrodynamic, and optical interactions between distant sections of the chain. In the last 10 years, therefore, more refined models were introduced in order to obtain agreement with experiments. Their success makes worthwhile a short survey with emphasis on the remaining gaps that it will be necessary to cover in the future.

The actual shape of statistically coiled linear macromolecule depends on valency angle between subsequent monomers, steric and energetic hindrance of rotation around the chemical bond (short-range interactions), on the volume requirement of the monomers, and on energetic interaction between any two monomers and between the monomer and the surrounding medium (long-range interactions). The short-range interactions determine not only the length of the statistically independent segment, its optical and hydrodynamic properties, but also the resistance of the chain against the rate of shape change of the coil. The long-range interactions, however, do not appreciably change the character of the segment but influence the overall coil dimensions by excluding sterically or energetically unfavored configurations. As a consequence, the root-mean-square (r.m.s) gyration radius does not increase as the square root of molecular weight. Proportionality with  $M^{1/2}$  is found only exceptionally, that is, in "ideal" solvent. The size and shape of the coil in turn influence the hydrodynamic and optical interaction.

The non-Gaussian character of actual coil, the anisotropy of hydrodynamic and optical interaction, and the resistance of the coil against rapid shape changes influence the gradient dependence of limiting viscosity and streaming birefringence. In spite of the fact that the basic character of

\* The investigation reported in this paper was supported in part by a research grant from SKNE, Beograd, Yugoslavia.

† On leave of absence from the Department of Physics, University Ljubljana, Ljubljana, Yugoslavia.

‡ Present address: Physikalisches Institut, Technische Hochschule, München, Germany.



the single contributions is already known, no one has yet succeeded in considering them all together in the full gradient range.

### Introduction

In dilute solution a linear unbranched macromolecule containing  $P$  monomers in the chain assumes a coillike shape and steadily changes its configuration so that in any experiment mean values over all possible configurations are observed. From investigation of monomers one knows, at least in principle, their volume  $v_0$ , link length  $b_0$ , valency angle  $180^\circ - \alpha$ , electric charge  $e_0$ , dipole moment  $\mu_0$ , optical polarizability tensor  $\alpha_0$ , hydrodynamic resistance coefficient  $\Lambda_0$  and so on. By taking into account all kinds of possible mutual interactions of monomers and averaging over all permitted configurations under the eventual influence of an external field one expects to be able to explain the effects observable with dilute polymer solutions and their dependence on molecular weight, temperature, solvent, and solvent composition (ionic strength,  $pH$ , mixture of solvents). The interactions may be due to the geometry of monomers, their space requirement, to attractive and repulsive forces between two monomers and between a monomer and a molecule of the solvent, and to hydrodynamic forces and electric fields originating from free charges and electric dipoles.

The effects concerned are primarily X-ray and light scattering, dielectric polarization, sedimentation in gravitational and inhomogeneous electric field, viscosity, electrical and streaming birefringence. What matters is always the excess effect of solution over that of solvent divided by concentration and extrapolated to infinite dilution. These *specific* or *intrinsic* effects all depend on the properties of the monomer in given solvent and on their mutual geometric arrangement in the chain and at the special conditions of experiment, that is, on shape and size of the macromolecular coil, which, for example, determine the extent of optical and hydrodynamic interaction and the resulting modification of observable intrinsic effects. This fact stresses the importance of coil geometry, which therefore must be considered first. In order not to complicate the situation too much let us start with solution at rest without any external field.<sup>1,2</sup>

A very rough but useful model for such a randomly coiled macromolecule is a chain with  $Z$  statistically independent segments of equal length  $A$  joined in such a way that the orientation of any segment is, at least in first approximation, independent on that of its neighbors. Within a polymer series and under unchanged experimental conditions  $Z$  is proportional to  $P$ , the proportionality factor  $\zeta$  being the number of monomers in a segment. Some properties, such as the volume and the charge of the segment, are strictly equal to  $\zeta$  times the corresponding values of monomer. In general, however, they are influenced by the special geometry of monomer arrangement in the segment and on their interaction so that they are smaller than  $\zeta$  times the values of monomer.

*Field Free Solution at Rest*

Chain configurations and their probability of occurrence are determined by forces among all chain atoms and those of solvent. In this generality, the problem is unduly complicated and must be simplified properly by applying generally accepted geometric and energetic formulations of above mentioned forces. Thus, for example, forces between first neighbors result in special valency angles and interatom distances and in a more or less fixed monomer structure that is usually known from crystallographic and X-ray investigation. The monomer unit may be rigid (cellulose) or flexible due to single bonds with more or less free rotation around it (for example, vinyl polymers, polyesters, and polyamides). The same forces also determine the possible geometric arrangement of subsequent monomer units and hence the geometrical properties of statistical segment.

With monomer units symmetric in chain direction, as for example in polyethylene  $-(CH_2 \cdot CH_2)-$ , and with those that, although asymmetric, require special orientation for regular valency bond between subsequent monomers, as for example in polysiloxanes  $-(SiR_1R_2 \cdot O)-$  and cellulose  $-(C_6H_{10}O_5)-$ , the atom or atom group sequence in unbranched polymer chain is absolutely determined and regular. With most vinyl polymers such as  $-(CH_2 \cdot CHR)-$ , however, the longitudinal assymetry gives rise to four possible arrangements (head-head, head-tail, tail-head, tail-tail), which in polymer chain may occur either in high order (*positionally isotactic* -ht-ht-ht- or *syndiotactic* -hh-tt-hh-tt- polymer) or distributed at random (*positionally atactic* polymer -ht-hh-th-tt-hh-), depending on polymerization conditions. Moreover with monomers exhibiting two-mirrored *d*- and *l*-isomers (most vinyl polymers are built from such monomer units  $-CH_2 \cdot CHR-$ ), the resulting polymer may contain both, either in well-ordered arrangement or distributed at random, or only one. In the case of positional order (positional tacticity) this monomer isomerism leads to *sterically isotactic* (all monomers are either *d*- or *l*-isomers), *syndiotactic* (*d-l-d-l* sequence) or *atactic* (random distribution of both isomers) polymers. A similar situation arises with monomers exhibiting *cis*- and *trans*-isomery, as for example in polybutadiene and polyisoprene, leading to *cis*- and *trans*-tacticity, syndiotacticity, and atacticity respectively.

The above-mentioned polymers with regular chain order are positionally tactic, but may show different degrees of sterical tacticity. Polyethylene, of course, exhibits complete positional and sterical order (isotacticity).

The spatial conformation that results with given fine structure of the chain, however, still depends on many other factors that may be either purely geometrical, due to volume requirement of single constituents and valency angles between adjacent groups, or energetic, due to special interaction between any two monomers' units or between such a unit and the solvent. It was soon found that some factors affect chiefly the single seg-



ment (*short-range* interactions) and that others affect the mutual arrangement of segments in the random coil (*long-range* interactions). A special situation arises with electric charges that influence both. This last effect will be only mentioned at the proper place without going into any further detail, because this would require an extended review by itself.

### Short-range Interactions

For sake of simplicity let us first consider the polyethylene chain. One can take  $\text{CH}_2$  as monomer,  $b_0 = 1.53 \text{ \AA}$ , valency angle  $109.5^\circ = 180^\circ - \alpha$  (tetrahedral bond with  $\cos \alpha = 1/3$ ). With completely free rotation around the valency bond the mean square end-to-end distance of such a chain with  $P = N + 1$  monomers reads<sup>3</sup>

$$h^2 = \langle \mathbf{r}^2 \rangle = \langle (\sum_{j=1}^N \mathbf{b}_j)^2 \rangle = \sum_j^N \sum_{k=1}^N \langle \mathbf{b}_j \mathbf{b}_k \rangle \quad (1)$$

$$= b_0^2 [N(1 - \cos^2 \alpha) - \cos \alpha (1 - \cos^N \alpha)] / (1 - \cos \alpha)^2$$

with  $\mathbf{b}_j$  the link joining the  $j$ th and the  $j + 1$ st monomer. But there is no experimental possibility for direct determination of  $h$ . Experiments yield only the mean square gyration radius<sup>4</sup>

$$R^2 = \sum_j^N \sum_{k=1}^N \langle \mathbf{r}_{jk}^2 \rangle / 2(N + 1)^2 = \sum_{s=1}^N (N + 1 - s) h_s^2 / (N + 1)^2$$

$$= b_0^2 \left\{ \frac{1 + \cos \alpha}{1 - \cos \alpha} \cdot \frac{N(N + 2)}{6(N + 1)} - \frac{\cos \alpha}{(1 - \cos \alpha)^4} \left[ \frac{N}{N + 1} \right. \right. \quad (2)$$

$$\left. \left. - \frac{2N(N + 2)}{(N + 1)^2} \cos \alpha + \frac{N + 2}{N + 1} \cos^2 \alpha - \frac{2 \cos^{N+2} \alpha}{(N + 1)^2} \right] \right\}$$

$\mathbf{r}_{jk}$  vector joining the  $j$ th and  $k$ th monomer,  $h_s$  r.m.s. end-to-end distance of a chain with  $s$  links or  $s + 1$  monomers. With increasing  $N$  both expressions may be simplified to

$$h^2 = Nb_0^2(1 + \cos \alpha)/(1 - \cos \alpha) = Nb^2 = KM \quad (3)$$

$$R^2 = Nb_0^2(1 + \cos \alpha)/6(1 - \cos \alpha) = Nb^2/6 = h^2/6 = KM/6$$

The effective link length

$$b = b_0[(1 + \cos \alpha)/(1 - \cos \alpha)]^{1/2} = b_0 \cot(\alpha/2) \quad (4)$$

is always larger than the true link length  $b_0$ . In the case of tetrahedral bond angle one has  $b = 2^{1/2}b_0 = 1.414b_0$ .

An additional useful quantity for characterizing the chain and especially the short-range interactions on segment length is the *persistence length*

$$a = b/(1 - \cos \alpha) \quad (5)$$



introduced by Kratky and Porod.<sup>5,5a</sup> It equals the mean length of projection of infinitely long chain on the direction of first link.

The model with  $Z$  independent segments of length  $A$  yields

$$\begin{aligned}h_z^2 &= ZA^2 \\ R_z^2 &= ZA^2/6\end{aligned}\tag{6}$$

for mean square of end-to-end distance and gyration radius respectively. In order to obtain  $Z$  and  $A$  from  $M$  or  $P$  or  $N$  and  $R$  or  $h$  one wants additional relationship between  $Z$ ,  $A$ , and an observable quantity. Kuhn and Kuhn<sup>6</sup> introduced the rather arbitrary condition that the model and the molecule have the same extended length

$$L = Z_m A_m = N b_0 \cos (\alpha/2)\tag{7}$$

Combination of Equations 3, 6, and 7 then yields Kuhn's preferential quantities

$$\begin{aligned}A_m &= h^2/L = b_0 \frac{\cos (\alpha/2)}{\sin^2 (\alpha/2)} = b/\sin (\alpha/2) = 2a \cos (\alpha/2) \\ Z_m &= (N/2)(1 - \cos \alpha) = N \sin^2 (\alpha/2) \\ \zeta_m &= N/Z = 2/(1 - \cos \alpha) = 1/\sin^2 (\alpha/2)\end{aligned}\tag{8}$$

One must not forget, however, that Equation 7 is rather unrealistic, yielding too high values for  $A_m$ . The actual statistically independent segment is shorter:  $A < A_m$ .

According to Equation 3 both quantities  $h$  and  $R$  in the limit of large  $N$  are proportional to the square root of molecular weight. With small  $N$ , however, the increase of  $R^2$  and  $h^2$  with  $M$  is more than linear. The corresponding effective bond length  $b_N$  starts with  $b_0$  at  $N = 1$  and approaches asymptotically the limiting value  $b$  (FIGURE 1), the approach being the slower the closer  $\cos \alpha$  to unity. The ratio  $6R^2/h^2$  also appreciably differs from unity at low  $N$ . It starts with 1.5 at  $N = 1$ , rapidly decreases to a minimum and then rather slowly approaches from below the limiting value 1 (FIGURE 2). In that which follows  $N$  will be always so large that all these effects, characteristic for short chain, that is, for chains having small  $Z$ , may be neglected and the asymptotic formulas Equation 3 used instead of Equations 1 and 2. In such a case the distribution function of interchain distances, with exception of those between closest neighbors, is Gaussian.

Experiments, that is, angular dependence of light scattering,<sup>7</sup> combination of intrinsic viscosity and sedimentation or diffusion constant<sup>8</sup> yield  $R^2$ . Proportionality with molecular weight is found in *ideal solvent* characterized by vanishing of second virial coefficient, that is, at the so-called Flory's  $\Theta$ -point. The corresponding gyration radii  $R_0$  are markedly smaller than in good solvents, but they are definitely higher than predicted by

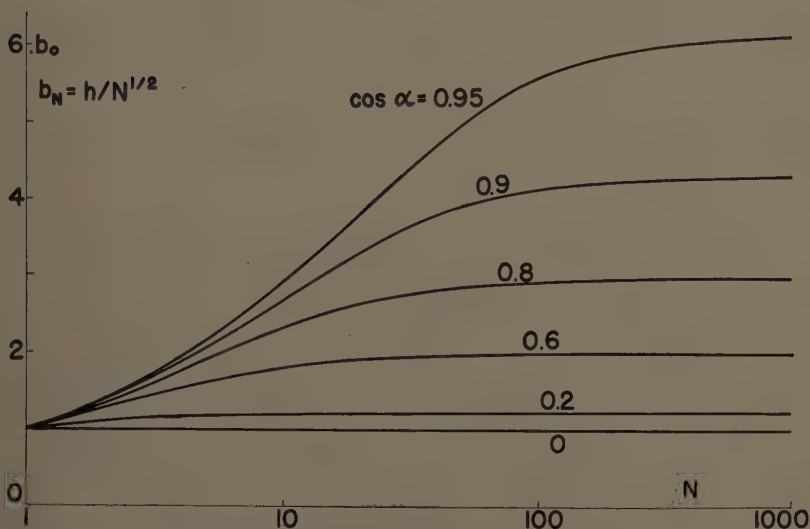


FIGURE 1. Initial increase of effective link length  $b_N = h/N^{1/2}$  with  $N$  from  $b_0$  at  $N = 1$  till  $b = b_0 [(1 + \cos \alpha)/(1 - \cos \alpha)]^{1/2}$  at  $N = \infty$ .

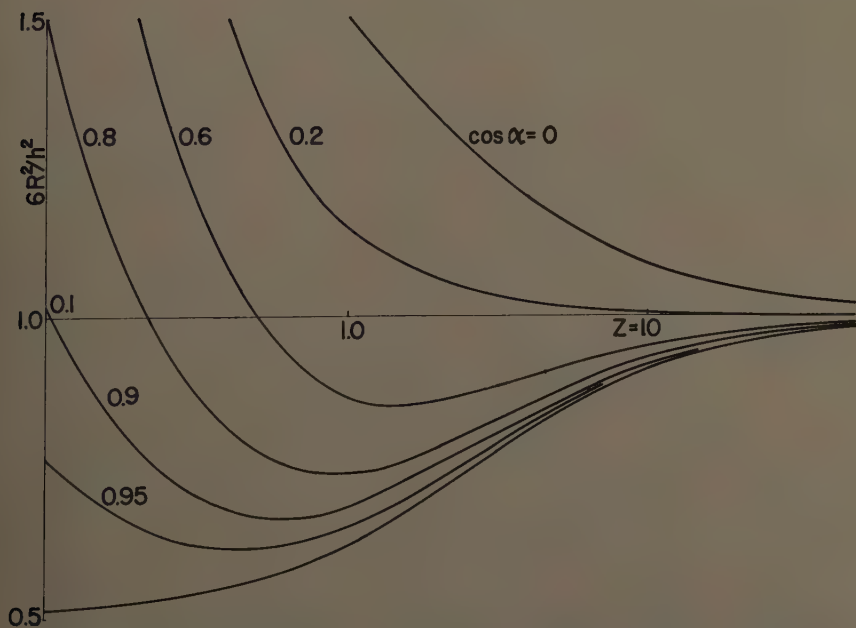


FIGURE 2. Initial changes of the ratio  $6R^2/h^2$  for different valency angles  $180^\circ - \alpha$ . Except for the shortest chains—the ratio starts with 1.5 at one link with two beads—and very small  $\cos \alpha$  the square of gyration radius is slightly less than  $h^2/6$ . The lowest curve corresponds to a wormlike chain<sup>5, 6a</sup> with  $Z = L/2a$ .

Equation 3. An experimental effective link length  $b_\theta$  can be calculated by applying Equation 3

$$b_\theta = R_\theta(6/N)^{1/2} \quad (9)$$

The ratio  $b_\theta/b$  is always larger than unity (TABLE 1). It is 1.2 for polyethylene and 2.1 for polymethylmethacrylate.

TABLE 1  
COIL EXTENSION DUE TO HINDERED ROTATION AS MEASURED BY  
 $b_\theta/b = [(1 + \langle \cos \varphi \rangle)/(1 - \langle \cos \varphi \rangle)]^2$  FOR DIFFERENT  
POLYMERS AT  $\theta$ -POINT

		$b_\theta/b$	Reference
Polyvinylbromide	$-\text{CH}_2-\text{CH}-$ Br	1.9	9
Polyacrylic acid	$-\text{CH}_2-\text{CH}-$ COOH	1.8	10
Polyvinylacetate	$-\text{CH}_2-\text{CH}-$ COOCH <sub>3</sub>	2.3	11
Polystyrene	$-\text{CH}_2-\text{CH}-$ C <sub>6</sub> H <sub>5</sub>	2.2-2.4	12, 13
Poly-4-vinyl pyridine	$-\text{CH}_2-\text{CH}-$ C <sub>5</sub> H <sub>4</sub> N	2.2	14
Polyisobutylene	$-\text{CH}_2-\text{C}(\text{CH}_3)_2-$	2.3 1.7-1.8	12 13, 15, 16
Polymethylmethacrylate	$-\text{CH}_2-\text{C}(\text{CH}_3)-$ COOCH <sub>3</sub>	2.0-2.2 1.68-1.89	10, 17, 18 19
Polyethylmethacrylate	$-\text{CH}_2-\text{C}(\text{CH}_3)-$ COOC <sub>2</sub> H <sub>5</sub>	1.9	20
Polybutylmethacrylate	$-\text{CH}_2-\text{C}(\text{CH}_3)-$ COOC <sub>4</sub> H <sub>9</sub>	2.1	21
Poly-2-ethylbutylmethacrylate	$-\text{CH}_2-\text{C}(\text{CH}_3)-$ COOC <sub>4</sub> H <sub>8</sub> (C <sub>2</sub> H <sub>5</sub> )	2.3	22
Polyhexylmethacrylate	$-\text{CH}_2-\text{C}(\text{CH}_3)-$ COOC <sub>6</sub> H <sub>13</sub>	2.4	23
Polyoctylmethacrylate	$-\text{CH}_2-\text{C}(\text{CH}_3)-$ COOC <sub>8</sub> H <sub>17</sub>	2.3	24
Polylaurylmethacrylate	$-\text{CH}_2-\text{C}(\text{CH}_3)-$ COOC <sub>12</sub> H <sub>25</sub>	2.8	24a
Polydimethylsiloxane	$-\text{Si}(\text{CH}_3)_2-\text{O}-$	1.2	25
Poly- <i>cis</i> -isoprene	$-\text{CH}_2-\text{CH}=\text{C}(\text{CH}_3)-\text{CH}_2-$	1.5	26
Poly- <i>trans</i> -isoprene	$-\text{CH}_2-\text{CH}=\text{C}(\text{CH}_3)-\text{CH}_2-$	1.3	26



In order to explain this additional chain extension one has to consider restriction of rotation around the chemical bond caused by geometric and energetic interaction of close-by monomers. In the limit of sufficiently high  $N$ , restricted rotation influence, calculable by the same scheme as demonstrated in Equation 1, leads to the following modification<sup>27</sup> of Equation 4

$$b^2 = b_0^2 \frac{1 + \cos \alpha}{1 - \cos \alpha} \cdot \frac{1 + \langle \cos \varphi \rangle}{1 - \langle \cos \varphi \rangle} \quad (10)$$

with  $\varphi$  the angle between the planes through the  $j$ th link and the preceding and subsequent link respectively. With pure *trans* (*cis*) configuration one has  $\varphi = 0$  ( $180^\circ$ ). Restricted rotation therefore may either increase or decrease the effective link length and hence  $R$  and  $h$  according to which configurations, *cis* or *trans*, are favored by neighbor interaction. Bulky side groups have high space requirement and hence prevent chain configurations at which the groups would partially overlap, and these are mainly configurations yielding a shorter segment. Very efficient are phenyl and methyl groups. Rather long aliphatic side chains do not matter very much since their bulk can be easily accommodated far enough from the main chain. There may be a special temperature effect found by Schulz and Kirste<sup>19</sup> on polymethylmethacrylate. The ratio  $b_0/b$  steadily rises from 1.68 at  $\Theta = -40^\circ \text{C}$ . (2-methylpentanon-4 and methylisovalerate as solvents) till 1.89 at  $+60^\circ \text{C}$ . (isoamylacetate). The authors propose as explanation that, with increasing temperature, the side groups have more motional freedom and hence increased space requirements so that the rotational restrictions to the main chain are greater than at lower temperature.

Forces between adjacent monomers and among neighboring groups, characterized by a distance-dependent interaction energy  $u(r)$ , may have various effects, all of them primarily showing a temperature dependence of the type  $\exp(-u/kT)$ . With exception of forces between free electrical charges in a solvent of low ionic strength they are typical short-range forces decaying with a very high power of mutual distance so that one has to consider the interaction of but a small number of neighbors.<sup>28, 28a</sup> For the most part merely the influence of first neighbor is taken into account. The solvent is considered only in so far as it changes the coefficients in the interaction energy. In the simple polyethylene chain one has to do only with the repulsion of protons favoring *trans* configuration and hence increasing the effective link length. With increasing temperature these limitations get less severe, the corresponding decrease of the average  $\langle \cos \varphi \rangle$  leading to a reduction of  $b$  and hence of coil diameter and gyration radius.

Side chains with active groups complicate the situation. An extreme case is DNA and other polynucleotides in which the strong hydrogen bonds between the sugars lead to double or even triple stranded helical configurations<sup>29</sup> that enormously increase  $b$  and persistence length  $a$  ( $\sim 300 \text{ \AA}$ ).<sup>30, 30a</sup> Such a helix is an extremely rigid structure as compared with single chain,

even when the latter exhibits high rotational restriction. As a consequence the deviations in coil structure from the limit (Equations 3 and 10) are not completely negligible as may be seen from angular dependence of light scattering (FIGURE 3). Hydrogen bonds and electrostatic interaction of charges in this kind of molecules are very sensitive to solvent composition, that is, ionic strength,  $pH$ , presence of groups competing with the intra-

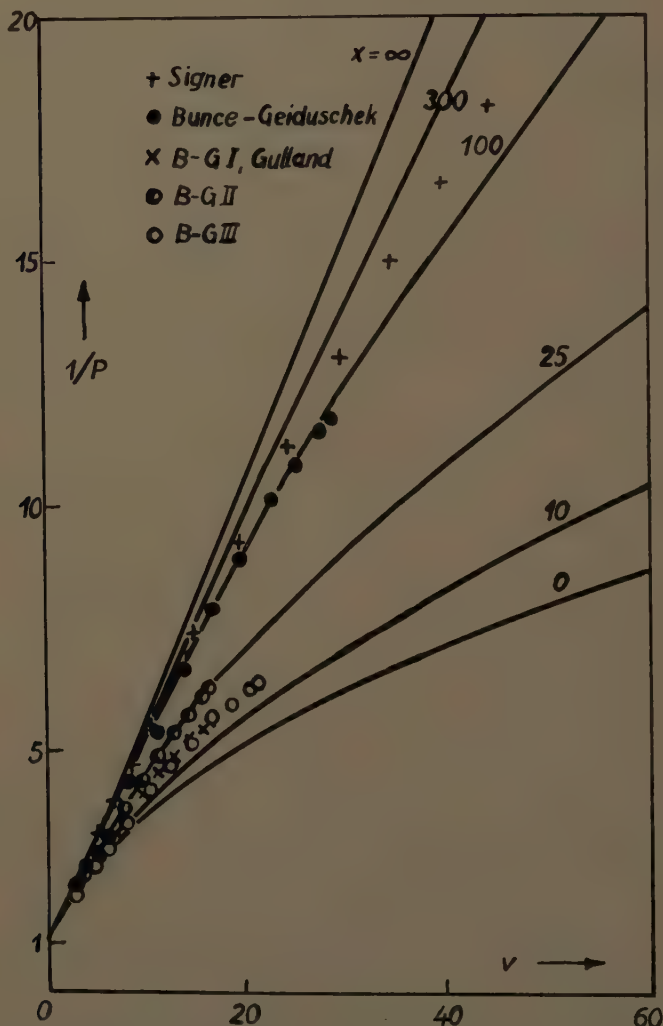


FIGURE 3. Angular dependence<sup>30a</sup> of scattering intensity  $P^{-1}(\vartheta)$  over  $v = (ksR)^2$  for coils with different persistence length  $a = L/x$ . Experimental points correspond to DNA samples of Signer, Bunce-Geiduschek and Gulland. Reproduced by permission of *Journal of Polymer Science*, Volume 41, copyright 1959 by Interscience Publishers, Inc., New York, N. Y.

helical hydrogen bonds (for example, urea), and one actually observes "melting" and a net influence of these factors on "melting" temperature at which the helices transform in normal chains with high flexibility.<sup>31</sup> A limited amount of helical arrangement is also found with isotactic polystyrene where, according to Birstein and Ptitsyn,<sup>32</sup> sections of left- and right-handed helices alternate, the single helical section containing three monomer units in the average. As a consequence  $b_\theta$  of isotactic polystyrene is larger than that of atactic one.<sup>33</sup>

Net electric charges yield an interaction energy proportional to the inverse distance between the charges. That is a typical long-range force. However it also very strongly influences the arrangement of next neighbors strongly favoring configurations with largest possible next-neighbor inter-charge distance. These are not always the most extended chains because in special cases, for example, in positionally isotactic acrylic acid (*ht*-chain), the nearest charges are farther away at *cis* than at *trans* configuration so that  $b$  decreases with ionization and decreasing ionic strength of solution.<sup>34</sup> Hence in every case, the effect of free charges requires a special study of the basis of the actual fine structure of the chain and of the charge position.

Dipole interaction decreases with the inverse third power of distance and hence chiefly influences the orientation of next neighbors. When the main component of dipole moment is parallel to the chain axis, electrical interaction favors *trans* configurations with parallel dipole arrangement. As a consequence the square of total dipole moment of macromolecule is greater than the sum of squares of single moments, the value resulting in a chain with tetrahedral valency angle and no dipole interaction.<sup>35</sup> Typical examples are poly-*o*-chlorstyrene and poly-*o*-bromstyrene, showing an increase by a factor of 1.3 and 1.1 respectively (TABLE 2). When, however, the main component is perpendicular to the chain axis the antiparallel *cis* configurations are favored, yielding a lower contribution to the mean square of total moment (polyvinylchloride 0.87, polyoxymethylene 0.87, polymethylmethacrylate 0.73 to 0.81). The contribution, of course, is still less when the dipole-bearing group can at least partially rotate independently on the chain (polyparachlorphenylmethacrylate 0.58). Investigations on dipole moment in good solvents agree with those at  $\Theta$  point, hence demonstrating that dipole interaction only influences the short-range structure of the chain and is not affected by coil dimensions.<sup>30,40,42</sup>

As already mentioned, the chief experimental method for investigation of short-range interaction, that is, of the effective link length, is measurement of gyration radius in ideal solvent. The same information may be obtained from small-angle X-ray scattering.<sup>5,41,44</sup> By plotting (FIGURE 4) the relative intensity  $P(\vartheta) = I(\vartheta)/I(0)$  multiplied by  $s^2$  over  $s = \sin(\vartheta/2)$  a distinct knee is obtained at  $s^* = 2/ka$  ( $k = 2\pi/\lambda$ ), yielding<sup>43</sup>

$$a = 2/ks^* \quad (11)$$



The effective link length follows from Equation 4 and 5:

$$b = b_0(2a/b_0 - 1)^{1/2} = b_0(4/k_s^*b_0 - 1)^{1/2} \quad (12)$$

This method is independent of coil dimensions and therefore may be applied also to nonideal solutions, permitting study of the changes of short-

TABLE 2

RATIO OF OBSERVED R.M.S. DIPOLE MOMENT OF MACROMOLECULE AND THAT PREDICTED FOR COMPLETELY UNRESTRICTED MONOMER ORIENTATION

		$(\mu_{\text{obs}}^2/P\mu_0^2)^{1/2}$	Reference
Poly- <i>o</i> -chlorstyrene	$\begin{array}{c} \text{---CH}_2\text{---CH---} \\   \\ \text{C}_6\text{H}_4\text{Cl} \end{array}$	1.3	36
Poly- <i>o</i> -bromstyrene	$\begin{array}{c} \text{---CH}_2\text{---CH---} \\   \\ \text{C}_6\text{H}_4\text{Br} \end{array}$	1.1	36
Polyoxyethylene	$\text{---CH}_2\text{---CH}_2\text{---O---}$	0.87	37, 38
Polyvinylchloride	$\text{---CH}_2\text{---CHCl---}$	0.87	39
Polymethylmethacrylate	$\begin{array}{c} \text{---CH}_2\text{---C(CH}_3\text{)---} \\   \\ \text{COOCH}_3 \end{array}$	0.73-0.81	38, 40
Poly- <i>p</i> -bromstyrene	$\begin{array}{c} \text{---CH}_2\text{---CH---} \\   \\ \text{C}_6\text{H}_4\text{Br} \end{array}$	0.71	36, 39
Poly- <i>p</i> -chlorphenylmethacrylate	$\begin{array}{c} \text{---CH}_2\text{---C(CH}_3\text{)---} \\   \\ \text{COO---C}_6\text{H}_4\text{---Cl} \end{array}$	0.59	41

range order in good solvents and the eventual influence of long-range interaction on the structure of short-chain segments.

Additional information may be obtained from measurement of excess dielectric polarization, as already mentioned above, and of optical anisotropy of macromolecules. The latter has to be derived from streaming birefringence. It turns out to be independent of coil dimensions, that is, on long-range interactions, but again larger as calculated on the assumption of free rotation around the chemical bond.<sup>46</sup> However, the calculated data of optical anisotropy are still so much affected by the uncertainty of orientation possibilities of optically anisotropic groups in the monomer that

they can not be used for a quantitative estimate of hindered rotation in the main chain although they yield a good qualitative support to results obtained by other methods.

### Long-range Interactions

In good solvents, characterized by positive value of second virial coefficient  $A_2$  (Equation 18), the square of gyration radius increases more than linearly with  $M$ . Very generally one can put

$$R^2 = KM^{1+\epsilon} \quad (13)$$

$\epsilon$  being 0.25 for polymethylmethacrylate<sup>47</sup> in acetone at 20° C., 0.33 for cellulose nitrate<sup>48</sup> in acetone at 20° C. and 0.005, 0.07, 0.22 for polystyrene<sup>49</sup> in

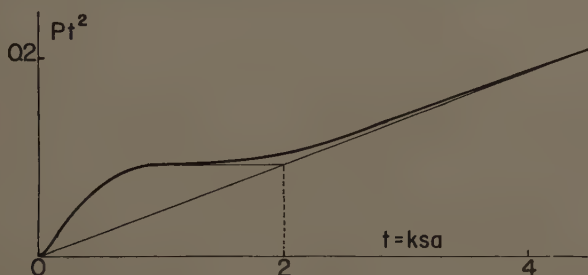


FIGURE 4. The product  $Pt^2$  over  $t = ksa$  for a chain with 800 monomers and  $\cos \alpha = 0.9$ . Note the knee at  $t = 2$ .<sup>45</sup>

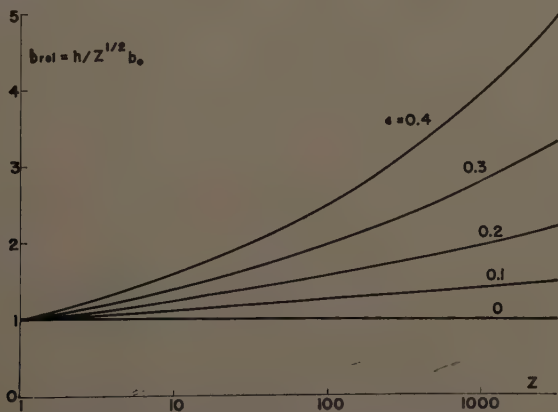


FIGURE 5. Relative increase of effective link length  $b/b_0 = h/b_0 Z^{1/2} = Z^{\epsilon/2}$  for non-Gaussian chains.

cyclohexanone at 43° and 57° C., and in toluene at 20° C., respectively. Such a behavior cannot be explained by hindered rotation, due to any of the sources mentioned above with short-range interactions, because in the limit of sufficiently high degree of polymerization it always leads to  $\epsilon = 0$ . The difference may be seen best by comparing the effective link length  $b$  in both cases (FIGURES 1 and 5). Valency angle and hindered rotation yield curves concave to the  $N$  axis, while Equation 13 produces an upward

curvature with the increase in  $b$  becoming more marked with increased degree of polymerization.

In order to account for this additional coil expansion which, in the same polymer series, increases with molecular weight, interactions between any two monomers must be considered, regardless of the length of the section of the chain by which they are separated. In spite of the fact that (with the exception of electrostatic forces between free charges, which are considered later) all interactions between monomers are rather short-ranged; they are not negligible because there are chain configurations that bring any pair of distant monomers to direct contact. The number of possible contacts increases with the square of degree of polymerization since any monomer has the chance to get in contact with any other monomer. The exception to this is the case of closest neighbors, which are prevented from that contact by restrictions imposed on them by valency angle and limited rotation, that is, by short-range interactions. On the other side, the volume of polymer coil increases as  $R^3$ , that is, as  $P^{3(1+\epsilon)/2}$ , so that the probability of a contact per unit volume (contact density) increases as  $P^{(1-3\epsilon)/2}$ . As long as  $\epsilon$  is smaller than one third, the contact density increases with molecular weight, and the corresponding contribution of interaction energy does likewise.

The energy of interaction between two monomers in a given solvent must express the impenetrability of monomer and eventual difference of affinity between the monomers and between the monomer and the solvent. Its precise dependence on distance  $r$  between the monomers does not matter very much, at least in the present stage of investigation. Therefore, one prefers to choose functions permitting the easiest calculation of interaction energy averages. Bueche<sup>50</sup> and Yamakawa and Kurata<sup>51</sup> assume (FIGURE 6)

$$\begin{aligned} u(r) &= +\infty & r < 2a^* \\ &= -u_0 \exp(-3r^2/2d^2) & r > 2a^* \end{aligned} \quad (14)$$

$a^*$  radius of monomer,  $d$  range of interaction  $< A$  (segment length). In good solvents the monomer prefers to be surrounded by solvent molecules, the forces between any two monomers are repulsive ( $u_0 < 0$ ). In poor solvents one has the opposite situation,  $u_0 > 0$ . At the  $\Theta$  point the attraction forces favor a just sufficiently close approach of segments to compensate for the effect of monomer impenetrability.

The exclusion of configurations with overlapping segments yields a more extended coil because the excluded configurations are chiefly those leading to small end-to-end distance. This increase of average dimensions is even greater with repulsive forces,  $u_0 < 0$ ; but it can be overcompensated by strong attractive forces ( $u_0 > 0$ ). Lattice model investigations of "excluded volume" effect on coil dimensions were done by Wall and Mazur,<sup>52</sup> who by the use of an electronic computer derived the average end-to-end



distance of chains and its dependence on molecular weight and average energy of interaction. A great advantage of this treatment is that it is not limited to small deviations from ideal solvent.

A similar interaction between free segments occurs in oligomer solution. As a consequence of interaction the osmotic pressure is not more proportional to concentration. The deviations are considered by a power expansion (Equation 18) in which the two-segment interaction is represented by the second virial coefficient  $A_2$ . By a rather rough procedure Peterlin<sup>53</sup> was able to show proportionality of  $\epsilon$  and  $A_2$ , which seems to be supported by experimental evidence. However, his treatment did not yield quantitatively the proportionality factor; it is also not rigorous enough.

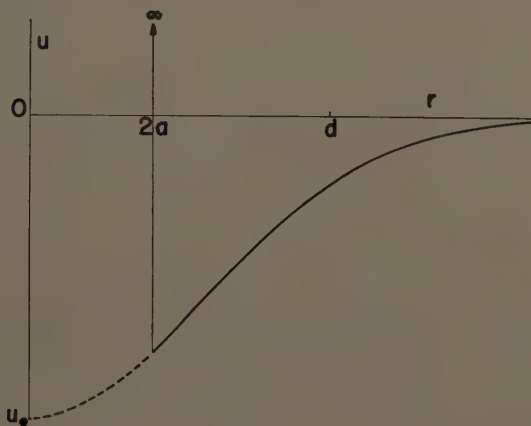


FIGURE 6. Interaction energy between two monomers according to Equation 14.

Flory<sup>54</sup> assumed a uniform coil expansion measured by a factor

$$\alpha = R/R_0 = h/h_0 \quad (15)$$

and derived the following basic relationship

$$\alpha^5 - \alpha^3 = 2C_M\psi_1(1 - \Theta/T)M^{1/2} \quad (16)$$

$$C_M = (27/2^{5/2}\pi^{3/2})(v^2/N_A v_1)(M_0/b_0^2)^{3/2} \quad (17)$$

$v$  = specific volume of polymer,  $N_A$  Avogadro's number,  $v_1$  molar volume of solvent,  $M_0$  molecular weight of monomer,  $\psi_1$  an empirical constant  $\sim 1/2$ . The same parameter enters the second virial coefficient  $A_2$  in osmotic pressure

$$\begin{aligned} \pi/c &= N_A kT(1/M + A_2 \cdot c + \dots) \\ A_2 &= (16\pi/3^{3/2})(N_A R^3/M^2) \ln [1 + (\pi^{1/2}/2)(\alpha^2 - 1)], \end{aligned} \quad (18)$$

leading to the power expansion

$$\alpha = 1 + (27/2)(M_0/2\pi b_\Theta^2)^{3/2}(A_2/N_A)M^{1/2} + \dots \quad (19)$$

$$= 1 + 1.299z + \dots$$

where  $z$  is defined in Equation 21. By uniform expansion the Gaussian distribution of intrachain distances remains unchanged.

Nonuniform coil expansion was considered by a long series of investigators.<sup>51,55-63</sup> They all closely agree with the following series expansion of  $h$  and  $R$

$$h^2 = h_\Theta^2(1 + 4z/3 + \dots) = h_\Theta^2(1 + 1.33z + \dots)$$

$$R^2 = R_\Theta^2(1 + 134z/105 + \dots) = R_\Theta^2(1 + 1.286z + \dots) \quad (20)$$

$$6R^2/h^2 = 1 - 0.047z + \dots$$

with

$$z = 2(3M_0/2\pi b_\Theta^2)^{3/2}(A_2/N_A)M^{1/2}/F(z)$$

$$F(z) = 1 - 2.865z + \dots \quad (21)$$

The end-to-end distance increases faster than the gyration radius. The expanded coil is definitely non-Gaussian. The value of  $\alpha^2$  from Equation 19 lies exactly between those given by the first two Equations of 20 when only the factor 27/2 in the linear term of Equation 19 is replaced by 27/4: 1.333, 1.299, and 1.286 are the corresponding numerical coefficients at  $z$ . The higher coefficients of series expansions in Equation 20 are rather uncertain.

Further modifications in the treatment of excluded volume effect were made recently<sup>61-67</sup> in order either to obtain higher terms in power expansions for  $R$ ,  $h$ , and  $A_2$  or to get better functional expressions valid in a greater range of  $z$ , which would agree with experimental data and the lattice model investigations. Both yield an increase of  $(\alpha^5 - \alpha^3)/M^{1/2}$  with  $M$ , indicating a nonuniform coil expansion. A more direct proof would be highly desirable.

Combination of X-ray and visible light scattering may provide a means for such a check. The latter yields the mean square gyration radius and the former the persistence length. At uniform expansion  $a$  and  $R$  must increase by the same factor when going from ideal to good solvent, while nonuniform expansion requires a net increase of  $R$  and nearly constant  $a$ . Indeed, when the short-range interactions are unaffected by the change of solvent and temperature,  $a$  ought to be strictly constant.

The scattering envelope with visible light yields an additional means of investigating the distribution function of intrachain distances. When the mean square of distance between any two chain elements obeys the same

power rule as the end-to-end distance (Equation 13)

$$\langle r_{jk}^2 \rangle = KM_{jk}^{1+\epsilon} \quad (22)$$

with  $M_{jk}$  molecular weight of the chain section between the  $j$ th and the  $k$ th element, the ratio between gyration radius and end-to-end distance decreases to<sup>68</sup>

$$6R^2/h^2 = 1/(1 + 5\epsilon/6 + \epsilon^2/6) = v/\tau \quad (23)$$

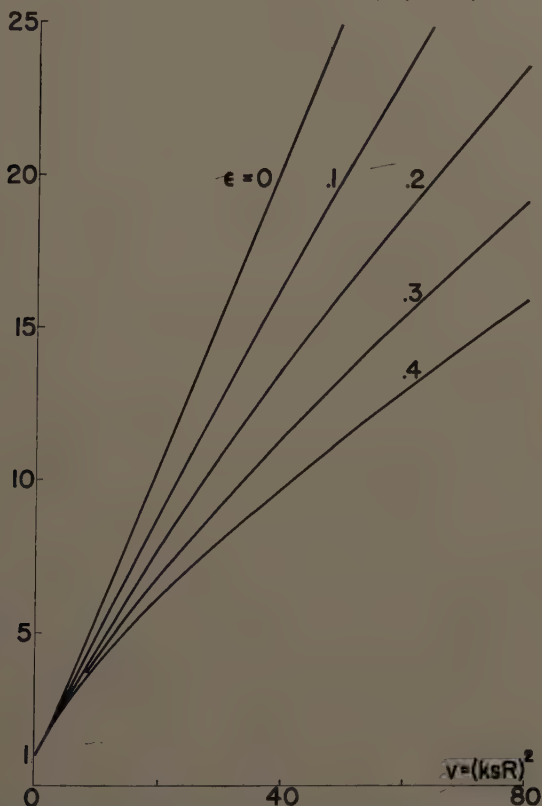


FIGURE 7. Angular dependence<sup>72</sup> of scattering intensity  $P^{-1} = cKM/R(\vartheta)$  over  $v = (ksR)^2$ , for coils with intrachain distances according to Equation 22. The calculation is based on a Gaussian distribution of distances between any two monomers.

with  $v = (ksR)^2$  and  $\tau$  parameter wanted in  $P(\vartheta)$ , and the scattering function<sup>69-72</sup> becomes (FIGURE 7)

$$P(\vartheta) = [2/(1 + \epsilon)] \{ \tau^{-1/(1+\epsilon)} [-\epsilon/(1 + \epsilon), \tau]! - \tau^{-2/(1+\epsilon)} [(1 - \epsilon)/(1 + \epsilon), \tau]! \} \quad (24)$$

$$[y, \tau]! = \int_0^\tau w^y \exp(-w) dw \text{ incomplete factorial function}$$

Its main characteristics are a persistent downward curvature of  $P^{-1}$  plot over  $\sin^2(\vartheta/2)$  in contrast with the persistent upward curvature in the case of  $\epsilon = 0$ . The downward curvature becomes still more marked in the case of coils with finite number of segments.

This check, however, is not unambiguous because polydispersity distorts the scattering envelope in exactly the same sense. Moreover, chains with  $\epsilon = 0$  but with sufficiently small  $Z$  yield scattering curves that lie between the curve for a rigid rod and that for an infinite coil with  $\epsilon = 0$  (FIGURE 3). Although the curves are definitely different from those corresponding to a nonvanishing  $\epsilon$ , the difference is not so striking that from the scattering envelope  $P^{-1}$  it could be decided with certainty whether the coil structure corresponds to  $\epsilon \neq 0$ , or to  $\epsilon = 0$  and small  $Z$ , or whether the whole effect is due simply to polydispersity.

A special case of long-range interaction occurs with charged polymers. The electrostatic repulsion potential energy between two chain elements having each a charge  $e$  reads

$$u = e^2 \exp(-\kappa r) / \epsilon_s r \quad (25)$$

with

$$\kappa = 4\pi \sum_i c_i e_i^2 / \epsilon_s kT$$

Dielectric constant of solution  $\epsilon_s$ ;  $c_i$  concentration; and  $e_i$  charge of ions of the  $i$ th kind. As a consequence of electrostatic repulsion the coil strongly expands with increasing ionization, that is, increasing number of charged chain elements and decreasing ionic strength  $\sum c_i e_i^2$ . The expansion is not uniform, the inner parts of the coil expanding more than the ends.<sup>73</sup> At the same time, however, the charges also influence the organization of next neighbors; there, as already mentioned with short-range interaction, under special steric conditions, configurations leading to a contraction of chain segment may be favored when this configuration increases the distance between neighboring charges. This possibility of simultaneous contraction of short segments and expansion of the whole coil requires a detailed study of positional and sterical particularities of chain structure in order to obtain the final effect of charges on coil dimensions.<sup>73a,b</sup> On the other hand, at finite concentration of polymer solution there is always a marked increase of gegenion concentration inside the coil, providing a more efficient shielding of charges on the macromolecule.<sup>74,74a</sup> Therefore, the condition of constant ionic strength during dilution can be guaranteed only by adding low molecular ions in proper amount, for example, by dialysis with a standard solution of constant ion concentration.<sup>75</sup> Until now there has been neither enough experimental data at sufficiently well defined conditions nor a satisfying theory<sup>76-77h</sup> available that could be checked by experiments, although there is a very rough qualitative agreement of rather rudimentary theoretical consideration with observations.



*Solution in Laminar Flow*

*Hydrodynamic interaction.* Hydrodynamic interaction is a typical long-range interaction that decreases with inverse distance of interacting chain elements. Two cases are of interest: (1) the macromolecule moving with constant velocity through the solution at rest (pure *translation*: sedimentation, electrophoresis), (2) the macromolecule in a linear flow field (*rotation* and *deformation*: viscosity, streaming birefringence). In both cases the effects are determined by the hydrodynamic resistance coefficient  $\Lambda_0$  of monomer and by their interaction, which in first approximation is proportional to inverse distance and also depends on the angle between velocity and distance of interacting units.

Let us first consider velocities and gradients so low that the deformation of coil by the flow may be neglected. This is nearly always the case with translational motion and with intrinsic viscosity at zero gradient. In a very rough but quite satisfactory approximation, the polymer coil behaves like a semipermeable sphere with two characteristic parameters: diameter and permeability. Both may be determined from combination of translational resistance and intrinsic viscosity data. The sphere diameter yields the gyration radius of coiled macromolecule in fairly good agreement with determinations by other methods.<sup>8,78</sup>

However, one may also start with average coil configuration in studying the effect of hydrodynamic interaction. In order to do that, the averaged values of all intrachain distances must be known. Most calculations are based on Equation 3, and therefore their results are applicable only to the coil in ideal solutions.<sup>53,79-82</sup> By taking into account the unavoidable polydispersity, it was possible to use the results for determination of hydrodynamic resistance  $\Lambda_0$  in satisfactory agreement with geometric expectations.<sup>83</sup> Treating the case with nonvanishing excluded volume effect<sup>60,62</sup> has also proved successful, so that the hydrodynamic interaction at translation and rotation of undeformed coil is fairly well understood. The results were extensively reviewed quite recently<sup>62,78</sup> so that it seems justified here to omit a treatment of this case. Let us consider in more detail, however, the effects when chain deformation and orientation are of primary concern, that is, the gradient dependence of intrinsic viscosity and streaming birefringence.

With increasing gradient  $G$ , the observed intrinsic viscosity decreases in close agreement with the series expansion<sup>84</sup>

$$[\eta] = [\eta]_0(1 - B'G^2 + \dots) = [\eta]_0(1 - B\beta_0^2 + \dots) \quad (26)$$

$$\beta_0 = M[\eta]_0\eta_0 G / N_A kT$$

and it is very likely that it approaches a new limit  $[\eta]_\infty < [\eta]_0$ , although no experiment has yet demonstrated it. Due to the rather difficult extrapolation to zero concentration, there is also some uncertainty as to whether the

initial drop of intrinsic viscosity is indeed proportional to the square of the gradient, although no clear-cut case demonstrates a different type of dependence.

Theory always yields a quadratic term in the series expansion Equation 26, but there is no final agreement about the value of  $B$ , and still less about higher coefficients. Moreover, all calculations are based on Gaussian coil and therefore can be applied only to ideal solutions.

Without any hydrodynamic interaction, intrinsic viscosity<sup>85</sup>

$$[\eta] = (N_A R^2 / 6M_0) \Lambda \quad (27)$$

turns out to be independent on gradient (FIGURE 8). Isotropic hydrodynamic interaction changes  $\Lambda_0$  into  $\Lambda_0^*$ , which, in first approximation, may be written

$$\begin{aligned} \Lambda_0^* &= \Lambda_0 / (1 + e) \\ e &= (2/27\pi^3)^{1/2} \Lambda_0 P^{1/2} / b \end{aligned} \quad (28)$$

More detailed treatment of hydrodynamic interaction<sup>82</sup> using Rouse's model<sup>86</sup> slightly modifies Equation 28 without changing the functional connection between  $[\eta]$  and  $\Lambda$  as the average value of resistance coefficient of monomer in laminar flow.<sup>53,81,87</sup> This reduction is the consequence of two opposing effects. In laminar flow the ends of coiled macromolecule have average velocities that are equal in amount but opposite in direction. Monomers of one half of the chain therefore move in the same direction and by hydrodynamic interaction reduce  $\Lambda_0$  of any monomer of this same half of the chain. Since monomers of the other half are moving in opposite direction, they increase  $\Lambda_0$ , their effect being smaller because they are farther away from the monomer under consideration.

With increasing  $\beta$  the coil gets more and more extended

$$h^2 = h_0^2 (1 + 2\beta^2/3) \quad (29)$$

However, the extension is not uniform,<sup>88</sup> since the distances between remote elements increase more rapidly than those between closer neighbors. As a first consequence, the influence of the more distant parts of the coil rapidly vanishes so that the reduction of  $\Lambda_0$  to  $\Lambda_0^*$  becomes still larger. Therefore, intrinsic viscosity decreases as<sup>89</sup>

$$[\eta]^* = [\eta]_0^* [1 - 0.152e\beta^2 / (1 + e) + \dots] \quad (30)$$

At still higher coil extension, the contributions of the close-by neighbors also markedly decrease and yield a rather slow increase of  $[\eta]^*$  (FIGURE 8). The effect is limited by the model to such  $\beta$  values that  $h \ll Pb_0$ . When  $h$  reaches the extended length  $Pb_0$  no further expansion can occur so that  $[\eta]^*$  has to decrease and to approach a limit  $[\eta]_\infty^*$ , roughly corresponding to that of rodlike particles of similar length-to-thickness ratio at maximum orientation.<sup>89a</sup>

Hydrodynamic interaction is not isotropic, and its average strongly depends on space distribution of all chain segments. As a consequence  $\Lambda_{l_0}^*$  for longitudinal (radial) movement of chain segments is smaller than  $\Lambda_{t_0}^*$  for transversal (rotational) motion. Intrinsic viscosity at zero gradient remains nearly unchanged, the coefficient  $\Lambda_0^*$  merely being replaced by  $\Lambda_{l_0}^*$ . But the increase in rotational resistance results in better orientation, yielding smaller extinction angle  $\chi$  of streaming birefringence. The decrease in longitudinal resistance, however, results in a smaller extension of

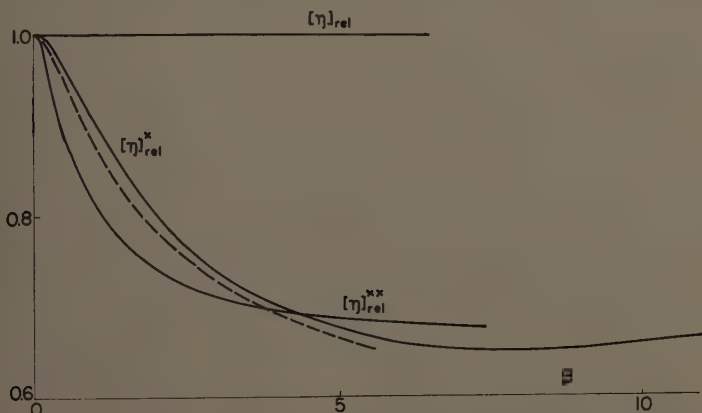


FIGURE 8. Relative intrinsic viscosity  $[\eta]_{rel} = [\eta]/[\eta]_0$  for free draining coil, coil with hydrodynamic interaction according to Equation 30 with  $e/(e+1) = 1([\eta]_{rel}^*)$ , and for coil with finite inner viscosity ( $[\eta]^{**}$ ) according to Cerf.<sup>94</sup> The broken line represents Čopič's measurement on polystyrene.<sup>90</sup>

the coil in flow. Therefore, even in the case that the direct influence of coil expansion on hydrodynamic interaction is neglected,  $[\eta]$  decreases

$$[\eta]_a^* = [\eta]_0(1 - B_a\beta^2 + \dots) \quad (31)$$

The coefficient  $B_a$  is 0.148 according to Čopič and Peterlin<sup>84,90,90a</sup> and 0.0196 according to Ikeda.<sup>87</sup> The difference is due to a different way of averaging. In order to include the effect of coil expansion on hydrodynamic interaction, it is necessary to multiply Equations 30 and 31, that is, to add the respective coefficients  $B$  of the linear term. The resulting initial drop in  $[\eta]$  is greater than according to either Equation 30 or 31.

In order to explain the steady decrease of  $[\eta]$  with  $G$ , it is necessary to make the additional assumption that in laminar flow the coil does not expand as much as given by Equation 29. Such a behavior may be easily understood. During one full rotation with the period  $T = 4\pi/G$ , the coil must change its shape four times from maximum expansion to maximum compression or vice versa, and in so doing, a great many changes in angular orientation of adjacent monomers must take place in a rather short time. Any restriction in free rotation around the valency bond opposes such a

sudden change. This short-range interaction effect can be described as a force proportional to the rate of shape change of the coil<sup>91-94</sup>

$$-F \, dh/dt \quad (32)$$

The coefficient  $F$  of "inner viscosity" has the dimension of viscosity times length. In order to account for the change of extinction angle of streaming birefringence with the gradient<sup>95</sup> the factor  $F$  must be independent of degree of polymerization. With such an assumption alone and neglecting the change of hydrodynamic interaction with the still remaining coil expansion, one obtains the curve  $[\eta]**$  (FIGURE 8). For a complete fit or comparison with experiment one will have to include the effect of anisotropy of hydrodynamic interaction and the influence of actual coil extension which, although smaller than according to Equation 29 is not negligibly small.

Some experiments with extremely viscous solutions, lubricating oils at low temperature,  $\eta \sim 10^4 P$ , containing small amount of polymer added as improver,<sup>96</sup> show a gradient dependence that is strikingly similar to that of  $[\eta]^*$ . The experiments, of course, were performed at too high concentrations, so that they do not yet represent the properties of isolated macromolecule, and it is always hard to estimate how much of the observed effect is due to interaction effects. Nevertheless, these experiments are an indication that at special conditions, that is, extremely viscous solvent and low gradient, one may find a situation where the macromolecular coil markedly expands under the influence of laminar flow because the high solvent viscosity seems to overshadow completely the influence of "inner viscosity." At  $\beta$  values, high enough for marked gradient dependence of viscosity, the gradient  $G$  is still so low that the macromolecular coil has no special difficulty in changing shape, and the forces exerted by the solvent so high that the "inner viscosity" resistance may be completely neglected. As a consequence, the intrinsic viscosity first decreases and then increases in qualitative agreement with the curve  $[\eta]^*$ . Further experiments at lower polymer concentration will be necessary before the soundness of this preliminary extrapolation can be evaluated. Similar experimental evidence was presented by Merrill<sup>97</sup> on polyisobutylene solutions in benzene, a poor solvent just a few degrees above the  $\Theta$ -point. Because in this case the viscosity of the solvent is not high, it must be concluded that PIB molecules in this solvent must be extremely soft, so that they easily expand. Again, the solutions were too concentrated and it could not be ascertained how much of the observed effect is due to the contribution of a single macromolecule and how much to intermolecular interaction.

The "inner viscosity" concept satisfactorily explains the observed initial change of extinction angle  $\chi$  with gradient (FIGURE 9). With sufficiently viscous solvents, Equation 33 is obtained.<sup>95,98,99</sup>

$$-(d\chi/dG)_{G=0} = B + C\eta_0 \quad (33)$$



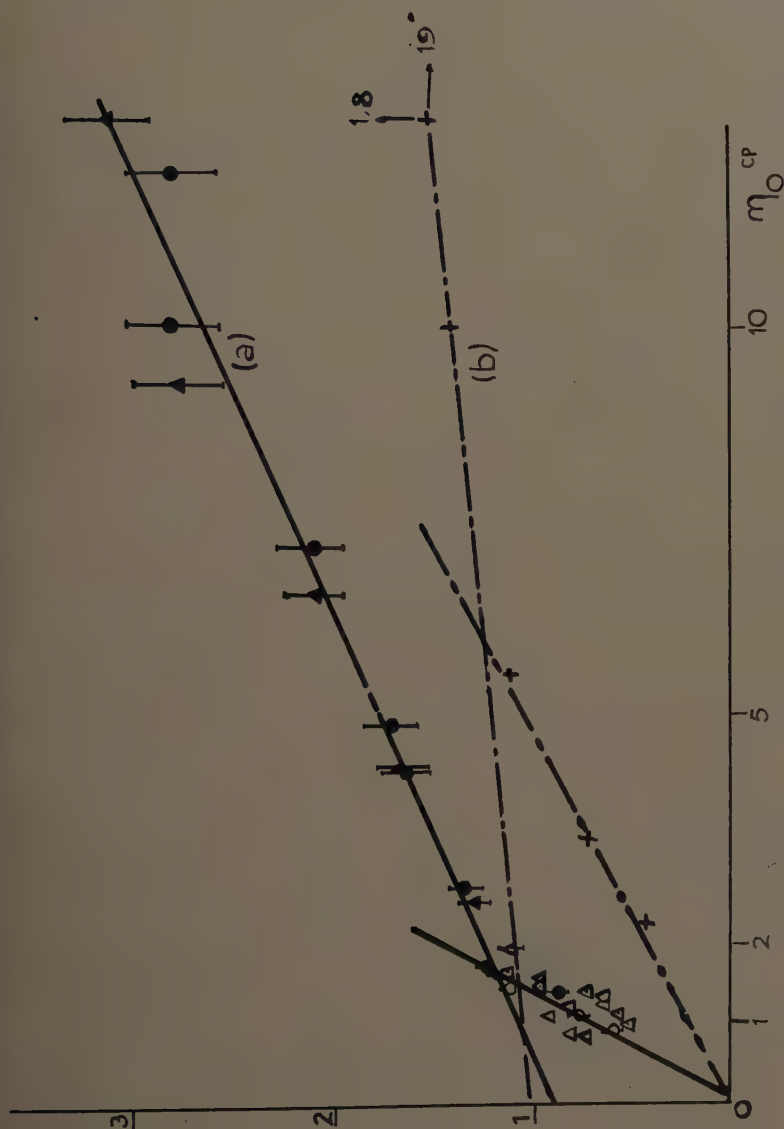


FIGURE 9.  $Tg \alpha = -(d\chi/dG)_{c=0}$  for two DNA samples (a.S. VIII, b.S. V sample of Schwander and Cerf<sup>100</sup>) over solvent viscosity  $\eta_0$  (water + glycerin). Reproduced by permission of *Journal of Polymer Science*,<sup>99</sup> Volume 23, copyright 1957 by Interscience Publishers, Inc., New York, N. Y.

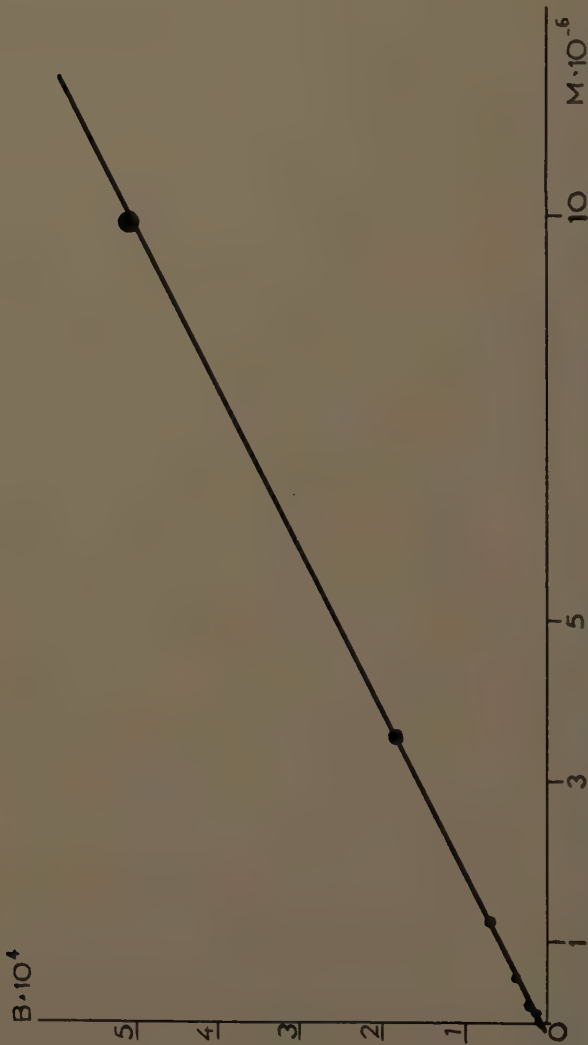


FIGURE 10. Intercept  $B$  (Equation 33) over  $M$  for different polystyrene samples.<sup>99</sup> Reproduced by permission of *Journal of Polymer Science*, Volume 23, copyright 1957 by Interscience Publishers, Inc., New York, N. Y.

The intercept  $B$  is proportional<sup>99</sup> to molecular weight of solute (FIGURE 10). When, however, the solvent viscosity is too low or the macromolecule too rigid the gradient dependence of extinction angle becomes the same as in the case of rigid particle: the coefficient  $B$  vanishes, and the curve

$$(d\chi/dG)_{G=0}$$

over  $\eta_0$  goes through the origin, the slope  $C$  being much higher than in Equation 33 with  $B \neq 0$ . Such a case occurs with deoxyribonucleic acid<sup>99,100</sup> (FIGURE 9), which is nearly rigid in water and relatively flexible in water-glycerin mixtures ( $\eta_0 > 2cP$ ). Theory<sup>99</sup> yields for not too low solvent viscosity

$$B = 0.0062FMb^2/M_0kT, \quad C = 0.2M[\eta]_0/N_AkT \begin{cases} \text{small} & \text{hydrodynamic} \\ 0.0045 & 0.1 & \text{strong} & \text{interaction} \end{cases} \quad (34)$$

and for nearly rigid particles ( $\eta_0 \rightarrow 0$ )

$$B = 0, \quad C = 0.9M[\eta]_0/N_AkT \begin{cases} \text{small} & \text{hydrodynamic} \\ 0.705 & \text{strong} & \text{interaction} \end{cases} \quad (34a)$$

*Optical interaction.* In an external electric field, the induced dipoles in the macromolecule interact and change the field value inside the coil. The interaction is proportional to the third power of inverse distance between the interacting chain dipoles. The effects are so small that in most cases they can be neglected, for example, in dielectric polarization and in light scattering when depolarization of scattered light is not in question. The effects, however, do matter in birefringence measurements where they influence the relatively small difference of main refractive indices in the oriented and deformed macromolecule.

The average over-all macromolecular configurations leading to the same end-to-end vector  $r_{1z}$  yields a nearly ellipsoidal monomer distribution instead of spherical one that results merely at vanishing end-to-end distance. As a consequence, the macromolecule exhibits a shape birefringence,<sup>101,102</sup> which according to Čopić<sup>101</sup> reads

$$(\gamma_1 - \gamma_2)_f = \theta_f h/h_0 = \frac{r}{h_0^4} \left( \frac{9M}{4\pi\rho N_A} \right)^2 \left[ \frac{n_0(n^2 - n_0^2)}{n^2 + 2n_0^2} \right]^2 \quad (35)$$

$n$  refractive index,  $\rho$  density of macromolecule. This contribution has to be added to intrinsic birefringence<sup>103</sup>

$$(\gamma_1 - \gamma_2)_i = \theta_i r^2/h_0^2 = \frac{3r^2}{5h_0^2} (\alpha_1 - \alpha_2) \quad (36)$$

$\alpha_1$ ,  $\alpha_2$  polarizability of chain segment in chain direction and perpendicular to it, in order to obtain the total optical anisotropy of macromolecular coil

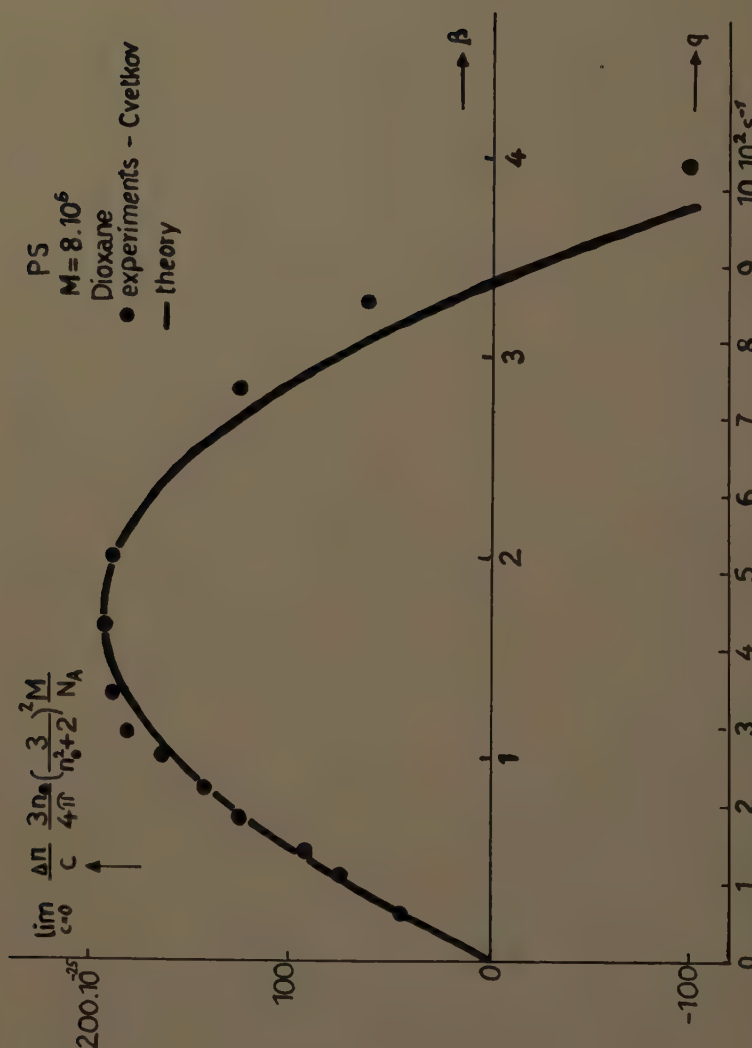


FIGURE 11. Streaming birefringence of polystyrene ( $M = 8 \cdot 10^6$ ) in dioxane as function of  $\beta$ . Experimental points from Tsvetkov *et al.*,<sup>109</sup> theoretical curve from Čopič.<sup>105</sup> Reproduced by permission of *Journal of Polymer Science*, Volume 20, copyright 1956 by Interscience Publishers, Inc., New York, N. Y.



with the end-to-end distance  $r$ . Intrinsic anisotropy may be either positive or negative depending on the optical properties of monomer unit. Form anisotropy, however, is always positive.

The resulting birefringence in laminar flow turns out to be<sup>101</sup>

$$\Delta n = (4\pi N_A/3n_0M)(n_0^2 + 2)^2\beta[0.86\theta_f + (1 + \beta^2)^{1/2}\theta_i] \quad (37)$$

The contributions of both kinds of optical anisotropy vary with the gradient or  $\beta$  in a different way. The corresponding effects are most conspicuous

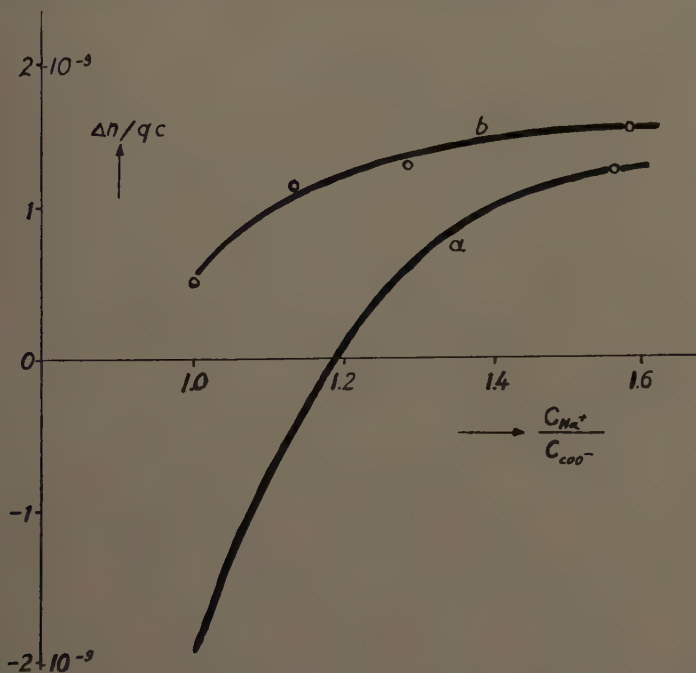


FIGURE 12. Streaming birefringence  $\Delta n/cG$  of polyacrylic acid solutions<sup>106</sup> at  $G = 19600\text{s}^{-1}$  and ionization degree 0.5 as function of added  $\text{Na}^+$ : (a) polymer concentration  $0.92 \times 10^{-3}$ ; (b)  $2.36 \times 10^{-3}$  gm./cm.<sup>3</sup> Reproduced by permission of Academic Press, Inc.<sup>110</sup>

with systems exhibiting negative intrinsic birefringence, for example, polystyrene and polyacrylic acid. In dioxane with considerable difference between  $n_0$  and  $n$  a high molecular  $PS^{104}$  ( $M = 8.10^6$ ,  $[\eta] = 930 \text{ cm.}^3/\text{gm.}$ ) yields a positive streaming birefringence at small gradient, indicating a greater absolute value of  $\theta_f$  than of  $\theta_i$  (FIGURE 11). With increasing gradient the factor  $(1 + \beta^2)^{1/2}$  lets the influence of intrinsic anisotropy prevail over that of form anisotropy. The birefringence, after reaching a maximum, drops, and becomes negative (FIGURE 11). From experimental data the values  $\theta_f = 312.10^{-25} \text{ cm.}^3$ ,  $\theta_i = -78.10^{-25} \text{ cm.}^3$ ,  $\alpha_1 - \alpha_2 = -130.10^{-25} \text{ cm.}^3$  may be calculated.<sup>105</sup>

As a consequence of contribution of form anisotropy the initial specific streaming birefringence

$$\left( \frac{\Delta n}{C n_0 \eta_0 G} \right)_{G=0} = \frac{4\pi}{3} \left( \frac{n_0^2 + 2}{3n_0} \right)^2 \frac{[\eta]}{kT} (0.86 \theta_f + \theta_i) \quad (38)$$

changes with shape of macromolecular coil or/and with the solvent. The first case is easily observable with polyelectrolytes in which added salt

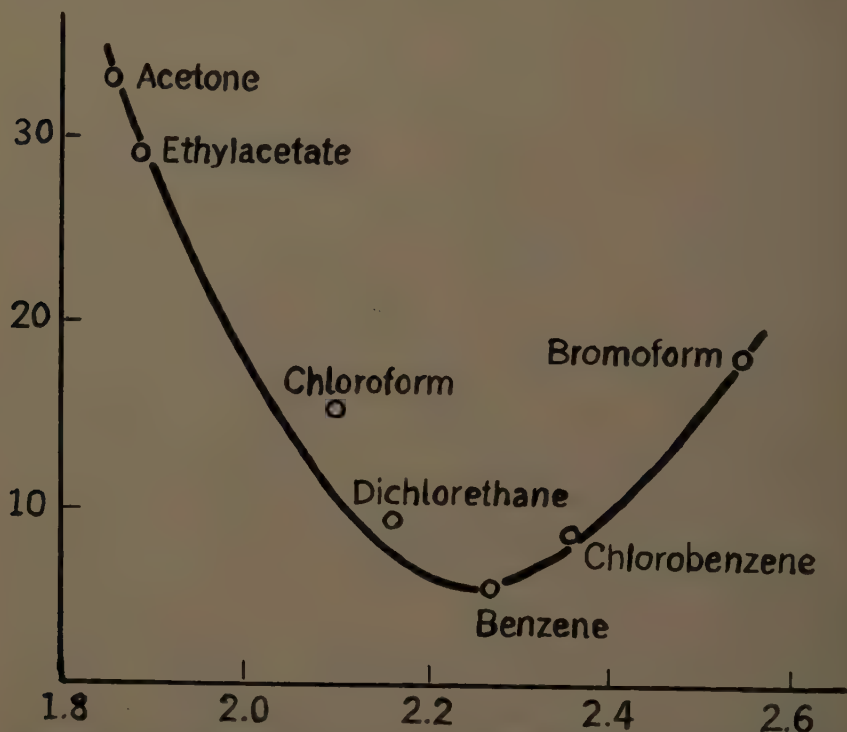


FIGURE 13. The birefringence  $\Delta n/cg$  at  $G = 1000s^{-1}$  for polymethylmethacrylate in several solvents of different index of refraction.<sup>108</sup> Reproduced by permission of Academic Press, Inc.<sup>111</sup>

increases the ionic strength, by electrostatic shielding reduces the repulsive forces in the coil, and hence reduces its size. Polyacrylic acid in water solution<sup>106</sup> changes the sign of birefringence from negative to positive with increased  $Na^+$  concentration (FIGURE 12). At low salt concentration, the coil is rather extended so that the negative intrinsic birefringence prevails. With more added salt the coil contracts,  $\theta_f$  increases rapidly due to the factor  $h_0^{-3}$  and results in positive streaming birefringence.

The theory also satisfactorily explains the solvent effect,<sup>107-109</sup> yielding a nearly parabolic curve for  $(\Delta n/cn_0\eta_0G)_{G=0}$  plotted over  $n_0^2$  (FIGURE 13). In the case of negative intrinsic anisotropy, the birefringence van-

ishes for two distinct values of solvent refractive index. The agreement in most cases is fairly good. However, some effects of molecular weight on gradient dependence of streaming birefringence<sup>109</sup>—the sign change in the system polystyrene–dioxane occurs at higher  $\beta$  with lower molecular weight—cannot be explained by Equation 37, which does not consider the partial coil rigidity and the limitations of coil extensibility by the requirement that the r.m.s. end-to-end distance must be always smaller than the extended length of the macromolecule. Exactly the same situation occurs with the gradient dependence of intrinsic viscosity.<sup>89,91-94</sup>

### References

1. PETERLIN, A. 1958. Reports J. Stefan Inst. Yugosl. **5**: 61.
2. PTITSYN, O. B. 1959. Uspekhi Fiz. Nauk. **69**(3): 371.
3. EYRING, H. 1932. Phys. Rev. **39**: 746.
4. BRINI, M. & H. BENOIT. 1955. Ricerca sci. **25**(Suppl.): 543.
5. KRATKY, O. & G. POROD. 1949. Rec. Trav. Chim. **68**: 1106.
- 5a. POROD, G. 1949. Monatsh. Chem. **9**: 244.
6. KUHN, W. & H. KUHN. 1943. Helv. Chim. Acta. **26**: 1394.
7. DEBYE, P. 1947. J. Appl. Phys. **15**: 338.
8. PETERLIN, A. 1955. J. Colloid Sci. **10**: 587.—Makromol. Chem. **18/19**: 254.
9. CIFERRI, A. & M. LAURETTI. 1958. Ann. Chim. (Rome). **48**: 198.
10. NEWMAN, S., W. KRIGBAUM, C. LANGIER & P. FLORY. 1954. J. Polymer Sci. **14**: 451.
11. SHULTZ, A. 1954. J. Am. Chem. Soc. **76**: 3422.
12. KUNST, E. 1950. Rec. Trav. Chim. **69**: 125.
13. KRIGBAUM, W. & P. FLORY. 1953. J. Polymer Sci. **11**: 371.
14. BOYES, A. & P. STRAUSS. 1956. J. Polymer Sci. **22**: 463.
15. FOX, T., JR. & P. FLORY. 1951. J. Am. Chem. Soc. **73**: 1909.
16. BAWN, C. & R. PATEL. 1956. Trans. Faraday Soc. **52**: 1669.
17. CANTOW, H. & O. BODMANN. 1955. Z. physik. Chem. **3**: 65.
18. CHINAI, S., J. D. MATLACK, A. J. RESNICK & R. J. SAMUELS. 1955. J. Polymer Sci. **17**: 391; CHINAI, S. & C. BONDURANT. 1956. J. Polymer Sci. **22**: 555.
19. SCHULZ, G. V. & R. KIRSTE. In press.
20. CHINAI, S. & R. SAMUELS. 1956. J. Polymer Sci. **19**: 463.
21. CHINAI, S. & R. GUZZI. 1956. J. Polymer Sci. **21**: 417.
22. DIDOT, F. E., S. CHINAI & D. W. LEVI. 1960. J. Polymer Sci. **43**: 557.
23. CHINAI, S. 1957. J. Polymer Sci. **33**: 471.
24. CHINAI, S., A. RESNICK & H. LEE. 1958. J. Polymer Sci. **33**: 471.
- 24a. CHINAI, S. & R. GUZZI. 1959. J. Polymer Sci. **41**: 475.
25. FLORY, P., L. MANDELKERN, J. KINSINGER & W. SHULTZ. 1952. J. Am. Chem. Soc. **74**: 3364.
26. WAGNER, H. & P. FLORY. 1952. J. Am. Chem. Soc. **74**: 195.
27. BRESLER, S. E. & J. FRENKEL. 1939. Acta Physicochim. USSR. **11**: 485.
28. PTITSYN, O. B. & J. A. SHARANOW. 1957. Zhur. Tekh. Fiz. **27**: 2744, 2762.
- 28a. LIFSON, S. 1958. J. Chem. Phys. **29**: 80; 1959. J. Chem. Phys. **30**: 964.
29. DOTY, P. 1957. Collection Czechoslov. Chem. Commun. **22**: 5.
30. REICHMAN, M. E., S. A. RICE, C. A. THOMAS & P. DOTY. 1954. J. Am. Chem. Soc. **76**: 3407.
- 30a. PETERLIN, A. 1953. J. Polymer Sci. **10**: 425; Makromol. Chem. **9**: 244; Nature. **171**: 259.
31. THOMAS, A. 1954. Biochim. Biophys. Acta. **14**: 231.
32. BIERSTEIN, T. M. & O. B. PTITSYN. 1959. Zhur. Tekh. Fiz. **29**: 1048.
33. KRIGBAUM, W., D. CARPENTER & S. NEWMAN. 1958. J. Phys. Chem. **62**: 1586.
34. LIFSON, S. 1958. J. Chem. Phys. **29**: 89.
35. GOTLIEB, YU. YA., M. V. VOLKENSTEIN & E. K. BUETNER. 1954. Doklady Akad. Nauk SSSR. **49**: 935.
36. FATTACHOV, K. Z. 1954. Zhur. Tekh. Fiz. **24**: 1401.
37. MARCHAL, J. & H. BENOIT. 1955. J. chim. phys. **52**: 818.
38. MARCHAL, J. & C. LAPP. 1958. J. Polymer Sci. **27**: 571.
39. DEBYE, P. & F. BUECHE. 1951. J. Chem. Phys. **19**: 589.

40. MARCHAL, J. & H. BENOIT. 1957. *J. Polymer Sci.* **23**: 223.
41. BIERSTEIN, L. L. & G. P. MIHAILOV. 1957. *Zhur. Tekh. Fiz.* **27**: 694.
42. MARCHAL, J., C. WIPPLER & H. BENOIT. 1955. *Compt. rend.* **241**: 1266.
43. POROD, G. 1953. *J. Polymer Sci.* **10**: 157.
44. KRATKY, O. & H. SEMBACH. 1956. *Makromol. Chem.* **18/19**: 463; KRATKY, O. & R. BREINER. 1957. *Makromol. Chem.* **25**: 134.
45. PETERLIN, A. *J. Polymer Sci.* In press.
46. TSVETKOV, V. N., V. E. BYCHKOVA, S. M. SAVVON & I. K. NEKRASOV. 1959. *Vysokomolekulyarnye Soedineniya*. **1**: 1407.
47. SCHULZ, G. V. & G. MEYERHOFF. 1953. *J. Polymer Sci.* **10**: 79.
48. MEYERHOFF, G. 1953. *J. Polymer Sci.* **29**: 399.
49. NOTLEY, N. & P. DEBYE. 1955. *J. Polymer Sci.* **17**: 99.
50. BUECHE, F. 1953. *J. Chem. Phys.* **21**: 205.
51. YAMAKAWA, H. & M. KURATA. 1958. *J. Phys. Soc. Japan*. **13**: 78.
52. WALL, F. T. & J. MAZUR. 1960. *Am. Phys. Soc. Meeting*. Detroit, Mich.
53. PETERLIN, A. 1948. *Internat. Congr. Les grosses molécules en solutions*. Paris: 70; 1950. *Diss. Acad. Ljubljana (3A)* **1**: 77.
54. FLORY, P. 1949. *J. Chem. Phys.* **17**: 303; FLORY, P. & T. FOX, JR. 1950. *J. Polymer Sci.* **5**: 745; *J. Am. Chem. Soc.* **73**: 1904; OROFINO, T. & P. FLORY. 1957. *J. Chem. Phys.* **26**: 1067.
55. TERAMOTO, E. 1951. *Busseiron Kenkyu*. **39**: 1; **40**: 18; **41**: 14; **42**: 24.
- 55a. YAMAMOTO, M., M. MATZUDA & E. TERAMOTO. 1951. *Busseiron Kenkyu*. **39**: 14.
- 55b. YAMAMOTO, M. 1951. *Busseiron Kenkyu*. **44**: 36.
- 55c. TERAMOTO, E. & M. YAMAMOTO. 1952. *Busseiron Kenkyu*. **47**: 18.
- 55d. MATSUDA, H. 1952. *Busseiron Kenkyu*. **51**: 46.
- 55e. FLORY, P. (Summary in English). 1954. *J. Polymer Sci.* **14**: 1.
56. GRIMLEY, B. 1953. *J. Chem. Phys.* **21**: 185.
57. JAMES, H. M. 1953. *J. Chem. Phys.* **21**: 1628.
58. ZIMM, B. H., W. H. STOCKMAYER & M. FIXMAN. 1953. *J. Chem. Phys.* **21**: 1716.
- 58a. SAITO, N. 1954. *J. Phys. Soc. Japan*. **9**: 780.
59. FIXMAN, M. 1955. *J. Chem. Phys.* **23**: 1656.
60. ISIHARA, A. & R. KOYAMA. 1956. *J. Chem. Phys.* **25**: 712.
61. ALBRECHT, A. 1958. *J. Chem. Phys.* **27**: 1002.
62. KURATA, M., H. YAMAKAWA & E. TERAMOTO. 1958. *J. Chem. Phys.* **28**: 785.
- 62a. KURATA, M., H. YAMAKAWA & H. UTIYAMA. 1959. *Makromol. Chem.* **34**: 139.
63. STOCKMAYER, W. H. *Lecture on the Inter. Macromol. Symposium*. 1959. Wiesbaden, Germany.
64. CASSASSA, E. F. & H. MARKOWITZ. 1958. *J. Chem. Phys.* **29**: 311.
65. PTITSYN, O. B. 1959. *Vysokomolekulyarnye Soedineniya*. **1**: 785.
66. PTITSYN, O. B. & YU. YE. EISNER. 1959. *Vysokomolekulyarnye Soedineniya*. **1**: 1200.
67. KURATA, M., W. H. STOCKMAYER & A. ROIG. 1960. *Am. Chem. Soc. Meeting*. Cleveland, Ohio.
68. PETERLIN, A. 1955. *J. Chem. Phys.* **23**: 2464.
69. PTITSYN, O. B. 1957. *Zhur. Tekh. Fiz.* **31**: 1091.
70. BENOIT, H. 1957. *Compt. rend.* **245**: 2244.
71. LOUCHEUX, C., G. WEILL & H. BENOIT. 1958. *J. chim. phys.* **55**: 540.
72. HYDE, A., J. RYAN & F. T. WALL. 1958. *J. Polymer Sci.* **33**: 129; PTITSYN, O. B. & YU. YE. EISNER. 1959. *Vysokomolekulyarnye Soedineniya*. **1**: 966.
73. PETERLIN, A. 1957. *Collection Czechoslov. Chem. Commun.* **22**: 84.
- 73a. HARRIS, F. E. & S. A. RICE. 1954. *J. Phys. Chem.* **58**: 725.
- 73b. RICE, S. A. & F. E. HARRIS. 1954. *J. Phys. Chem.* **58**: 733.
74. WALL, F. T. & J. BERKOWITZ. 1957. *J. Chem. Phys.* **26**: 114.
- 74a. WALL, F. T., J. A. COTE & S. M. RUCKER. 1959. *J. Chem. Phys.* **31**: 1640.
75. EISENBERG, H. & E. F. CASSASSA. 1960. *Am. Chem. Soc. Meeting*. Cleveland, Ohio.
76. HERMANS, J. J. & J. T. G. OVERBECK. 1948. *Bull. soc. chim. Belges*. **57**: 154; *Rec. Trav. Chim.* **67**: 761.
77. KUHN, W., O. KÜNZLE & A. KATCHALSKY. 1948. *Helv. Chim. Acta*. **31**: 1994; *Bull. soc. chim. Belges*. **57**: 421.
- 77a. KÜNZLE, O. 1949. *Rec. Trav. Chim.* **68**: 699.
- 77b. KATCHALSKY, A., O. KÜNZLE & W. KUHN. 1950. *J. Polymer Sci.* **5**: 283.
- 77c. KATCHALSKY, A. & S. LIFSON. 1953. *J. Polymer Sci.* **11**: 409.
- 77d. KIMBALL, G. E., M. CUTLER & M. SAMUELSON. 1952. *J. Phys. Chem.* **56**: 57.



- 77e. FLORY, P. J. 1953. *J. Chem. Phys.* **21**: 162.  
77f. OSAWA, F., N. IMAI & I. KAGAWA. 1954. *J. Polymer Sci.* **13**: 93.  
77g. KRIEGER, I. M. 1955. *J. Chem. Phys.* **26**: 1.  
77h. FISHER, M. E. 1958. *J. Chem. Phys.* **28**: 756.  
78. PETERLIN, A. 1959. *Makromol. Chem.* **34**: 89.  
79. KUHN, H. & W. KUHN. 1947. *Helv. Chim. Acta.* **30**: 1233.  
79a. KUHN, H. & W. KUHN. 1948. *J. Chem. Phys.* **16**: 838.  
79b. KUHN, H. & W. KUHN. 1950. *J. Polymer Sci.* **5**: 519.  
79c. KUHN, H. & W. KUHN. 1952. *J. Polymer Sci.* **9**: 1.  
79d. KUHN, H. 1950. *J. Colloid Sci.* **5**: 331.  
79e. KUHN, H., W. KUHN & A. SILBERBERG. 1953. *J. Polymer Sci.* **10**: 79.  
80. KIRKWOOD, J. G. & J. RISEMAN. 1948. *J. Chem. Phys.* **16**: 565.  
80a. KIRKWOOD, J. G., R. W. ZWANZIG & R. J. PLOCK. 1955. *J. Chem. Phys.* **23**: 213.  
80b. AUER, P. L. & C. S. GARDNER. 1955. *J. Chem. Phys.* **23**: 1545.  
81. PETERLIN, A. 1950. *Diss. Acad. Ljubljana (3A)*. **1**: 39; also *J. Polymer Sci.* **5**: 473.  
82. ZIMM, B. H. 1956. *J. Chem. Phys.* **24**: 269.  
83. MARRIMAN, H. & J. J. HERMANS. 1960. *Am. Chem. Soc. Meeting. Cleveland, Ohio*.  
84. PETERLIN, A. & M. ČOPIČ. 1956. *J. Appl. Phys.* **27**: 434.  
85. KRAMERS, H. A. 1946. *J. Chem. Phys.* **14**: 415.  
86. ROUSE, P. E. 1953. *J. Chem. Phys.* **21**: 1272.  
87. IKEDA, Y. 1957. *J. Phys. Soc. Japan*. **12**: 378.  
88. PETERLIN, A., W. HELLER & M. NAKAGAKI. 1958. *J. Chem. Phys.* **28**: 470.  
89. PETERLIN, A. *J. Chem. Phys.* In press.  
89a. PETERLIN, A. *Makromol. Chem.* In press.  
90. ČOPIČ, M. 1957. *J. chim. phys.* **54**: 348.  
90a. ČOPIČ, M. 1956. *J. chim. phys.* **53**: 440.  
91. KUHN, W. & H. KUHN. 1945. *Helv. Chim. Acta.* **28**: 1533; also 1946. *Helv. Chim. Acta.* **29**: 71.  
92. GOTTLIEB, YU. YA. & M. V. VOLKENSTEIN. 1953. *Zhur. Tekh. Fiz.* **23**: 1936.  
93. VAN BECK, L. H. J. 1955. *Thesis. Leiden, Germany*.  
94. CERF, R. 1958. *J. Phys. Radium*. **19**: 122.  
95. CERF, R. 1956. *Compt. rend.* **243**: 1875.  
96. SELBY, T. W. 1960. *ASTM Symposium on Non-Newtonian Viscometry. Washington, D. C.*  
97. MERRILL, E. W. 1960. *ASTM Symposium on Non-Newtonian Viscometry. Washington, D. C.*  
98. CERF, R. 1950. *J. chim. phys.* **47**: 663.  
99. LERAY, J. 1957. *J. Polymer Sci.* **23**: 167.  
100. SCHWANDER, H. & R. CERF. 1953. *Helv. Chim. Acta.* **34**: 436.  
101. ČOPIČ, M. 1953. *Bull. Sci. Conseil Acad. RPF. Yougoslavie*. **1**: 103; also 1957. *J. Chem. Phys.* **26**: 1382.  
102. TSVETKOV, V. N. & E. V. FRISMAN. 1954. *Doklady Akad. Nauk SSSR*. **97**: 647; TSVETKOV, V. N. 1955. *Ricerca sci.* **25A**: 413; TSVETKOV, V. N., E. V. FRISMAN, O. B. PITTSYN & S. T. KOTLIAR. 1958. *Zhur. Tekh. Fiz.*  
103. KUHN, W. & F. GRÜN. 1942. *Kolloid Z.* **101**: 248.  
104. CVETKOV, V. N. 1955. *Chem. listy*. **49**: 1419; FRISMAN, E. V. & V. N. TSVETKOV. 1956. *Doklady Akad. Nauk SSSR*. **106**: 42.  
105. ČOPIČ, M. 1956. *J. Polymer Sci.* **20**: 593.  
106. KUHN, W., H. OSWALD & H. KUHN. 1953. *Helv. Chim. Acta.* **36**: 1209.  
107. SIGNER, R. 1930. *Z. physik. Chem.* **150A**: 257; SIGNER, R. & H. GROSS. 1933. *Z. physik. Chem.* **165A**: 161.  
108. TSVETKOV, V. N. & A. J. PETROVA. 1944. *Zhur. Tekh. Fiz.* **14**: 289; also 1949. *Zhur. Fiz. Khim.* **23**: 368; also 1950. *Zhur. Fiz. Khim.* **24**: 992.  
108a. TSVETKOV, V. N. & E. V. FRISMAN. 1945. *Acta Physicochim. USSR*. **20**: 61, 363. 1946. *Acta Physicochim. USSR*. **21**: 978. 1947. *Zhur. Fiz. Khim.* **21**: 261.  
108b. TSVETKOV, V. N., E. V. FRISMAN & L. S. MUCHINA. 1956. *Zhur. Eksp. Teor. Fiz.* **30**: 449.  
109. FRISMAN, E. V. & V. N. TSVETKOV. 1958. *J. Polymer Sci.* **30**: 297.  
110. PETERLIN, A. 1956. *Rheology I. Academic Press, New York, N. Y.* p. 631, Fig. 11.  
111. *Ibid.* p. 638, Fig. 15.

# STATISTICAL THERMODYNAMICS OF COILING-TYPE POLYMERS\*

Frederick T. Wall and Jacob Mazur†

*Noyes Chemical Laboratory, University of Illinois, Urbana, Ill.*

## *Introduction*

During recent years a considerable amount of work has been carried out on the thermodynamics of coiling-type polymer molecules.<sup>1,2</sup> From a statistical point of view, one of the important considerations deals with the over-all dimensions of such molecules, taking into account the fact that any given molecule can assume numerous configurations. An appreciable amount of statistical work, including Monte Carlo-type calculations using high speed computers, has been directed toward establishing the mean square end-to-end separations of flexible polymer chains. This Monte Carlo-type work has been carried out by generating nonintersecting random walks in various lattice systems.<sup>3,4</sup>

The model assumed for the nonintersecting random walks, in which double occupancy of any site is forbidden, implies an infinite potential energy when two elements of the chain are superimposed. It was also tacitly assumed, in the work carried out heretofore, that the potential energy was constant (for example, zero) for all configurations except those involving double occupancy. Thus two values for the intrachain interaction energies were implied, infinity and zero.

In this paper we shall report the results of carrying out somewhat more elaborate calculations, assuming a potential energy function different from that implicit in the earlier Monte Carlo-type calculations. As before, we shall stipulate that double occupancy, or approaches within a certain specified short distance, will correspond to infinite energy. We shall further assume that there will be a short range of intrachain element separations, just outside the above-mentioned excluded range, for which there will be a finite energy of interaction different from zero. Finally, for intrachain element separations beyond the range of nonzero finite interaction energies, we shall assume that the energies are zero. In this way our model becomes slightly more sophisticated than before, because we now assume three (instead of two) possible interaction energies, namely, infinity, a constant different from zero, and zero. This does not mean, of course, that the energy of a given molecule cannot assume more than three values. Actually the energy of a molecule will range from zero (for an extended configuration) to an upper or lower bound (depending upon the sign of the finite interaction term) for molecules that are tightly coiled. To establish the

\* The investigation reported in this paper was supported in part by a research grant from the National Science Foundation, Washington, D.C.

† Present address: National Bureau of Standards, Washington, D.C.

potential energy of a molecule, it is necessary only to count the number of intrachain interactions with energies different from zero that occur in a given configuration. The use of this model should introduce some interesting new features into the problem of coiling-type polymer dimensions. In particular, it should provide a means of learning more about the effect of temperature on the size and shape of molecules.

At this juncture, we should point out that if the intrachain interactions were restricted to near-contour neighbors only, an analytic solution of the problem might be obtained through consideration of Markoff chains. A solution of this problem was attempted by Montroll,<sup>5</sup> who treated random walks in a two-dimensional 90° lattice with exclusions limited to loops of four steps. Various other mathematical procedures have been adopted by a number of authors to deal with the problem of configurations of real polymers subject to interaction energies. However, these mathematical treatments are not only complex, but they involve serious approximations, the validities of which cannot be readily checked. The simplified problem of configurations of coiling chains subject to the excluded volume effect belongs to this category of problems for, as indicated above, the excluded volume concept can always be regarded as corresponding to hard sphere interaction potentials between the elements of a polymer chain.

The computations were carried out in the following way. As with the earlier Monte Carlo work, we generated random walks in various lattice systems, rejecting those walks involving either double occupancy of lattice sites or, in some instances, approaches within a finite distance such as those corresponding to nearest-neighbor sites. In addition, we counted the number of intrachain approaches lying in a specified middle-distance range. Having counted the number of such interactions, each of which would contribute to the molecule a finite amount of energy different from zero, it was possible to classify the configuration by its energy value. All this work was carried out using the Illiac, a high-speed digital computer, at the University of Illinois.

### *Theory*

In the following discussion, we shall assume that the polymer chain consists of  $n$  links or  $n + 1$  chain elements. A given polymer configuration will be characterized by its end-to-end separation,  $r_n$ , and by a number,  $z$ , which equals the number of intrachain interactions corresponding to the afore-mentioned intermediate distance range with potential energy of interaction,  $\epsilon$ . The total potential energy of such a molecule will therefore be  $z\epsilon$ , and the partition function for the system will be given by

$$Q = \sum_z N_z \exp(-z\epsilon/kT) \quad (1)$$

where  $N_z$  is the number of ways a molecule can exhibit configurations with

$z$  interactions of the type specified (for our purpose, we shall let  $N_z$ , which also depends on  $n$ , equal the number of samples found by the Monte Carlo technique).

Expressions may now be written for certain average physical properties. For example, the mean square end-to-end separation will be

$$\langle r_n^2 \rangle = \frac{\sum_z \langle r_n^2 \rangle_z N_z \exp(-z\epsilon/kT)}{Q} \quad (2)$$

where  $\langle r_n^2 \rangle_z$  is the mean square end-to-end separation of molecules with  $z$  interactions.

The average energy,  $\langle E \rangle$ , will equal  $\langle z \rangle \epsilon$  and will be given by

$$\begin{aligned} \langle E \rangle = \langle z \rangle \epsilon &= \frac{\sum_z z \epsilon N_z \exp(-z\epsilon/kT)}{Q} \\ &= kT^2 \frac{\partial \ln Q}{\partial T} \end{aligned} \quad (3)$$

The free energy will, of course, be given by

$$F = -kT \ln Q \quad (4)$$

and the thermodynamic potential associated with a chain element (or "partial-link" free energy) will be

$$\begin{aligned} \mu = \frac{\partial F}{\partial n} &= -kT \frac{\partial \ln Q}{\partial n} \\ &= \frac{-kT}{Q} \sum_z \frac{\partial N_z}{\partial n} \exp(-z\epsilon/kT) \end{aligned} \quad (5)$$

### Computations

Our Monte Carlo calculations, performed on a high-speed computer, all involved random walks that were carried out, subject to appropriate rules, in several different lattice systems, both in two and in three dimensions. Six different sets of computations were carried out, four of them in two-dimensional lattices and two in three-dimensional lattices. The essential characteristics of these lattices and the distance ranges to be associated with intramolecular interaction energies are summarized in TABLE 1. The first two entries ( $a$ ,  $b$ ) deal with walks in the two-choice square lattice, the second involving a wider range of distances associated with the finite energy of interaction. The third and fourth entries ( $c$  and  $d$ ) both deal with walks in the two-choice hexagonal plane lattice, once again with interaction energies identified with different distance ranges. The fifth entry ( $e$ ) deals with walks in the four-choice ( $90^\circ$  bond angle) three-dimensional simple cubic lattice. The last ( $f$ ) deals with the three-choice tetrahedral lattice.



The columns in TABLE 1 are, for the most part, self-explanatory. The next to the last column, "Possible number of intermediate neighbors," is essentially a type of coordination number applicable to interior points of a chain. Because of the constraints imposed, an interior point in a walk of type *c*, for example, can have only one intermediate neighbor, not counting those that must lie within the specified range because of the continuous contour of the chain (the end point of a *c*-type chain can have two intermediate-range neighbors). For each entry, the last column denotes the initial number of samples, subject to attrition, employed in the calculations.

For all the computations we assumed the step lengths or distances between adjacent lattice sites to equal unity. Some of the random walks (those designated *c*, *e*, and *f* in TABLE 1) were generated by using the simple techniques employed in the earliest studies carried out in this laboratory.<sup>3,4</sup> This procedure consisted essentially of generating a string of unit vectors,

TABLE 1

Designation	No. of dimensions	Bond angle	No. of lattice choices	Excluded range ( $\epsilon_{ij} = \infty$ )	Intermediate range ( $\epsilon_{ij} = e \neq 0$ )	Outer range ( $\epsilon_{ij} = 0$ )	Possible No. of intermediate neighbors	<i>N</i>
<i>a</i>	2	90°	2	$0 < r_{ij} < 1$	$1 < r_{ij} < \sqrt{2}$	$\sqrt{2} < r_{ij} < \infty$	2	200,000
<i>b</i>	2	90°	2	$0 < r_{ij} < 1$	$1 < r_{ij} < 2$	$2 < r_{ij} < \infty$	4	200,000
<i>c</i>	2	120°	2	$0 < r_{ij} < 1$	$1 < r_{ij} < \sqrt{3}$	$\sqrt{3} < r_{ij} < \infty$	1	50,000
<i>d</i>	2	120°	2	$0 < r_{ij} < 1$	$1 < r_{ij} < 2$	$2 < r_{ij} < \infty$	5	60,000
<i>e</i>	3	90°	4	$0 < r_{ij} < 1$	$1 < r_{ij} < \sqrt{2}$	$\sqrt{2} < r_{ij} < \infty$	4	100,000
<i>f</i>	3	Tetrahedral	3	$0 < r_{ij} < 1$	$1 < r_{ij} < 2$	$2 < r_{ij} < \infty$	16	220,000

which in the aggregate would represent a molecular chain. The individual vectors were chosen by a pseudorandom number technique and, after each selection of an additional vector, the chain was tested to make sure that the last-added vector did not terminate on a site already occupied. When such exclusion was encountered, the sample was rejected and a new chain was begun. Other walks (designated *a*, *b*, and *d* in TABLE 1) were generated by the "stride" technique described by Wall *et al.*<sup>6</sup>

In carrying out the computations it was necessary to count the number of intrachain interactions falling within the prescribed intermediate range. Once the value of the interaction energy has been fixed, this count determines the energy of the chain. From this it is easy to establish the partition function and the other derived quantities by making use of Equations 1 through 5.

The results of the calculations here reported are limited to values of  $n < 60$ . Collection of statistical data for polymers with a greater number of steps was seriously limited by time considerations for the following reasons: (1) the number of tests that the computer must perform to check all

possible intralattice distances corresponding to nonzero interaction energies is of the order of  $n^2$ ; (2) the rejection of random walks with double occupancies seriously diminishes the computer yield of chains with a large number of steps (the procedure of Wall and Erpenbeck<sup>7</sup> for chain enrichment had not been fully developed when the present work was done); and (3) the spread of possible end-to-end distances increases rapidly with increasing  $n$ , and more data are required for large  $n$  to eliminate excessive scattering of the data.

The data have all been analyzed through further computations involving the use of Equations 2 and 4. The reliability of the data diminishes as we depart from values of  $\epsilon = 0$ , because the relative weights of the samples are changed. For positive values of  $\epsilon$ , smooth graphs can be obtained with  $\epsilon$  less than  $0.75 kT$  for small  $n$ . However, for  $\epsilon > 0.5 kT$  there is serious scattering of data when  $n$  is greater than 40.

For model polymer chains with negative values of  $\epsilon$ , we could not extend our calculations much below  $\epsilon = -0.5 kT$  because of the scattering of the results. The lowest value of  $\epsilon$  that still yields reliable results depends very strongly on the maximal number of intermediate-range neighbors and on the maximal number of choices in the propagation of the random walk. The reason for this lies in the fact that coiled molecules will be identified with high Boltzmann weight factors even when the coiled molecules correspond to configurations whose yield from the computer is small.

### Discussion

The results of our computations are presented in graphical form. In FIGURES 1 and 2 are plotted the quotient of the mean square end-to-end separation,  $\langle r_n^2 \rangle$ , by the number of steps,  $n$ , as a function of  $n$ . The curves in FIGURE 1 refer to two-dimensional walks carried out in the two-choice ( $90^\circ$  bond angle) square lattice, designated *a* in TABLE 1. The several curves in FIGURE 1 correspond to different values of the parameter  $\epsilon/kT$ . It will be observed that as  $\epsilon/kT$  increases the afore-mentioned quotient increases for a given value of  $n$ . This, of course, is to be expected since a repulsive potential will tend to elongate the molecules. For negative values of  $\epsilon/kT$ , the chains become more compact relative to the simple models that exclude double occupancy but for which  $\epsilon = 0$ . It will be further observed that none of the curves in FIGURE 1 exhibits values of the ordinate less than unity, for reasons discussed below.

FIGURE 2 is a similar graph for four-choice ( $90^\circ$  bond angle) restricted walks carried out in a simple cubic three-dimensional lattice. Qualitatively, the considerations cited with respect to the two-dimensional system described above are once again valid, except that when  $\epsilon/kT$  is sufficiently negative the values of  $\langle r_n^2 \rangle/n$  can be less than unity. As a matter of fact, when  $\epsilon/kT = -0.50$  the function  $\langle r_n^2 \rangle/n$  appears to be constant and equal

to unity for all values of  $n$ . This is an interesting phenomenon, corresponding to what is observed when the pressure-volume product of a nonideal gas is plotted against pressure at various temperatures. At low-enough temperatures, the slopes of such curves are negative, whereas at high temperatures they are positive. At a particular temperature, known as the Boyle temperature,  $pV$  is constant. In precisely the same way,  $\langle r_n^2 \rangle/n$  is constant at what is substantially the Flory  $\Theta$  temperature<sup>8</sup> which, for our simple

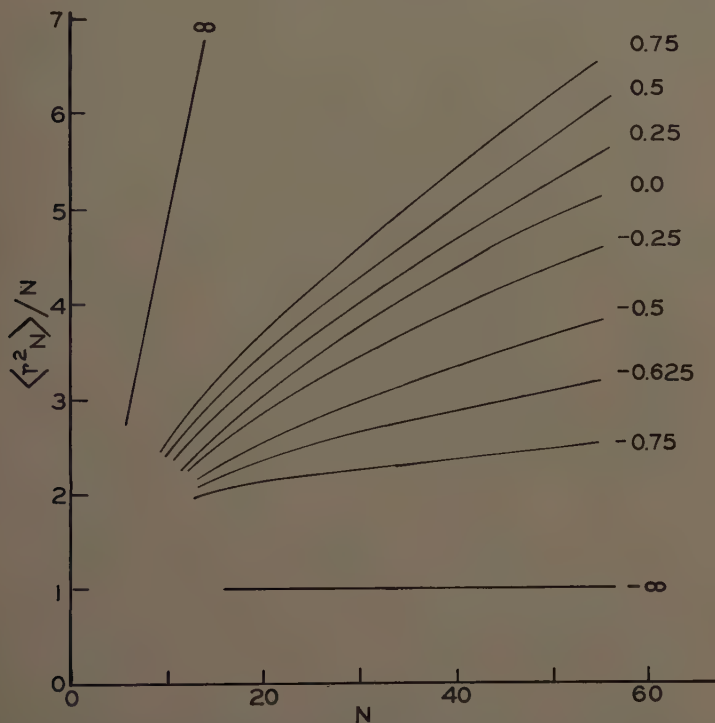


FIGURE 1. Graphs of  $\langle r_n^2 \rangle/n$  versus  $n$  for chains with 90° bond angles in the two-dimensional square lattice (designation  $a$  in TABLE 1) for various values of  $\epsilon/kT$  indicated next to curves.

three-dimensional model, would equal  $-\epsilon/0.50k$ . At such a temperature, the attractive forces just compensate the hard-sphere repulsions that are implied by exclusion of double occupancy.

At this point, it may properly be asked why no theta temperature is observed for the two-dimensional model while it shows up in the three-dimensional model. The reason is clear from simple geometrical considerations. In two dimensions, the most tightly packed molecule would correspond roughly to a spiral with an area proportional to  $\langle r_n^2 \rangle$ . This same area would also be substantially equal to  $n$ , the number of points in the chain,

assuming unit distances between points in a square lattice. Hence  $\langle r_n^2 \rangle / n$  would be constant in two dimensions for the most tightly packed form of molecule. Such a molecular state could be realized at finite temperatures only if the attractive potential were infinite. Alternatively, for a finite

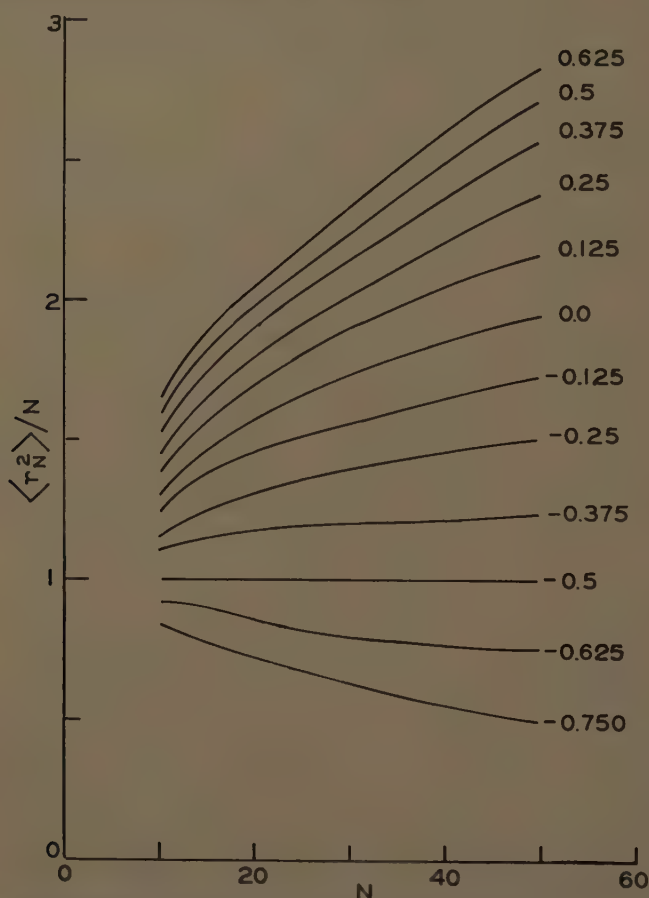


FIGURE 2. Graphs of  $\langle r_n^2 \rangle / n$  versus  $n$  for chains with 90° bond angles in the three-dimensional simple cubic lattice (designation  $\epsilon$  in TABLE 1) for various values of  $\epsilon/kT$  indicated next to curves.

attractive potential, the two-dimensional, closely packed spiral could exist only at absolute zero (one could therefore say that absolute zero is the theta temperature for a two-dimensional polymer). In three dimensions the situation is somewhat different. The most closely packed random coil would be like a tight ball of yarn with volume proportional to  $\langle r_n^2 \rangle^{3/2}$ . The volume of this sphere would likewise be substantially equal to  $n$ , the number of lattice sites occupied in a simple cubic lattice. This would imply



that  $\langle r_n^2 \rangle$  is proportional to  $n^{2/3}$  and hence that  $\langle r_n^2 \rangle/n$  is proportional to  $n^{-1/3}$ , indicating that with an infinite attractive potential the quotient that has been plotted would diminish with increasing  $n$ . Hence there should be

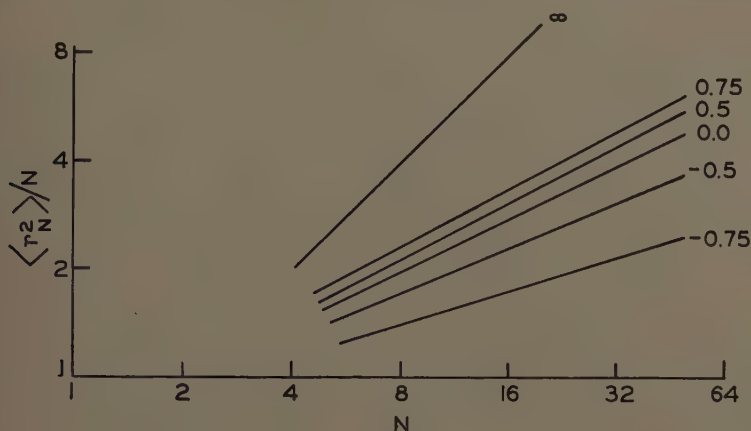


FIGURE 3. Graphs corresponding to those of FIGURE 1 drawn on a log-log scale.

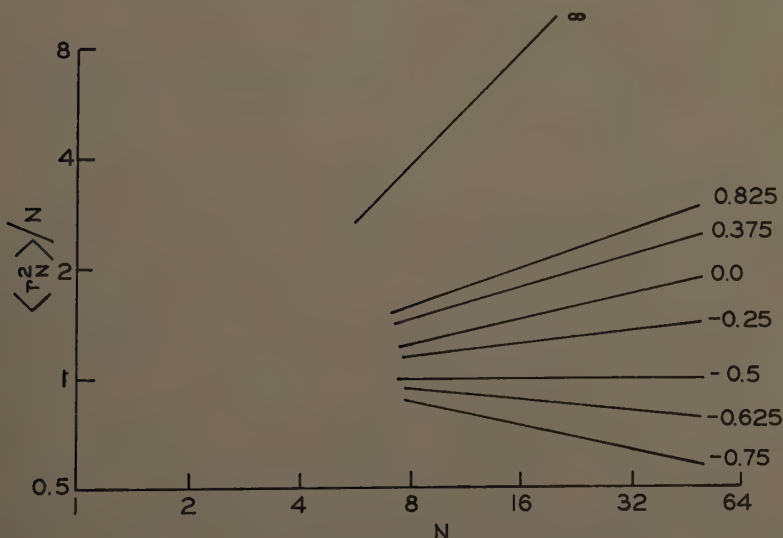


FIGURE 4. Graphs corresponding to those of FIGURE 2 drawn on a log-log scale.

a finite attractive potential at a temperature other than absolute zero, for which the slope of the  $\langle r_n^2 \rangle/n$  plot would be zero. This is, in fact, found to be the case in the three-dimensional lattice.

When the logarithm of  $\langle r_n^2 \rangle/n$  is plotted against the logarithm of  $n$ , reasonably straight lines are obtained, as indicated in FIGURES 3 and 4. These

curves reveal that, except for low values of  $n$ , all such plots are linear. This means that a relationship of the form

$$\langle r_n^2 \rangle = an^b \quad (6)$$

provides an adequate description of random-walk polymers even with interaction energies.

Graphs for the other kinds of walks described in TABLE 1 have also been prepared; they are not reproduced here since no significantly new features arise that would alter the general discussion or interpretation. It should be mentioned, however, that the values of the exponent  $b$  depend mainly on the number of dimensions and are little dependent on the lattice details. For category  $c$ , the molecular properties do not exhibit a strong dependence on  $\epsilon$ , except for extreme values, since the possible number of intermediate neighbors is only equal to 1. For the tetrahedral lattice, denoted by  $f$ , some minor differences in behavior were encountered, because the excluded range covered not only occupied lattice sites but also nearest-neighbor sites adjacent to the chain. This subject is being investigated further.

### *Thermodynamic Properties*

By using Equation 4 one can readily calculate the free energies of coiling-type molecules for different interaction energies. What we actually calculated is a difference in free energy,  $F - F^0$ , choosing as our standard state that corresponding to  $\epsilon = 0$ . For the two lattices already discussed, namely, the two-choice square lattice in two dimensions and the four-choice simple cubic lattice in three dimensions, this difference in free energy is found to be a linear function of the number of bonds. This means, in accordance with Equation 5, that the partial-link free energy, or the chemical potential per link, is independent of  $n$ . As  $\epsilon/kT$  increases, the free energy likewise increases; for negative values of  $\epsilon$ ,  $F - F^0$  becomes negative. This behavior results principally from the contribution of the energy of the system, which more than compensates for any entropy effect. Regardless of the sign of  $\epsilon$ , the entropy difference,  $S - S^0$ , is never positive, because the new distribution resulting from the introduction of an interaction potential will necessarily be less random than the old. It will be observed in FIGURES 5 and 6 that the lines representing  $F - F^0$  as functions of  $n$  fan out in both directions from the line corresponding to  $\epsilon = 0$ . The behavior may be empirically represented by Equation 7

$$F - F^0 = (n - 2)AkT \ln(1 + B\epsilon/kT) \quad (7)$$

where  $A$  and  $B$  are constants.

From Equation 7 it is easy to establish equations for  $S - S^0$  and for  $H - H^0$  (which will be the same as  $E - E^0$ ), as follows:

$$S - S^0 = -(n - 2)Ak \ln (1 + B\epsilon/kT) + \frac{(n - 2)AB\epsilon/T}{1 + B\epsilon/kT} \quad (8)$$

$$H - H^0 = \frac{(n - 2)AB\epsilon}{1 + B\epsilon/kT}. \quad (9)$$

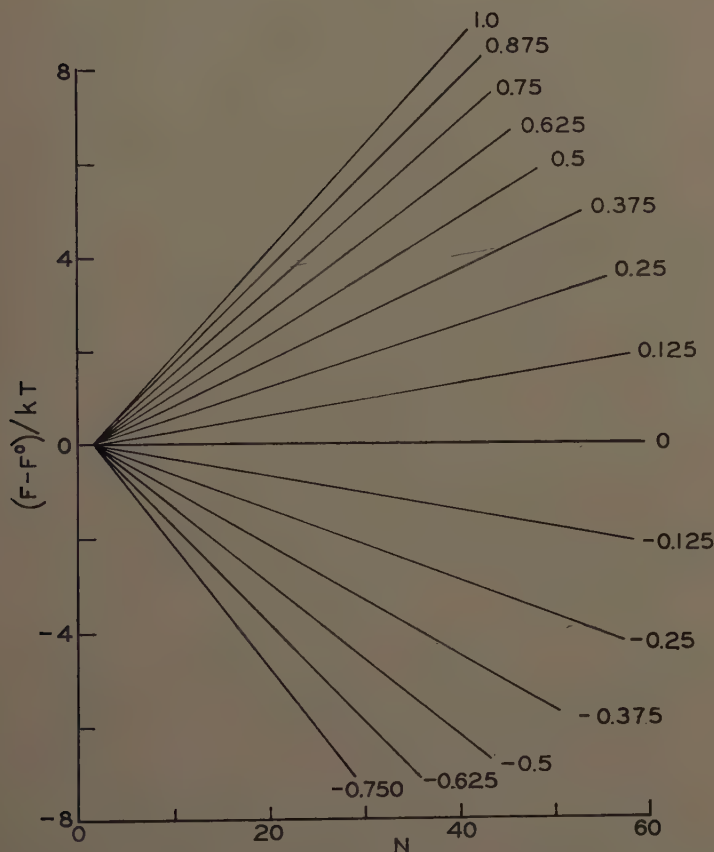


FIGURE 5. Graphs showing how the free energy of chains in two dimensions (designation *a*) depends on *n* for different values of  $\epsilon/kT$ .

It is evident that both *S* and *H* are linear functions of *n*.  $H - H^0$  was also calculated directly on the computer by using Equation 3, and the linear dependence of *H* on *n* was confirmed. The aforementioned linear dependence of the several important thermodynamic functions of *n* was established for all six designations, *a* through *f*, including the tetrahedral system. These thermodynamic properties are established with considerable accuracy, even up to  $n = 60$ , since no excessive scattering of the data occur, as was the case with computations of the mean square end-to-end separations.

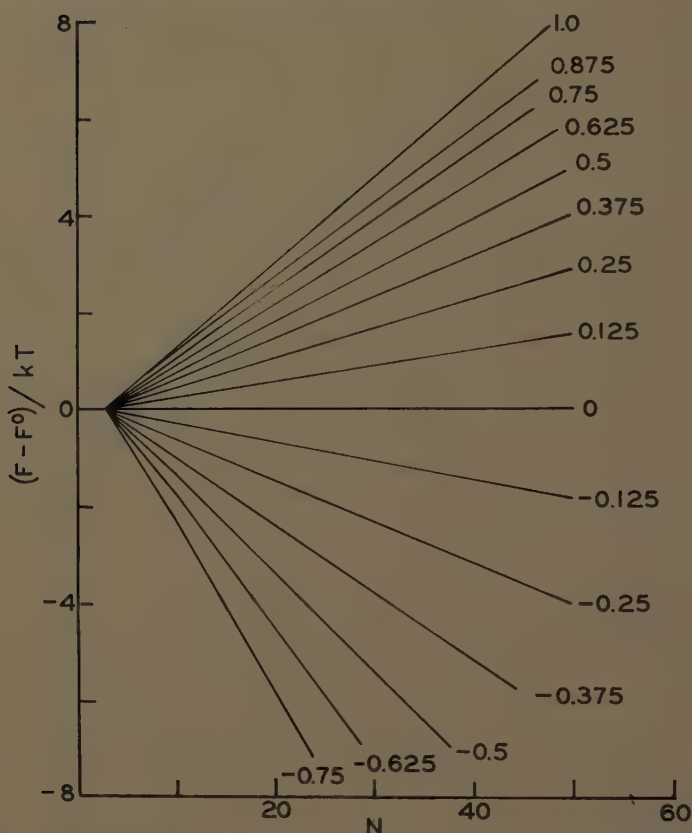


FIGURE 6. Graphs showing how the free energy of chains in three dimensions (designation *e*) depends on *n* for different values of  $\epsilon/kT$ .

TABLE 2

Designation	$\frac{\langle s^2 \rangle_0}{n-2}$	<i>B</i>
<i>a</i>	0.285	0.288
<i>b</i>	0.332	1.131
<i>d</i>	0.463	0.979
<i>e</i>	0.274	1.428
<i>f</i>	0.865	1.500

Another interesting result may be deduced from the thermodynamic computations. Since we are dealing with a single-step type of potential energy function, Equation 9 may be rewritten in terms of the average number of intrachain interactions corresponding to the given value of  $\epsilon$ :



$$\langle z \rangle = \frac{AB(n-2)}{1 + B\epsilon/kT} \quad (10)$$

If  $\epsilon = 0$ , then

$$\langle z \rangle_0 = AB(n-2) \quad (11)$$

where  $\langle z \rangle_0$  is the average number of intrachain distances lying within the specified intermediate separation range for an excluded volume polymer with  $\epsilon = 0$ .

For small values of  $B\epsilon/kT$ , the logarithmic term in 7 can be linearized and, with the help of 11, we obtain

$$F - F^0 = \langle z \rangle_0 \epsilon \quad (12)$$

Therefore the free-energy difference changes linearly with  $\epsilon$  when the potential energy of intrachain interaction is sufficiently small. Moreover when  $\epsilon$  is small, it is also clear that

$$H - H^0 = \langle z \rangle_0 \epsilon \quad (13)$$

and

$$S - S^0 = 0 \quad (14)$$

Actually,  $S - S^0$  must be negative, but this shows up only with higher-order terms in  $\epsilon$ . TABLE 2 summarizes the pertinent thermodynamic parameters.

### References

1. FLORY, P. J. 1953. Principles of Polymer Chemistry. Chapters X and XIV. Cornell Univ. Press. Ithaca, N. Y.
2. ZIMM, B. H., W. H. STOCKMAYER & M. FIXMAN. 1953. Excluded volume in polymer chains. J. Chem. Phys. **21**: 1716.
3. WALL, F. T., L. A. HILLER, JR. & D. J. WHEELER. 1954. Statistical computation of mean dimensions of macromolecules. I. J. Chem. Phys. **22**: 1036.
4. WALL, F. T., L. A. HILLER, JR. & W. F. ATCHISON. 1955-1957. Statistical computation of mean dimensions of macromolecules. I, III & IV. J. Chem. Phys. **23**: 913, 2314; **26**: 1742.
5. MONTROLL, E. W. 1950. Markoff chains and excluded volume effect in polymer chains. J. Chem. Phys. **18**: 734.
6. WALL, F. T., R. J. RUBIN & L. M. ISAACSON. 1957. Improved statistical method for computing mean dimensions of polymer molecules. J. Chem. Phys. **27**: 186.
7. WALL, F. T. & J. J. ERPENBECK. 1959. New method for the statistical computation of polymer dimensions. J. Chem. Phys. **30**: 634.
8. FLORY, P. J. *Op. cit.* : 600 602.

# THERMODYNAMICAL EXPLANATION OF LARGE PERIODS IN HIGH POLYMER CRYSTALS AND DRAWN FIBERS

E. W. Fischer

*University of Mainz, Mainz, Germany*

## *Introduction*

Nearly all crystallizable high polymers show one or more structural periodicities between 50 and 500 Å, revealing themselves in small-angle X-ray scattering. The occurrence of long-period diffraction is always associated with the existence of crystallites. Therefore it is very reasonable to assume that the origin of the long periods is the regular placement of the crystallites. I shall call the process leading to this regular arrangement "periodic crystallization." This paper deals with the reasons for the special process of crystal growth that occurs in polymer systems. For this purpose the experiments that led to the introduction of the concept of periodic crystallization will be considered. Then some experimental features will be discussed in order to decide whether the cause of periodic crystallization is kinetical or thermodynamical. Finally the fundamentals of a theoretical treatment developed by A. Peterlin and myself will be considered. This theory maintains that the phenomenon is caused by the anisotropy of lattice forces in chain crystals.

## *Periodic Crystallization*

Often the structure of the high-polymer system causing small-angle scattering is not known exactly. In three cases, however, the associated structure has been revealed by means of electron microscopy. These scattering effects are: (1) the numerous and sharp small-angle interference patterns of certain natural fibers such as collagen; (2) the meridional reflections of synthetic drawn fibers; and (3) the small-angle interferences that originate from polymer single crystals grown from solution.

In the first case it was shown<sup>1,2</sup> that the periods measured by X-ray investigations correspond to a system of regular transverse stripes within the collagen fibrils. Probably the period is due to a certain order of the amino-acid residues within the protein chains.<sup>3</sup> This type of periodic structure in which large periods are caused in one way or another by the structure of the molecules will not be discussed in this paper.

However, the large periods obtained from synthetic drawn fibers cannot be explained by a periodicity within the molecule itself. According to Hess and Kiessig<sup>4</sup> the small-angle maxima are produced in this case by a periodic change of crystalline and amorphous regions.\* This idea is gen-

\* It must be remarked that some authors<sup>5,6</sup> believe that the large period in protein is also caused by alternation of ordered and disordered regions.

erally accepted today although there are differences of opinion about the inner structure of the amorphous areas.<sup>7</sup> FIGURE 1 shows the model of fiber polymers proposed by Hess and Kiessig<sup>4</sup> and constructed by Statton.<sup>8</sup> All the details of this model need not be accepted; for further consideration it is only essential that the fiber polymers consist of elementary fibrils having nearly *periodic* alternation of poorly and well-ordered regions.



FIGURE 1. Model of fiber structure with approximate periodic alternation of crystalline and amorphous regions (W. O. Statton).<sup>8</sup> Reproduced by permission of *Journal of Polymer Science*, vol. 41, copyright 1959 by Interscience Publishers, Inc., New York, N. Y.

The third case mentioned above deals with a cake of polyethylene single crystals. Here the reason for the small-angle period is obvious. During the crystallization of polyethylene from dilute solution, single crystals grow into the shape of a lamella in which the chains are perpendicular to the flat surfaces.<sup>9-11</sup> The average length of the chains is about 50 times greater than the thickness of the single crystals: therefore Keller<sup>10</sup> concluded that the molecules must be folded at the outer planes of the lamella. Such lamellae when arranged in layers form a cake, and Keller and O'Connor<sup>12</sup> showed that this cake gives a small-angle period up to the fourth order, corresponding exactly to the thickness of the platelike crystals.

In the alternation of crystalline and amorphous regions in drawn fibers as well as in the folding of the chains that occurs during the crystallization from dilute solution, the structure of the crystal is subjected to periodic

lattice distortions in chain direction. Furthermore investigations have shown that in polycrystalline high polymers crystallized from melt, from concentrated solution, or from the glassy state the crystallites have a small and uniform length in the chain direction. Electron-microscopy studies of the surface of bulk-crystallized polymers also often show a lamellar structure.<sup>13,14</sup> For special reasons, which cannot be considered in detail here, I am rather certain that the whole polymer solid consists of crystals similar to those seen on the surface. For example, the replicas of fracture

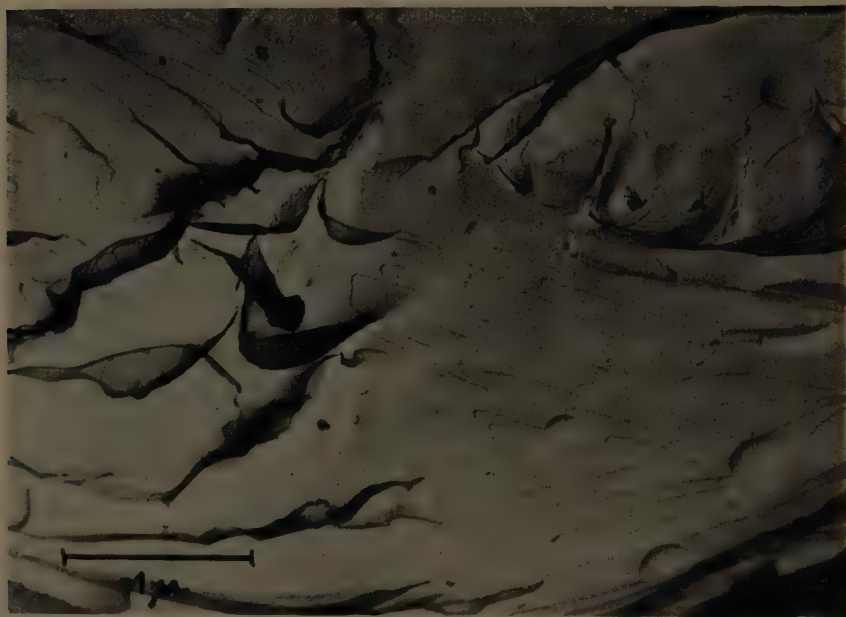


FIGURE 2. Fracture surface of high-density polyethylene, crystallized at 125° C.

surfaces from polyethylene show clearly the individual lamellae (FIGURE 2).<sup>\*</sup> This statement does not necessarily mean that in crystallization in bulk the chains are folded at the boundary surfaces of the crystallites. However, crystallites are always found to have the same thickness and to be arranged in a particular order with one another; the folding of the molecules is the simplest assumption to explain this morphological structure. Independently of this assumption I shall name the process that leads, at least in small regions, to a periodic arrangement of crystallites with nearly the same size "periodic crystallization." I believe that this special manner of crystallization is a general feature of all crystalline polymers.

<sup>\*</sup> See also the fracture experiments of Bunn *et al.*<sup>31</sup> with polytetrafluorethylene and of Geil<sup>14</sup> with polyoxymethylene.



*Kinetic or Thermodynamic Causes*

The cause of periodic crystallization is not yet known. There are two principal possibilities to explain the phenomenon. It may be that the periodic structure is kinetically caused. On the other hand is it conceivable that crystals with such a small thickness in chain direction can be in a state of lowest free energy for the polymer material.

The first idea was extended in the theories proposed by Lauritzen and Hoffmann<sup>15</sup> and independently by Price.<sup>16</sup> In the case of crystal growth from dilute solutions these authors assume that in the outer planes of the nucleus the molecules are already folded and therefore further growth of

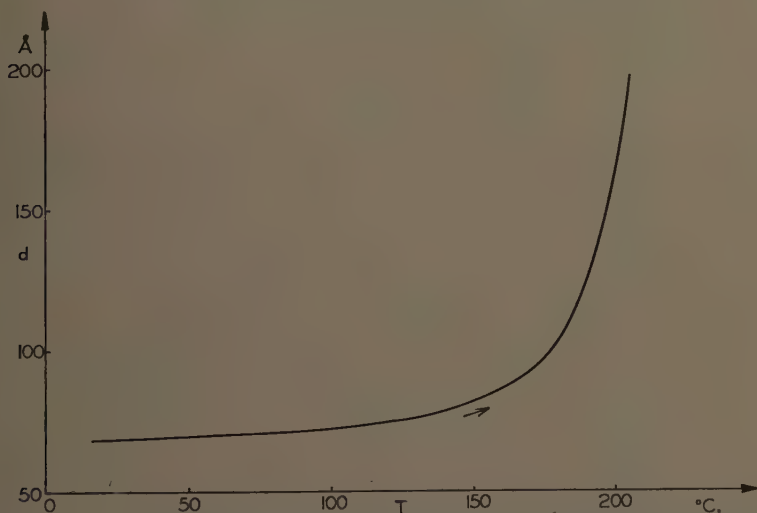


FIGURE 3. Dependence of the long period of drawn 6-nylon on the temperature (K. Kobayashi, private communication).

the crystal is kinetically retarded in chain direction. I shall not discuss this assumption because I believe that the cause for the periodic crystallization is the same in all the previously mentioned cases, that is, that the cause is the same whether the crystallization is from solution or from bulk or whether it is in the drawn state. This assumption excludes kinetic causes. It should not be forgotten that during the stretching the molecules are arranged to a great extent in a parallel way from the exterior. If the molecules are given enough mobility by annealing, there results extremely favorable kinetic conditions for the formation of large single crystals. However, this observation has not been made.

The assumption of periodic crystallization is supported by similar behavior of the long periods in drawn material and of polyethylene single crystals during annealing. In FIGURE 3 the dependence of the small-angle period of drawn 6-nylon fibers on temperature can be seen. These measurements

were carried out by K. Kobayashi (private communication). The long period increases with heating; the increase is particularly rapid at high temperatures.

A curve similar to FIGURE 3 is obtained by heating polyethylene lamellae crystallized from solution. Data for FIGURE 4 were obtained by Statton and Geil<sup>17</sup> and by G. F. Schmidt and E. W. Fischer (unpublished data). In the temperature range between 110°C. and the melting point, the fold

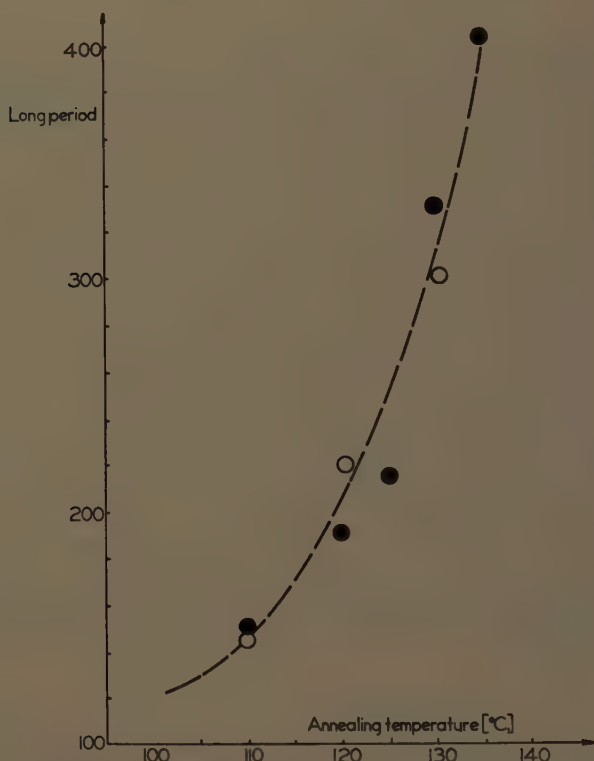


FIGURE 4. Dependence of the long period of polyethylene crystals on the annealing temperature. Key: ● = measured at room temperature by Statton and Geil<sup>17</sup> (original crystals 104 Å); ○ = measured at annealing temperature by G. F. Schmidt and E. W. Fischer (unpublished data; original crystals 120 Å).

period of the crystals changes, and the system comes to a new state of equilibrium. The points in FIGURE 4 obtained at the annealing temperature show that the new period had already formed at these temperatures before the sample was cooled. It is obvious that smaller crystals must melt at a lower melting point because of the large contribution of the surface energy to the whole energy per volume unit. This melting process could also be observed by means of the X-ray wide-angle scattering with cakes of polyethylene single crystals held at constant temperature (G. F.

Schmidt and E. W. Fischer, unpublished data). According to the kinetic theories, however, the crystals should grow infinitely because the kinetic hindrance of the prefolded surfaces has been removed. Nothing should prevent them from growing into their most stable thermodynamic configuration; that is, they should grow as large as possible. This phenomenon was not observed; however, with a small difference of temperature, a new fold period that is slightly longer is observed. In my opinion this can be explained only by the fact that for high-polymer crystals there exists a stable length, which depends on the temperature.

It seems useful to mention two other experiments. The first experiment concerned the dependence of the fold period on the chain length; the second concerned the structure of polyoxymethylene single crystals. It was shown by Keller and O'Connor<sup>18</sup> that the fold length of polyethylene crystals is independent of the molecule length even if there is a change of the molecular weight by a factor of about 100. It is important for the theory of periodic crystallization that this independence holds true even in the region where the molecular length becomes comparable with the fold length. Other experiments carried out by Zahn<sup>19</sup> with very short molecules of the 6-nylon type gave similar results. At first the long period increased with the number of the monomer units  $n$ , but above  $n = 6$  it remained constant at about 70 Å. This value corresponded exactly to the long period measured in high-molecular 6-nylon. I cannot believe that there is a kinetic reason for this behavior because kinetic theories start from the fact that the nucleus with folded chain configuration is formed by *only one* molecule.

Finally let us consider the structure of polyoxymethylene. Recently it was shown by Geil *et al.*<sup>20</sup> that this polymer grows from dilute solution in the form of lamellae about 100 Å thick; hence the molecules have a folded conformation. It is true that polyoxymethylene single crystals—however different—have been known for a long time.<sup>21,22</sup> This was the first and, to date, the only polymer that permitted the formation of crystals large enough to obtain rotation patterns for the determination of lattice. Obviously the production of crystals as large as 1 mm. was possible in this case only because the crystal growth coincided with the polycondensation. The building elements of these crystals were not previously formed chain molecules; instead the growth took place in such a manner that formaldehyde molecules were added to a nucleus. Nevertheless, according to the thermodynamic theory, the formation of single crystals consisting of chain molecules with such large macroscopic dimensions is highly improbable since the minimum of energy is within the range of about 100 Å. On the other hand, of course, kinetic theories concerning macromolecules cannot be applied to these crystals. Therefore it was important to study the possibility that these crystals might have a microstructure.

Indeed electron micrographs of surface replicas of macroscopic polyoxy-

methylenes single crystals\* show that the crystals are built up of many growth layers arranged extremely regularly (FIGURE 5). The period in chain direction amounts to approximately 200 Å; consequently it is exactly within the expected order of magnitude. There is no doubt that the macromolecules are longer than this period, and I believe that this experiment also favors a thermodynamic interpretation of the periodic crystallization.

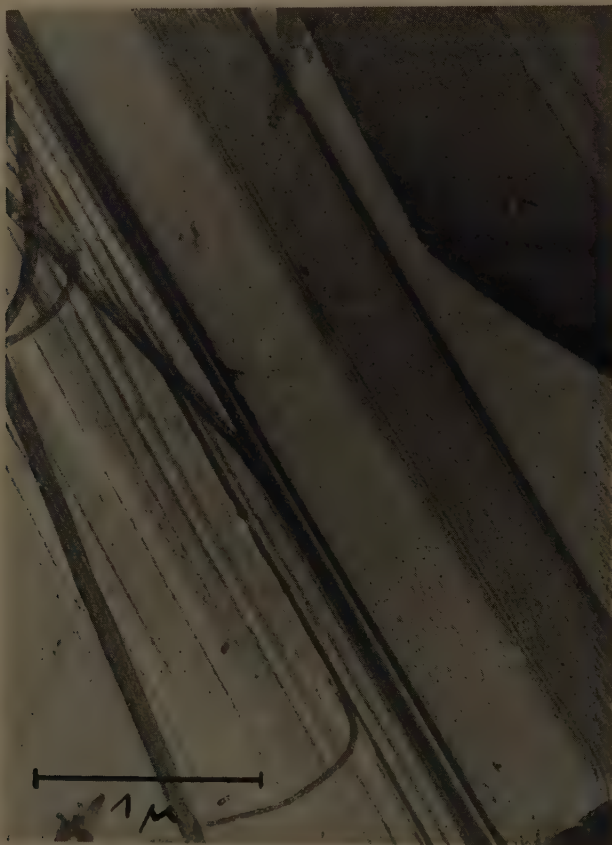


FIGURE 5. Electron-microscopic surface replica of a polyoxymethylene single crystal.

### *Basic Idea of the Theory*

What feature of a lattice built by chain molecules can cause the energy density of a crystal to be size-dependent? It must be a very general property of such lattices, and the main difference between polymer and low-molecular crystals is the extreme anisotropy of lattice forces in the polymers. In chain direction the forces are diamondlike; perpendicular to

\* I thank O. Schweitzer, Frankfurt/Mainz, Germany, for preparation of the sample.



chain direction the forces are considerably weaker, but those forces between neighboring chains preventing rotation around or translation along the chain axis are particularly weak. Stockmayer and Hecht,<sup>23</sup> for example, who calculated the heat capacity of chain crystals, proposed a model in which the forces perpendicular to the chain amount to only one twenty-fifth of the forces in the chain, and the force opposing the translation in chain direction amounts only to two thousandths of the force between adjacent groups in the chain.

What are the consequences of this anisotropy of the lattice forces? If distortions are introduced into an ideal lattice, the position of a mass point *s*, in first approximation, given only by the position of the immediately

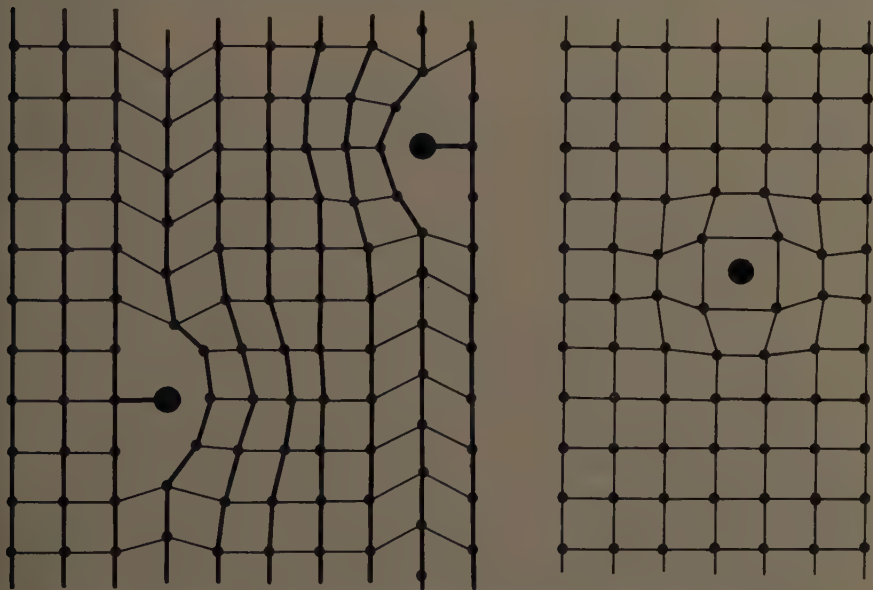


FIGURE 6. Lattice distortions in high-molecular and low-molecular lattices.

neighboring mass points within the molecular chain. The lattice forces are not strong enough to cause the fitting of the mass points into the ideal positions in the lattice. On the contrary the minimum of the potential energy of the lattice with an included defect is reached if the chain bonds and angles are only slightly deformed. This fact is demonstrated in FIGURE 6 by the example of a branching structure. Although this pattern is very much simplified it shows that in contrast to the case of low-molecular lattices such lattice defects do not heal easily with increasing distance. This one-dimensional defect is a case similar to that of dislocation. Therefore the density of the defects per unit volume and also the defect energy depend not only on the number of the branchings in the crystals but also on the size of the crystals in chain direction. It should be recalled that in normal lattices the energy of a linear dislocation is infinitely large for an

infinitely extended crystal. In such crystals only closed dislocation rings have a finite energy.

In high-polymer crystals distortions of this kind may be caused by various phenomena such as branchings, hydrogen bonds wrongly fitted, and distorted or entangled chains. It must be expected that in a crystal such as that shown in FIGURE 6 the long-range order in chain direction breaks down by introduction of further branchings. Therefore the crystal is no longer stable after it has exceeded a certain length. In agreement with this concept electron microscopy and X-ray small-angle scattering show that the sizes of the crystallites diminish with an increasing degree of branching<sup>28</sup> or with an increasing number of lattice failures caused by poor crystallization conditions.

### Lattice Vibrations

It can be demonstrated that in an ideal chain lattice "long-range" distortions can also be initiated through heat motion.<sup>24,25</sup> For this purpose

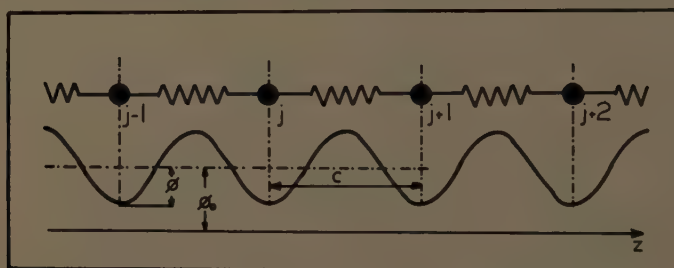


FIGURE 7. Model of a linear chain within a longitudinal lattice field.

FIGURE 7 represents a simple one-dimensional model. The groups of the molecular chain are represented by  $N$  mass points with the mass  $m$ , linked to one another by spring forces  $f$ . The simplifying assumption is made that the chains in the crystal fluctuate almost independently and that the force field due to the neighboring chains can be represented by a cos-potential function:

$$\phi_0 - \phi \cos \frac{2\pi z}{c} \quad (1)$$

The meaning of the potential amplitude can be seen in FIGURE 7;  $c$  is the repeating unit of the chain. If we assume that  $\phi = 0$ , it can easily be shown that the mean square deviation of the free chain with its center of mass fixed is given by

$$s_f^2 = \frac{1}{N} \sum_{j=1}^N \overline{z_j^2} = \frac{1}{6} \frac{kT}{f} N \quad (2)$$

Thus the mean square deviation of chain points from their equilibrium positions increases linearly with the number of the links of chain.

The energy of the chain embedded in the lattice field is the sum of the kinetic energy plus the potential energy of the springlike forces within the chain itself and of the intermolecular cosine field. The result is:

$$u = \frac{m}{2} \sum_{j=1}^N \dot{z}_j^2 + \frac{f}{2} \sum_{j=1}^{N-1} (z_j - z_{j+1})^2 + N\phi_0 - \phi \sum_{j=1}^N \cos \frac{2\pi z_j}{c} \quad (3)$$

Using this setup Peterlin and Fischer<sup>25</sup> calculated the state sum of the system in a relatively comprehensive calculation. From the state sum the mean square fluctuation of the chain links in the lattice can be derived. Equation 4 is obtained:

$$s_c^2 = \frac{NkT}{6} \left( 1 - \frac{0.4}{1 + 1/4N\beta A^2} \right) \quad (4)$$

with  $\beta = \phi/kT$  and  $A^2 = NkT/fc^2$ . It is apparent that the mean square fluctuation in the lattice is smaller than in the free chain (2); however, it increases with increasing  $N$ . This dependence is a specific property of polymer crystals with large anisotropy of lattice forces. Although the chains are prevented from making translation in the plane perpendicular to the chains, the groups can still move rather easily in chain direction. The same applies to the motion around the chain axis, as shown later.

In a former publication on this subject<sup>24</sup> I was of the opinion that this dependence of the fluctuation amplitude on  $N$  led to an increase of the energy density with increasing crystal thickness. F. C. Frank and M. H. L. Pryce have called my attention to the fact that this is not correct if the potential amplitude  $\phi$  is kept constant. This changes however, if it is taken into account that the potential is smeared by longitudinal oscillations of the neighboring groups. It is assumed that  $\phi = \phi_0$  for the case in which all neighboring groups are in state of rest. However, if all four neighbors oscillate independently of one another, it can easily be shown that:

$$\phi = \phi_0 \exp(-2\pi^2 s_c^2 / c^2) \quad (5)$$

That means that the potential amplitude  $\phi$  decreases with increasing mean square fluctuation  $s_c^2$  or with increasing number of chain groups in the chain direction. If the free-energy density is calculated from the state sum, taking into account the contribution of the surface energy, approximately the following expression for the energy density is obtained.

$$\begin{aligned} \frac{F}{NkT} = \text{const} + \frac{1}{N} \ln \frac{kT}{h\omega_0} - \frac{\phi}{kT} \\ + \frac{1}{N} [0.7 + 0.5 \ln N(1 + 4N\beta A^2) + 2b^2\sigma/kT] \end{aligned} \quad (6)$$

In Equation 6 the terms independent of  $N$  are included in the constant;

$b^2$  means the size of the boundary surface per chain. In this expression for the free-energy density, the potential function  $\phi$  contributes a term increasing with  $N$  as a consequence of the smearing-out effect. The term in brackets diminishes with increasing  $N$ , the term with the boundary surface energy being the most important one within the brackets. Thus a term increasing with  $N$  is obtained as well as another that decreases with  $N$ . Both terms together yield a minimum of free energy with a certain  $N$ , which depends mainly on the temperature and the intermolecular forces. A plot of this minimum  $N_{\min}$  representing the thermodynamically stable crystal thickness as a function of  $2b^2\sigma/kT$  with  $\beta_0 = \phi_0/kT$  as parameter is shown in FIGURE 8. The higher  $\beta_0$  is, the stronger the interchain forces and the

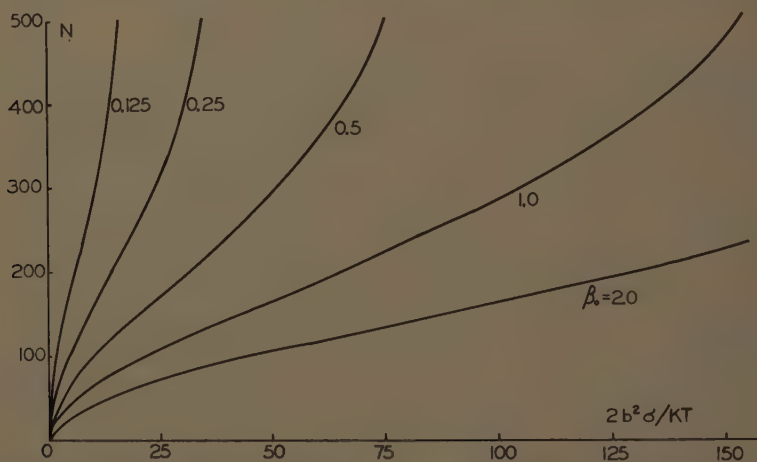


FIGURE 8. Stable crystal thickness  $N_{\min}$  as function of surface energy  $\sigma$  with  $\beta_0 = \phi_0/kT$  as parameter.

smaller the stable crystal thickness; this is in qualitative agreement with experimental data obtained from different polymers.

With increasing temperature the crystal expands chiefly in the direction perpendicular to the chain axis; consequently the interchain potential energy  $\beta_0$  decreases. Furthermore the number of thermic failures increases, and this also leads to a decrease of  $\beta_0$ . Since the changes in  $T$  are small compared with the absolute temperature  $T$  itself, there is only a small change in the abscissa. On the other hand, by using a smaller parameter in the plot an increased thickness of the thermodynamically stable crystal is obtained. The thickness increases more quickly the smaller the original  $\beta_0$ , that is, with increasing temperature the thickness increases faster the higher the temperature; this is in good qualitative agreement with the experimental results of Statton and Geil.<sup>17</sup>

The values of the parameters received from the theory are also in the right order of magnitude. I started from a boundary surface energy of



$\sigma = 50 \text{ erg/cm.}^2$ , a value also estimated by Price<sup>16</sup> from the heat of fusion. If a value of the surface energy is chosen then the magnitude of the lattice potential amplitude  $\phi_0$  can be obtained from the theory by means of the stable crystal thickness given experimentally. The result is

$$(\phi_0)_{\text{crystal thickness}} = 1.3 \cdot 10^{-14} \text{ erg.}$$

On the other hand, an estimation for  $\phi_0$  can be given with the aid of the well-known setup for the van der Waals potential between two  $\text{CH}_2$  groups of different molecules. From the values for the van der Waals constants found in the literature<sup>26</sup>  $\phi_0$  can be calculated by summation of the interaction potential for the four next neighbors, giving:  $(\phi_0)_{\text{van der Waals}} = 0.3 \times 10^{-14} \text{ erg}$ . This agreement, although not very good, is satisfactory considering the uncertainty of the constants.

### *Torsional Vibrations*

A similar dependence of the free-energy density on the chain length is obtained if the torsional vibrations of the chain are considered instead of the longitudinal vibrations. Again the chain is placed into a periodic lattice potential, and the following expression for the energy of the chain in question is obtained.

$$u = \frac{F}{2} \sum_{j=1}^N \phi_j^2 + \frac{c}{2 \sin^2 \frac{\theta}{2}} \sum_{j=1}^{N-1} (\varphi_j - \varphi_{j+1})^2 + NE_0 - E \sum_{j=1}^N \cos 2\varphi_j \quad (7)$$

$\varphi_j$  means the displacement of the  $j$ th chain link from its position of rest in radian measure. Instead of the spring constant  $f$  the expression

$$c/2 \sin^2(\theta/2)$$

is obtained; according to Szigeti<sup>27</sup> this amounts to  $0.64 \times 10^{-12} \text{ erg/group}$  when considering torsional vibrations of  $\text{CH}_2$  groups. In this case the angle  $\theta$  is the C—C— bond angle, the constant angle between three C atoms. Contrary to the calculation of the longitudinal vibrations, this case gives good approximations for  $E_0$ . According to Eicker<sup>26</sup>  $E_0$  is equal to  $1.75 \times 10^{-14} \text{ erg}$ . It can also be calculated from the heats of transition of paraffins. If these values are substituted into the equations for the free energy of the vibrating chain, the curve in FIGURE 9 is obtained. In this case too the minimum is placed near  $N = 100$  if the temperature  $T = 373^\circ \text{ K}$ . A corresponding boundary face energy of  $135 \text{ erg/cm.}^2$  is obtained, a value that is slightly too large. This is a consequence of the inaccuracy of the setup for the smearing of the potential. The mutual coupling of the chains markedly undergoes this effect so that the smearing actually appears less than calculated. With a smaller smearing-out effect, the theory also gives a smaller value for surface energy. Thus the incorrect value of  $135 \text{ erg/cm.}^2$

indicates that the torsional vibrations of the chain are not independent of those of the neighboring-chains.

### Branching and Other Lattice Failures

A consideration of the influences of branching and other lattice failures is in order here; therefore the scheme of a lattice with branchings shown in

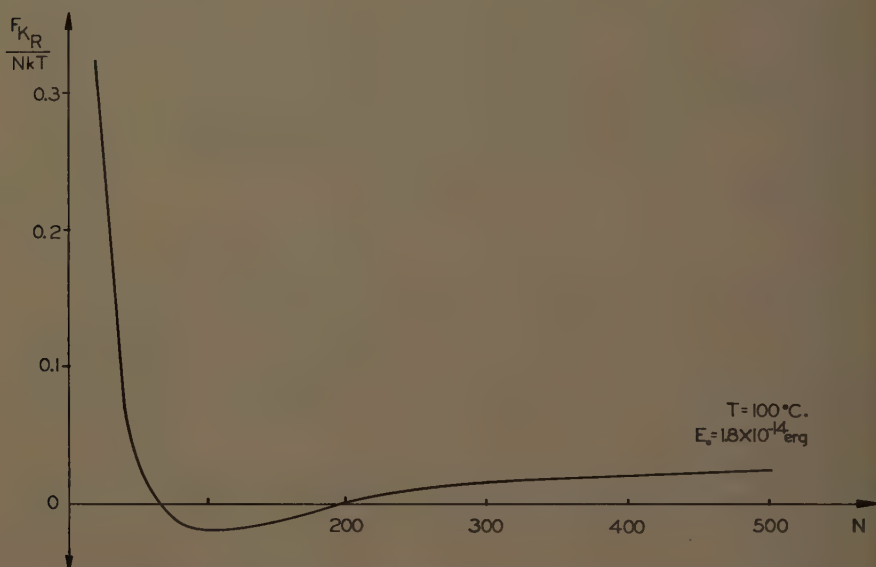


FIGURE 9. Free-energy density as function of crystal length for torsional vibrations.  $T = 100^{\circ}\text{C.}$ ;  $E_0 = 1.75 \times 10^{-14}$  erg.

FIGURE 6 should be reviewed. Obviously each of those failures causes a smearing of the potential in the same way as that shown in the case of longitudinal vibrations and torsional vibrations. In accordance with this observation Hendus *et al.*<sup>28</sup> found the dependence of the long period on the degree of branching plotted in TABLE 1. There are good reasons to

TABLE 1  
LONG PERIODS OF VARIOUS POLYETHYLENES\*

Degree of branching $\text{CH}_3/1000^{\circ}\text{C.}$	Slowly cooled		Quenched	
	1st period	2nd period	1st period	2nd period
1.5	344	165	222	86
5	310	140	204	78
15	280	85	184	60
25	218	—	154	—

\* From Hendus *et al.*<sup>28</sup> Reproduced by permission of *Ergebnisse der exakten Naturwissenschaften*.

assume that the second period gives the size of the crystals in *c* direction. The size decreases with increasing degree of branching as would be expected from the model in FIGURE 6.

### Conclusions

The mean amplitude of fluctuation of the thermal motion of groups in chain crystals depends on the thickness of the crystals in chain direction. These distortions cause a smearing of the lattice potential. Therefore the energy density of a crystal consisting of chain molecules increases with increasing length of the chains. It seems that this dependence is an appropriate explanation for the periodic crystallization observed in polymers. Having passed its critical length the nucleus of the crystal then continues to grow in chain direction until the minimum of free energy is attained. Then the chains fold, and the loops cause the decoupling of the longitudinal vibrations of subsequent parts of the chain. Another cause of this decoupling is to be found in the amorphous regions of drawn fibers.

Of course my model is not fully satisfactory in spite of qualitative agreement with the experimental results. It will be necessary to examine closely the chain motion in polymer crystals. Nuclear magnetic resonance (NMR) investigations form a suitable method for this purpose. These investigations have already shown that the chain mobility in the crystalline regions is greater than previously assumed. From their measurements McCall and Slichter<sup>29</sup> derived a value of the mean torsion amplitude very similar to the one I had assumed. Furthermore the NMR studies of Hugins *et al.*<sup>30</sup> force the conclusion that translational motion of appreciable magnitude occurs in polymer crystals below the crystal melting temperature.

Such investigations are suitable for reexamining the theory in a quantitative way, but I believe that the simple model gives a possible explanation for periodic crystallization.

### Acknowledgments

I thank H. A. Stuart, Mainz, Germany, for his helpful discussions during this work, and I am much indebted to A. Peterlin, Ljubljana, Yugoslavia, for permission to report on his studies.

### References

1. SCHMITT, F. O. 1956. *Proc. Am. Phil. Soc.* **100**: 477.
2. NEMETSCHKE, T. 1958. *Z. Naturforsch.* **13b**: 225.
3. SCHMITT, F. O. 1959. *Rev. Mod. Phys.* **31**: 349.
4. HESS, K. & H. KIESSIG. 1943. *Naturwiss.* **31**: 171; also 1944. *Z. Phys. Chem.* **194**: 196; 1953. *Kolloid-Z.* **130**: 10.
5. BEAR, R. S. 1952. *Advances in Protein Chem.* **7**: 69.
6. HESS, K., E. GUETTER & H. MAHL. 1960. *Kolloid-Z.* **168**: 37.
7. BONART, R. & R. HOSEMANN. 1959. *IUPAC-Symposium Makromoleküle. Wiesbaden, Germany.*
8. STATTON, W. O. 1959. *J. Polymer Sci.* **41**: 143.

9. TILL, P. H. 1957. *J. Polymer Sci.* **24**: 301.
10. KELLER, A. 1957. *Phil. Mag.* **2**: 1171.
11. FISCHER, E. W. 1957. *Z. Naturforsch.* **12a**: 753.
12. KELLER, A. & A. O'CONNOR. 1957. *Nature*. **180**: 1289.
13. EPPE, R., E. W. FISCHER & H. A. STUART. 1959. *J. Polymer Sci.* **34**: 721.
14. GEIL, P. H. 1960. *Am. Phys. Soc. Meeting.* Detroit, Mich.
15. LAURITZEN, J. I. & J. D. HOFFMANN. 1960. *Research Natl. Bur. Standards.* **A64**: 73.
16. PRICE, F. P. 1960. *J. Polymer Sci.* **42**: 49.
17. STATTON, W. O. & P. H. GEIL. 1960. *Am. Chem. Soc. Meeting.* Cleveland, Ohio.
18. KELLER, A. & A. O'CONNOR. 1960. *Polymer*. **1**: 163.
19. ZAHN, H. 1959. *IUPAC-Symposium Makromoleküle.* Wiesbaden, Germany.
20. GEIL, P. H., N. K. J. SYMONS & R. G. SCOTT. 1959. *J. Appl. Phys.* **30**: 1516.
21. STAUDINGER, H. & R. SIGNER. 1929. *Z. Kristall.* **70**: 193.
22. STAUDINGER, H. & O. SCHWEITZER. 1929. *Ann. Phys.* **474**: 238.
23. STOCKMAYER, W. H. & C. E. HECHT. 1953. *J. Chem. Phys.* **21**: 1954.
24. FISCHER, E. W. 1959. *Z. Naturforsch.* **14a**: 584.
25. PETERLIN, A. & E. W. FISCHER. 1960. *Z. Phys.* **159**: 272.
26. EICKER, F. 1958. *Z. Naturforsch.* **13a**: 126.
27. SZIGETTI, B. 1952. *Trans. Faraday Soc.* **48**: 400.
28. HENDUS, H., G. SCHNELL, H. THURN & K. WOLF. 1959. *Ergeb. exakt. Naturw.* **31**: 220.
29. MCCALL, D. W. & W. P. SLICHTER. 1957. *J. Polymer Sci.* **25**: 171.
30. HUGGINS, C. M., L. E. ST. PIERRE & A. M. BUECHE. 1960. *General Electric Research Rept.*
31. BUNN, C. W., A. J. COOBOLD & R. P. PALMER. 1958. *J. Polymer Sci.* **28**: 376.



# LATTICE THEORY OF CHAIN POLYMER SOLUTIONS

Michio Kurata\*

*Department of Chemistry, Massachusetts Institute of Technology, Cambridge, Mass.*

## *Introduction*

It is now well known that the Flory entropy of mixing for chain polymer solutions<sup>1</sup> is straightforwardly derivable from the phase integral of the system without the aid of a special model such as the lattice model, if the correlation between segments arising from the chain connectivity is entirely ignored.<sup>2,3</sup> This implies that the Flory entropy, although crude in itself, can be given a fundamental role in a more general polymer solution theory. Furthermore, the thermodynamic properties of systems characterized by the Flory entropy have been fully investigated by many authors in connection with phase separation and other practical problems.<sup>4,5</sup> For these two reasons, the Flory entropy may be adopted as the most convenient standard for thermodynamic description of general polymer solutions, and the entropy of dilution  $\tilde{S}_0$  and the heat of dilution  $\tilde{H}_0$  of the system may be written in the following forms:

$$\tilde{S}_0 = -R\{\ln(1 - \phi) + [1 - (1/n)]\phi + \sigma\phi^2\} \quad (1)$$

and

$$\tilde{H}_0 = RT\kappa\phi^2 \quad (2)$$

where  $R$  is the gas constant,  $T$  is the absolute temperature,  $\phi$  is the volume fraction of polymer, and  $n$  is the number of segments per molecule. More explicitly,  $n$  is defined as

$$n = \bar{v}M/V_0 \quad (3)$$

where  $M$  is the molecular weight,  $\bar{v}$  is the (partial) specific volume of polymer and  $V_0$  is the molar volume of solvent. The quantities  $\sigma$  and  $\kappa$  are respectively an entropy and a heat function, defined by **1** and **2** in a purely phenomenological sense. The chemical potential of the solvent is then written in the form

$$\mu_0 = \mu_0^* + RT\{\ln(1 - \phi) + [1 - (1/n)]\phi + \chi\phi^2\} \quad (4)$$

with

$$\chi = \sigma + \kappa \quad (5)$$

and the chemical potential of the polymer is obtained from  $\mu_0$  with the

\* Sloan Foreign Post-Doctoral Fellow of the School for Advanced Study, Massachusetts Institute of Technology. Permanent address: Department of Industrial Chemistry, Kyoto University, Kyoto, Japan.

Gibbs-Duhem equation. Here  $\mu_0^*$  represents the chemical potential of pure solvent.

At infinite dilution, the osmotic pressure derived from 4 should tend to the van't Hoff limiting law. This condition shows that both  $\sigma$  and  $\kappa$  approach a finite value at zero concentration. At reasonably low concentrations, therefore,  $\sigma$ ,  $\kappa$ , and  $\chi$  can be expanded in series form:

$$\sigma = \sum_i \sigma_i \phi^i = \sigma_0 + \sigma_1 \phi + \sigma_2 \phi^2 + \dots \quad (6)$$

$$\kappa = \sum_i \kappa_i \phi^i = \kappa_0 + \kappa_1 \phi + \kappa_2 \phi^2 + \dots \quad (7)$$

and

$$\chi = \sum_i \chi_i \phi^i = \chi_0 + \chi_1 \phi + \chi_2 \phi^2 + \dots \quad (8)$$

and the following expressions can be obtained for the second and the third osmotic virial coefficients:

$$A_2 = (\bar{v}^2/V_0)(\frac{1}{2} - \sigma_0 - \kappa_0) \quad (9)$$

$$A_3 = (\bar{v}^3/V_0)(\frac{1}{3} - \sigma_1 - \kappa_1) \quad (10)$$

It is now well established that the second virial coefficient  $A_2$  is a decreasing function of molecular weight. This indicates that in this formalism 9, the  $\sigma_0$  and  $\kappa_0$  should depend on the molecular weight in contrast to the prediction of the existing lattice theories.<sup>1,5-7</sup> It is also obvious that these functions should depend on the structural properties of polymer chains, such as flexibility and branching.

The theta temperature where the second virial coefficient vanishes may be defined by

$$\frac{1}{2} - \sigma_0(\Theta, M) = \kappa_0(\Theta, M) \quad (11)$$

where  $\sigma_0(\Theta, M)$  indicates the value of  $\sigma_0(T, M)$  at  $T = \Theta$ , and so on. According to the recent experiment on polystyrene-cyclohexane system by McIntyre *et al.*,<sup>8</sup> the  $\Theta$  value is found to increase slightly as the molecular weight is decreased. For the same system, Krigbaum and Geymer<sup>9</sup> have observed that the third virial coefficient  $A_3$  also vanishes at the theta temperature. A similar result has been obtained for polyisobutylene-benzene system by Flory and Daoust.<sup>10</sup> Thus I am almost sure that

$$\chi_1(\Theta, M) = \sigma_1(\Theta, M) + \kappa_1(\Theta, M) = \frac{1}{3} \quad (12)$$

The establishment of the dilute polymer solution theory in this decade is due largely to the experimental data obtained at the theta temperature or in its vicinity. For the same reason, the two facts mentioned above, that is, the molecular weight dependence of the  $\Theta$  value in the region of rather low molecular weight and the simultaneous vanishing of  $A_2$  and  $A_3$  at  $\Theta$ ,

will furnish a key for the determination of the functional form of  $\sigma$  and  $\kappa$  as functions of  $T$ ,  $M$ , and  $\phi$ .

Concerning the thermodynamic behavior in the more concentrated range, I refer to the interesting analysis by Zimm<sup>11</sup> and Zimm and Lundberg.<sup>12</sup> Based on the general solution theory of Kirkwood and Buff,<sup>13</sup> they derived an equation relating the pair distribution function  $F_2(i, j)$  to the activity of solvent  $a_0$ . This is

$$\frac{G_{00}}{V_0} = -\phi \frac{\partial}{\partial a_0} \left( \frac{a_0}{1 - \phi} \right) - 1 \quad (13)$$

with the definition

$$G_{00} = (1/V) \iint [F_2(i, j) - 1] d(i) d(j) \quad (14)$$

Since  $F_2(i, j)d(i) d(j)$  gives the probability of finding a solvent molecule  $i$  in the volume element  $d(i)$  at the position  $(i)$  and another solvent molecule  $j$  in  $d(j)$  at  $(j)$ , the quantity  $(1 - \phi)G_{00}/V_0$  represents the mean number of solvent molecules in excess of the random expectation in the neighborhood of a given solvent molecule. According to the analysis of the activity data of rubber-benzene and polystyrene-toluene systems by Zimm and Lundberg, the value of  $G_{00}/V_0$  exceeds unity over the whole range of concentration, indicating a strong clustering tendency. This observation is important, because the combination of the Flory or Huggins-Guggenheim-Miller theory with 14 leads to

$$\begin{aligned} G_{00}/V_0 &= 0 \text{ (Flory)} \\ &= 2/(z - 2) \text{ (Huggins-Guggenheim-Miller)} \end{aligned} \quad (15)$$

which can never exceed unity unless an unreasonably small value, for example, 3, is assigned for the lattice coordination number  $z$ . Accordingly, even in concentrated solutions the clustering effect of solvent molecules, which is undoubtedly in the closest connection with the chain connectivity, can no longer be neglected.

In this paper I shall develop a lattice model theory of concentrated polymer solutions and investigate the relation between the thermodynamic properties and the chain connectivity in the light of the presented theory. From a purely statistical mechanical point of view, there are at least three fundamental problems to be considered in the lattice model treatment of liquids or solutions: (1) the communal entropy, (2) the free volume, and (3) the combinatory problems.<sup>14,15</sup> The first problem is, of course, very important for detailed investigation of properties of pure liquids, but generally not for rather rough treatment of solution properties. Concerning the free volume problem, Prigogine<sup>16</sup> and his co-workers have recently developed an approximate treatment called the "average potential method"

and have applied it to liquid mixtures involving polymer solutions with considerable success. In the case of polymer solutions, however, the chief defect of existing theories seems to arise from the incomplete treatment of chain connectivity, as mentioned above. This is, of course, a typical configurational problem or, in the language of the lattice theory, the combinatorial problem. Thus in this paper I am principally concerned with the combinatorial problem, but not with the free volume problem.

### Basic Formalism

*Polymer solution as a special type of regular assembly.* Consider a polymer solution composed of  $N_0$  solvent molecules and of  $N_1$  polymer molecules of the same molecular weight  $M$ . Each polymer molecule consists of  $n$

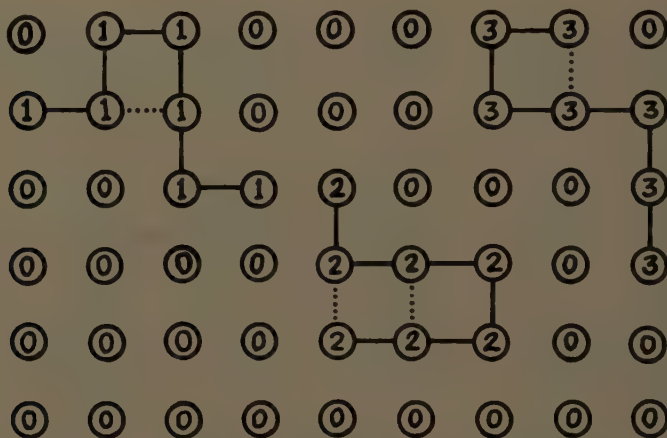


FIGURE 1. Schematic representation of polymer solutions.

identical segments, which are linearly connected by  $n - 1$  chemical bonds. A segment occupies one lattice point as well as a solvent molecule does. Later, I shall need to distinguish between two kinds of segment contact, that is, the intramolecular contact that is formed between two segments belonging to the same polymer molecule and the intermolecular contact. For this purpose, let us label the same index number  $j$  for all segments of the  $j$ th polymer molecule. In FIGURE 1 is presented a schematic illustration of the system. From FIGURE 1 it will be easily understood that the given system is nothing other than a special type of the so-called regular assemblies. In other words, the system is a regular solution composed of  $N_0$  molecules of type 0,  $n$  molecules of type 1,  $n$  molecules of type 2,  $\dots$ , and  $n$  molecules of type  $N_1$ , all having the same size. The number of components is thus counted as  $N_1 + 1$ . There is, of course, a remarkable specificity in the present system that distinguishes it from the regular solution of ordinary sense. This is the strong tendency to clustering of molecules



of the same kind or, in the usual language of the regular assembly statistics, the existence of an order of extremely high degree. This kind of peculiarity, however, will not obstruct the formal application of regular assembly theory to the present system in a decisive way.

*Short sketch of the regular solution theory.* According to the pseudoconfiguration method that was first proposed for treating the Ising ferromagnet by Kikuchi<sup>17</sup> and Kurata *et al.*,<sup>18</sup> the combinatory factor  $G$  of the *pair* approximation is formally written as

$$G = [N! / \prod_j (x_j N)!] \cdot (Q/P) \quad (16)$$

with

$$Q = \frac{1}{2} z N! / \prod_j \prod_k (y_{jk} \frac{1}{2} z N)! \quad (17)$$

for the regular assembly of multiple components. Here  $z$  is the coordination number of the lattice,  $x_j$  is the probability of finding a molecule of type  $j$  on a given lattice point, and  $y_{jk}$  is the probability of finding a molecule of type  $j$  on a given lattice point and another molecule of type  $k$  simultaneously on another given point adjacent to the former. By this definition Equation 18 is obtained:

$$x_j = \sum_k y_{jk} \quad (18)$$

The meaning of 16 is as follows. The first factor,  $N! / \prod_j (x_j N)!$ , is the combinatory factor of the *point* approximation, which obviously represents the number of distinguishable ways of distributing a given set of molecules, for example,  $x_j N$  molecules of type  $j$  and  $N$  molecules in total, on the lattice, irrespective of the number of molecular pairs. To obtain the combinatory factor corresponding to a fixed number of molecular pairs, it is necessary first to distribute the given set of molecular pairs,  $y_{jk} \frac{1}{2} z N$  pairs of type  $j = k$  and  $\frac{1}{2} z N$  pairs in total, on the lattice. This is done in  $Q$  distinguishable ways. However, the pairs are here independently distributed on the lattice; accordingly, these  $Q$  configurations include a large number of *wrong* configurations, in the sense that a certain lattice point is simultaneously occupied by more than one molecule. FIGURE 2a illustrates such wrong configurations in a one-dimensional assembly of two components, while FIGURE 2b illustrates a *right* configuration. Thus the combinatory factor  $G$  is obtained by picking out the *right* configurations from  $Q$  or multiplying  $Q$  by a selection factor  $\Gamma$ .

To evaluate  $\Gamma$ , we define the pseudoconfiguration  $P$  as the configuration consisting of the same number of molecules as that involved in the parent configuration  $Q$ . These are  $x_j z N$  molecules of type  $j$  (Equation 18) and

$zN$  molecules in total. Thus the number of pseudoconfigurations  $P$  is readily counted as

$$P = zN! / \prod_j (x_j zN)! \quad (19)$$

These  $P$  configurations also include a large number of *wrong* configurations of a nature similar to those included in  $Q$  in addition to the *right* configurations, whose number is obviously given by  $N! / \prod_j (x_j N)!$ . These are illustrated on FIGURE 2c and d. Thus if we use the selection factor of the

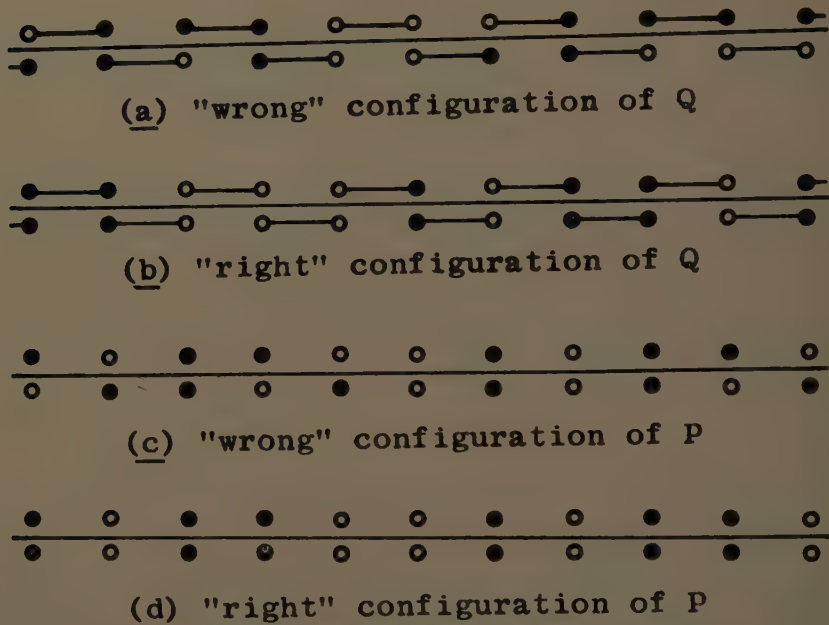


FIGURE 2. Parent configuration  $Q$  and its pseudoconfiguration  $P$ .

right configurations from  $P$  instead of  $\Gamma$  we can obtain 16 for the combinatory factor  $G$ . This approximation has been proved to be correct for such a singly connected lattice as the one-dimensional lattice or the dendritic lattice shown in FIGURE 3.<sup>18</sup>

The potential energy of the system is easily written as

$$E = \sum_j \sum_k (y_{jk} \frac{1}{2} zN) \varepsilon_{jk} \quad (20)$$

where  $\varepsilon_{jk}$  is the energy of each  $j = k$  contact. This energy  $E$  is then re-written in the form

$$E = \sum_j x_j \frac{1}{2} zN \varepsilon_{jj} + \sum_{j \neq k} y_{jk} zN \Delta \varepsilon_{jk} \quad (21)$$

with the aid of **18** and the definition that

$$\Delta\epsilon_{jk} = \epsilon_{jk} - \frac{1}{2}(\epsilon_{jj} + \epsilon_{kk}) \quad (22)$$

The most probable value of each  $y_{jk}$  is, of course, determined by minimizing the free energy of the system  $F = E - kT \ln G$  with respect to all independent variables, for example, all  $y_{jk}$ s but not  $y_{jj}$ s. This minimization yields

$$y_{jk}^2/y_{jj}y_{kk} = \exp(-2\Delta\epsilon_{jk}/kT) \quad (23)$$

which is usually called the equation of quasi-chemical equilibrium. Here  $k$  is the Boltzmann constant. If  $\Delta\epsilon_{jk}$ s are all negligibly small compared

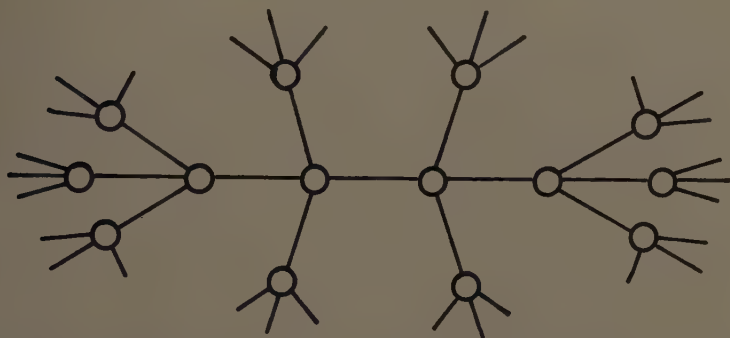


FIGURE 3. A dendritic lattice ( $z = 4$ ). Reproduced by permission of *The Journal of Chemical Physics*.<sup>18</sup>

to  $kT$ , the following solution of **23** is obtained:

$$y_{jk} = x_j x_k \quad (24)$$

which corresponds to the case of ideal or perfect solution. In general, **23** leads to a more complicated expression for  $y_{jk}$ , which is not reproduced here. Nevertheless, in the case of regular solutions, the most probable value of  $y_{jk}$  for solute-solute contacts tends to zero at infinitely high dilutions ( $x_0 \rightarrow 1$ ). This fact, while rather obvious, is important, especially in comparison with the following case of polymer solutions.

*Combinatory problem for polymer solutions.* Turning to the polymer solution defined above as a special type of regular assembly, the singlet probability  $x_j$  can be written as

$$x_0 = N_0/(N_0 + nN_1) = N_0/N, \quad (25)$$

$$x_j = n/N \quad \text{for } j = 1, 2, \dots, N_1$$

It is also obvious that each polymer molecule involves many intramolecular

segment contacts: at least  $n - 1$  corresponding to chemical bonds and, generally, more. Thus it may be stated

$$y_{11} \frac{1}{2} z N = (n - 1) + C \quad \text{for } j = 1, 2, \dots, N_1 \quad (26)$$

where  $C$  denotes the number of intramolecular segmental contacts in excess of the chemical bonds.

Concerning this quantity  $C$ , three properties are to be noted:

(1)  $C$  must have a very close relation to the average statistical dimension of polymer chain, which plays an essential role in the dilute solution theory. The value of  $C$  is naturally expected to vary with expansion of chains.

(2) The number of this kind of segmental contacts never tends to zero even at infinite dilution but reaches a finite value, depending on the nature of the given chain, such as flexibility or branching. In other words, to determine the equilibrium value of  $C$ , an equation other than the quasi-chemical equilibrium Equation 23 is needed. In this connection it is to be noted that in the case of rigid polymer solutions  $C$  is definitely a structural constant that depends on the geometrical shape or the compactness of the molecule. These facts indicate that in the present formalism the quantity  $y_{jj}$  for each molecule should be regarded as a structural quantity rather than a variable.

(3) The existence of  $C$  in excess of  $n - 1$  chemical bonds generally destroys the single connectivity of the chain; in other words, the chain cannot be separated into two fragments by removal of one of the  $n - 1 + C$  bonds unless  $C = 0$ . Since the pseudoconfiguration method, 19, is rigorously applicable to singly connected systems alone, these  $C$  excess bonds must be excluded from the pseudoconfigurational treatment.

Keeping the above three comments in mind, let us proceed to calculate the combinatory factor  $G$  of the polymer solution. The number of distinguishable ways of distributing a given set of molecular or segmental contacts on the lattice is straightforwardly written from 17 and 26 in the form

$$Q = \frac{\frac{1}{2} z N!}{(y_{00} \frac{1}{2} z N)! \prod_{j=1}^{N_1} (y_{0j} \frac{1}{2} z N)! \prod_{j=1}^{N_1} \prod_{\substack{k=1 \\ j \neq k}}^{N_1} (y_{jk} \frac{1}{2} z N)! [C!(n - 1)!]^{N_1}} \quad (27)$$

Here the chemical bonds were treated separately from the excess intramolecular segmental contacts. Because of the identity of the  $N_1$  polymer molecules Equation 28 can be written:

$$y_{0j} = y_{01} \quad \text{and} \quad y_{jk} = y_{11} \quad (28)$$

and then Equation 27 rewritten into a more simple form:

$$Q = \frac{\frac{1}{2} z N!}{(y_{00} \frac{1}{2} z N)! (y_{01} \frac{1}{2} z N)!^{N_1} (y_{11} \frac{1}{2} z N)!^{N_1(N_1-1)} [C!(n - 1)!]^{N_1}} \quad (29)$$

As for the mutual relation of variables, Equation 30 is obtained from 18, 25, and 26

$$\sum_{k \neq j} y_{jk} = x_j - y_{jj} = (N_0/N) - y_{00} \quad \text{if } j = 0, \\ = q/N \quad \text{if } j = 1, 2, \dots, N_1 \quad (30)$$

with the abbreviation that

$$q = n - (2/z)(n - 1 + C) \quad (31)$$

Then, using 28, we get

$$y_{00} = (N_0/N) - N_1 y_{01}, \\ (N_1 - 1) y_{11} = (q/N) - y_{01} \quad (32)$$

The number of molecules or fragments of the pairs used in the above  $Q$  configuration is as follows:  $zN_0$  of the solvent molecules,  $zq$  of the fragments of the intermolecular segment contacts for each polymer molecule,  $2(n - 1)$  of the fragments of the chemical bonds, and  $2C$  of the fragments of the excess intramolecular segment contacts. Thus applying the pseudoconfigurational method to the remaining part of  $Q$  except  $C$  term, we obtain

$$P = \frac{1/2 z N!}{(C!)^{N_1} (1/2 z N - C)!} \cdot \frac{(zN - 2C)!}{z N_0! (zq!)^{N_1} [2(n - 1)!]^{N_1}} \quad (33)$$

then, substituting 29, 33, and 25 into 16, we obtain

$$G = \frac{N!}{N_0! (n!)^{N_1}} \cdot \frac{z N_0! (zq!)^{N_1}}{(y_{00} 1/2 z N)! (y_{01} 1/2 z N!)^{N_1} (y_{11} 1/2 z N!)^{N_1 (N_1 - 1)}} \\ \cdot \frac{(1/2 z N - C)! [2(n - 1)!]^{N_1}}{(n - 1)!^{N_1} (zN - 2C)!} \cdot \frac{1}{N_1!} \quad (34)$$

where the last factor  $1/N_1!$  represents, of course, the indistinguishability of  $N_1$  polymer molecules.

The energy of the system is obviously given by

$$E = y_{00} 1/2 z N \varepsilon_{00} + \sum_{j=1}^{N_1} (y_{0j} + y_{j0}) 1/2 z N \varepsilon_{0j} \\ + \sum_{j=1}^{N_1} \sum_{\substack{k=1 \\ j \neq k}}^{N_1} y_{jk} 1/2 z N \varepsilon_{jk} + N_1 C \varepsilon_{jj} \quad (35)$$

Because of the identity of all segments, we can simply put

$$\varepsilon_{0j} = \varepsilon_{01} \quad \text{and} \quad \varepsilon_{jk} = \varepsilon_{jj} = \varepsilon_{11} \quad (36)$$

and rewrite the 35 as

$$E = 1/2 z N_0 \varepsilon_{00} + [1/2 z n - (n - 1)] N_1 \varepsilon_{11} + y_{01} z N N_1 \Delta \varepsilon \quad (37)$$



with

$$\Delta\epsilon = \epsilon_{01} - \frac{1}{2}(\epsilon_{00} + \epsilon_{11}) \quad (38)$$

The Equations **34** and **38** give the expression for the free energy of the system in terms of an independent variable  $y_{01}$ . Thus, minimizing the free energy with respect to  $y_{01}$ , we again find the equation of quasi-chemical equilibrium,

$$y_{01}^2/y_{00}y_{11} = \exp(-2\Delta\epsilon/kT) \quad (39)$$

which indicates, as usual, that the larger value of  $\Delta\epsilon$  is followed by the higher clustering tendency of the same kind of molecules. This kind of clustering tendency, however, is of minor importance in the polymer solution theory when compared with another extremely strong clustering tendency due to the chain connectivity. In other words, the adoption of the approximate solution of **39** corresponding to the Bragg-Williams approximation may be acceptable as a good approximation. Thus we obtain from **39** and **32**:

$$y_{00} = N_0^2/NN_q, \quad y_{01} = N_0q/NN_q, \quad \text{and} \quad y_{11} = q^2/NN_q \quad (40)$$

with the abbreviation;

$$N_q = N_0 + qN_1 \quad (41)$$

Then, substituting these  $y$ s into **34** and **37**, we obtain

$$G = \frac{N!}{N_0!(n!)^{N_1}} \cdot \frac{[\frac{1}{2}zN - (n-1+C)N_1]!(n-1)!^{N_1}}{(\frac{1}{2}zN - CN_1)!} \cdot \frac{1}{N_1!} \quad (42)$$

and

$$E = \frac{1}{2}zN_0\epsilon_{00} + [\frac{1}{2}zn - (n-1)]N_1\epsilon_{11} + (zN_0qN_1/N_q)\Delta\epsilon \quad (43)$$

As is easily seen, the first two terms in  $E$  represent the energies of pure solvent and polymer. The configurational entropy and the energy of mixing of the system are then written in the form

$$\begin{aligned} S = & -k\{N_0 \ln(1-\phi) + N_1 \ln \phi \\ & - [\frac{1}{2}zN - (n-1+C)N_1] \ln[1 - 2z^{-1}(1 - n^{-1} + Cn^{-1})\phi] \\ & - N_1(n-1) \ln[2z^{-1}(1 - n^{-1})\phi] \\ & + (\frac{1}{2}zN - CN_1) \ln[1 - 2C(zn)^{-1}\phi]\} \end{aligned} \quad (44)$$

and

$$E = (zN\Delta\epsilon) \frac{[1 - 2z^{-1}(1 - n^{-1} + Cn^{-1})]\phi(1-\phi)}{1 - 2z^{-1}(1 - n^{-1} + Cn^{-1})\phi} \quad (45)$$

where  $\phi$  is the volume fraction of polymer,

$$\phi = nN_1/(N_0 + nN_1) \quad (46)$$

The parameter  $C$  is generally expected to be a function of  $\phi$ ; therefore the entropy and the heat of dilution are respectively obtained from 44 and 45 as

$$\bar{S}_0 = -R \left[ \ln(1 - \phi) - \left( \frac{1}{2}z + \phi^2 \frac{d(C/n)}{d\phi} \right) \times \ln \left( \frac{1 - 2z^{-1}(1 - n^{-1} + Cn^{-1})\phi}{1 - 2z^{-1}Cn^{-1}\phi} \right) \right] \quad (47)$$

and

$$\bar{H}_0 = (zN_A\Delta\mathcal{E}) \frac{[1 - 2z^{-1}(1 - n^{-1} + Cn^{-1})]^2 + 2z^{-1}(1 - \phi)^2 \frac{d(C/n)}{d\phi}}{[1 - 2z^{-1}(1 - n^{-1} + Cn^{-1})\phi]^2} \phi^2 \quad (48)$$

ignoring the difference between  $E$  and  $H$ . These two are the basic equations of the present theory. Here  $N_A$  represents the Avogadro number. As is easily seen, these equations reduce to the Huggins-Miller-Guggenheim equations when  $C = 0$ .

#### *Systems Involving a Constant Number of Intramolecular Segmental Contacts*

*Lattice solutions of rigid polymers.* According to the definition, the quantity  $C$  must be a simple geometric constant in the case of rigid polymers. In such a case, therefore, we can always neglect the concentration dependence of  $C$  and obtain

$$\bar{S}_0 = -R \left[ \ln(1 - \phi) + \frac{1}{2}z \ln \left( \frac{1 - 2z^{-1}(1 - n^{-1} + Cn^{-1})\phi}{1 - 2z^{-1}Cn^{-1}\phi} \right) \right] \quad (49)$$

$$\bar{H}_0 = (zN_A\Delta\mathcal{E}) \frac{[1 - 2z^{-1}(1 - n^{-1} + Cn^{-1})]^2 \phi^2}{[1 - 2z^{-1}(1 - n^{-1} + Cn^{-1})\phi]^2} \quad (50)$$

Accordingly, the functions  $\sigma$  and  $\kappa$  defined by 1 and 2 are written as

$$\sigma = \frac{1}{\phi^2} \left[ \frac{1}{2}z \ln \left( \frac{1 - 2z^{-1}Cn^{-1}\phi}{1 - 2z^{-1}(1 - n^{-1} + Cn^{-1})\phi} \right) - \left( 1 - \frac{1}{n} \right) \phi \right] \quad (51)$$

and

$$\kappa = \left( \frac{zN_A\Delta\mathcal{E}}{RT} \right) \left( \frac{1 - 2z^{-1}(1 - n^{-1} + Cn^{-1})}{1 - 2z^{-1}(1 - n^{-1} + Cn^{-1})\phi} \right)^2 \quad (52)$$

respectively. Hence we have

$$\sigma_0 = \frac{1}{z} \left( 1 - \frac{1}{n} \right) \left( 1 - \frac{1}{n} + 2 \frac{C}{n} \right) \quad (53)$$

$$\kappa_0 = \left( \frac{z\Delta\mathcal{E}}{kT} \right) \left( 1 - \frac{2}{z} \left( 1 - \frac{1}{n} + \frac{C}{n} \right) \right)^2 \quad (54)$$

On the other hand, we already know the rigorous value of  $\sigma_0$  of several lattice chains, which were obtained by elementary geometric computation of the excluded volume of the chain.<sup>19,20</sup> These are shown in TABLES 1 and 2. The shape effect on  $\sigma_0$  is, in fact, dominant for both short and long chains.

In the present theory this kind of shape effect is expressed in terms of  $C$ , which can be easily evaluated from a molecular figure. As shown in TABLES 1 and 2, the values of  $\sigma_0$  calculated from **53** are generally in good agreement with the rigorous values, in spite of the simplicity of the equation. There are, however, some systematic deviations of the calculated values of  $\sigma_0$  from its rigorous values. As is easily seen from TABLES 1 and 2, the present theory often predicts an overestimated value for  $\sigma_0$ , and the overestimation becomes large for molecules of high compactness. Thus, for example, in the case of a cubical molecule of high molecular weight, the theory predicts a value, 0.833, for  $\sigma_0$ , which is considerably higher than the rigorous asymptotic value, 0.500. A value of  $\sigma_0$  higher than 0.500 is also obtained for the third example in TABLE 2: that is, a ribbon molecule with three-segment width in the two-dimensional square lattice. Since the second virial coefficient of athermal solutions is necessarily positive, such predictions of high value of  $\sigma_0$  are obviously wrong. In this meaning, the range of application of the present theory is restricted within the range that  $0 \leq C/n \leq (z - 2)/4$  or, more seriously, within the region of small value of  $C/n$  as 0.2 or 0.5 depending on  $z$ . It is also obvious from **53** that the present theory cannot predict the shape effect of bent molecules unless they involve at least one intramolecular segmental contact. The third and the fifth examples in TABLE 1 and the fourth example in TABLE 2 illustrate this effect. To treat this kind of bent effect, it is necessary to construct the combinatory factor of the system in a more detailed manner. For such treatment the reader may refer to theories presented by Guggenheim and McGlashan<sup>21</sup> and by Kurata *et al.*<sup>19</sup> However, apart from the mathematical interest, the bent effect is practically small, as shown in the tables, and so this defect of the present theory is probably not serious for most practical purposes.

*Theta solvent systems.* Another interesting example of a system with constant  $C$  is the so-called *theta* solvent system. According to the theory of excluded volume effect,<sup>22-24</sup> polymer molecules generally take a more or less expanded form in dilute solution, owing to the volume effect of the segments. This expansion effect, however, vanishes at the *theta* temperature, at which the second osmotic virial coefficient tends to zero, and the polymer molecules reduce to the so-called unperturbed Gaussian chain. It is also known that the volume effect generally diminishes with increasing concentration and most probably vanishes in the pure polymer state. These facts suggest that at the *theta* temperature the statistical dimension of the polymer chain is kept constant at its unperturbed dimension over the whole

TABLE 1  
RELATION BETWEEN THE ENTROPY PARAMETER  $\sigma_0$  AND THE MOLECULAR SHAPE  
Short Chains

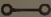












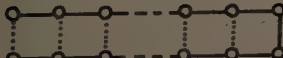

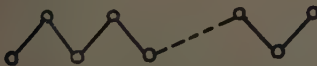
Mol. shape	$n$	$C$	Two-dimens. square lattice $z = 4$		Simple cubic lattice $z = 6$	
			Eq. 53	Rigorous	Eq. 53	Rigorous
	2	0	0.063	0.063	0.042	0.042
	3	0	0.111	0.111	0.074	0.074
	3	0	0.111	0.115	0.074	0.079
	4	0	0.141	0.141	0.094	0.094
	4	0	0.141	0.172	0.094	
	4	1	0.235	0.219	0.156	0.156
	5	0	0.160	0.160	0.107	0.107
	5	1	0.240	0.235	0.160	
	8	0	0.191	0.191	0.128	0.128
	8	5	—	—	0.310	0.289
	12	0	0.210	0.210	0.140	0.140
	12	9	—	—	0.369	0.337

TABLE 2  
RELATION BETWEEN THE ENTROPY PARAMETER  $\sigma_0$  AND THE MOLECULAR SHAPE  
Long Chains

Mol. shape ( $n = \infty$ )	$\frac{C}{n}$	Two-dimens. square lattice $z = 4$		Simple cubic lattice $z = 6$	
		Eq. 53	Rigorous	Eq. 53	Rigorous
	0	0.250	0.250	0.167	0.167
	$\frac{1}{2}$	0.500	0.438	0.333	0.333
	$\frac{2}{3}$	0.583	0.472	0.388	0.388
	0	0.250	—	0.167	0.208

range of concentration because of the lack of the excluded volume effect. Thus, at least in an approximate sense, theta solvent solutions may be characterized as systems of constant  $C$ .

For the sake of convenience, let us now define the coiling probability  $g$  by

$$C = \frac{1}{2}zn g \quad (55)$$

The  $g$  gives the probability that, if a segment of a molecule is on a given lattice point, another segment of the same molecule will be found on a nearest-neighbor site of the former. Here we neglect a minor end effect. The  $g$  is, of course, a function of  $T$ ,  $M$ , and  $\phi$ , in general; but at  $T = \Theta$ , it would be a function of  $M$  alone. We denote it by  $g_0(\Theta, M)$  or simply  $g_0$ .

Using this probability  $g$  we can rewrite 51 and 52 into

$$\begin{aligned} \chi(\Theta, M, \phi) &= \sigma(\Theta, M, \phi) + \kappa(\Theta, M, \phi) \\ &= \frac{1}{\phi^2} \left[ \frac{1}{2} z \ln \left( \frac{1 - g_0 \phi}{1 - (2z^{-1} + g_0) \phi} \right) - \phi \right] \\ &\quad + \frac{z \Delta \varepsilon}{k} \cdot \frac{1}{\Theta} \left( \frac{1 - 2z^{-1} - g_0}{1 - (2z^{-1} + g_0) \phi} \right)^2 \end{aligned} \quad (56)$$

Then we find:

$$\psi_0(\Theta, M) \equiv \frac{1}{2} - \sigma_0(\Theta, M) = \frac{1}{2}(1 - 2z^{-1} - 2g_0) \quad (57)$$

$$\kappa_0(\Theta, M) = (z \Delta \varepsilon / k \Theta) (1 - 2z^{-1} - g_0)^2 \quad (58)$$

Hence remembering the definition of the theta temperature (11) we obtain

$$\Theta = \frac{2z \Delta \varepsilon}{k} \left( \frac{z - 2}{z} \right) \frac{[1 - (z/z - 2)g_0]^2}{1 - 2(z/z - 2)g_0} \quad (59)$$

This equation indicates that the molecular weight dependence of  $\Theta$  is a second-order effect of  $g_0(\Theta, M)$  and is generally small, in accordance with the experimental knowledge.

For the corresponding monomer solution, we obtain from 11, 53, and 54

$$\Theta = 2z \Delta \varepsilon / k \quad (60)$$

by putting  $n = 1$  and  $C = 0$ . This implies that the  $\Theta$  of very low molecular substances is some 20 to 50 per cent (depending on the value of  $z$ ) above the  $\Theta$  of very high polymers of the same chemical species. If the latter is near room temperature, about 300° K., this difference ranges from 60° to 150° C. Thus even if  $1/n$  is as small as 0.01, the end effect on  $\Theta$  value still counts 1°. In the case of real polymers the molecule usually has an end group that is different from intermediate ones, and this end segment effect may enhance the variation of  $\Theta$  as the molecular weight is decreased.<sup>8</sup>



Now, substituting **59** into **56** for elimination of  $\Theta$  and expanding **56** in the form of **8** we obtain

$$\chi_1(\Theta, M) = (2z - \frac{8}{3})/z^2 + [(z - 4)/z]g_0 - g_0^2 \quad (61)$$

$$\chi_2(\Theta, M) = (6z - 10)/z^3 + [(6z - 20)/z^2]g_0 + [(\frac{3}{2}z - 12)/z]g_0^2 - 2g_0^3 \quad (62)$$

TABLE 3  
THEORETICAL VALUES OF THERMODYNAMIC QUANTITIES AT THE THETA TEMPERATURE

$z$	$g_0$	$\psi_0$	$\chi_0$	$\chi_1$	$\chi_2$	$\chi(\phi = 1)$	$\kappa(\phi = 1)/\kappa_0$
4	0	0.250	(0.500)	0.333	0.219	1.386	4.00
	0.05	0.200		0.330	0.227	1.482	4.94
	0.10	0.150		0.323	0.227	1.559	6.25
	0.15	0.100		0.310	0.216	1.590	8.16
	0.20	0.050		0.293	0.193	1.517	11.11
6	0	0.333	(0.500)	0.259	0.121	0.967	2.25
	0.10	0.233		0.283	0.158	1.115	3.11
	0.15	0.183		0.287	0.170	1.180	3.75
	0.20	0.133		0.286	0.173	1.229	4.59
	0.25	0.083		0.280	0.169	1.243	5.76
8	0	0.375	(0.500)	0.208	0.074	0.817	1.78
	0.10	0.275		0.248	0.116	0.953	2.37
	0.15	0.225		0.261	0.133	1.018	2.78
	0.20	0.175		0.268	0.146	1.077	3.31
	0.25	0.125		0.271	0.152	1.122	4.00
$\infty$	0	0.500	(0.500)	0	0	0.500	1.00
	0.10	0.400		0.090	0.013	0.605	1.23
	0.20	0.300		0.160	0.044	0.718	1.56
	0.30	0.200		0.210	0.081	0.836	2.04
	0.40	0.100		0.240	0.112	0.944	2.78
Complete vanishing of virial coefficients			0.500	0.333	0.250	$\infty$	—

It has been established in the past several years that the polystyrene-cyclohexane system is well specified by the following parameter values:<sup>25-30</sup>

$$\Theta = 307^\circ \text{K.} \quad \text{and} \quad \psi_0 = 0.19 - 0.23 \quad (63)$$

TABLE 3 shows the values of  $\psi_0$ ,  $\chi_1$ , and  $\chi_2$  calculated by **57**, **61**, and **62**, together with the used values of  $z$  and  $g_0$ . From TABLE 3 the following combinations of parameter values may be adopted as the best choice for the polystyrene-cyclohexane system:

$$\begin{aligned} z = 4 \quad & \text{and} \quad g_0(\Theta, M) = 0.02 - 0.07, \\ z = 6 \quad & \text{and} \quad g_0(\Theta, M) = 0.10 - 0.15, \\ z = 8 \quad & \text{and} \quad g_0(\Theta, M) = 0.15 - 0.20 \end{aligned} \quad (64)$$

It is to be noted here that the predicted values of  $(\frac{1}{3} - \chi_1)$ , hence the third virial coefficient  $A_3$  is in fact very small at theta temperature, although it does not completely vanish.

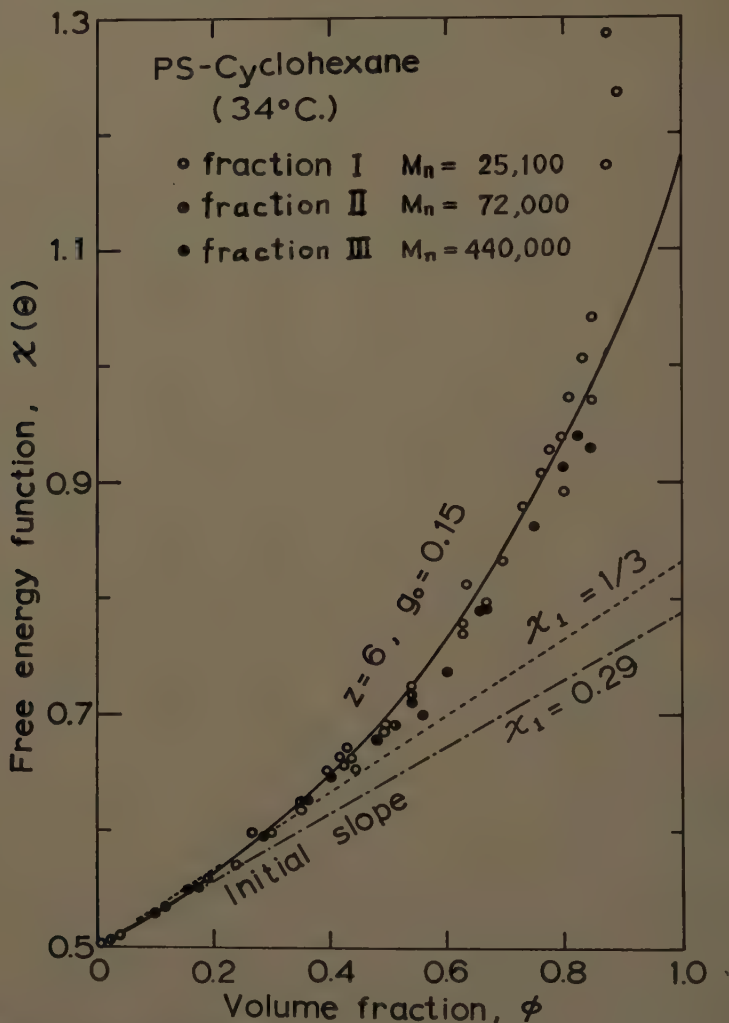


FIGURE 4. Free energy function  $\chi$  for polystyrene-cyclohexane system at 34° C. and its theoretical values.

After the values of  $z$  and  $g_0$  are once determined, the values of  $\sigma$ ,  $\kappa$ , and  $\chi$  can easily be calculated over the whole range of concentration, with the aid of 56 and 59. FIGURES 4 and 5 show the results in comparison with the recent experimental data obtained by Krigbaum and Geymer.<sup>9</sup> Agreement between theory and experiment is satisfactory over a wide range of concentration, but an appreciable discrepancy is observed in the concen-

trated region higher than 60 or 80 per cent of volume fraction, especially in the case of the heat function  $\kappa$ . In this region, however, the system is probably in the glassy state or in a transition state, as pointed out by Krigbaum and Geymer.

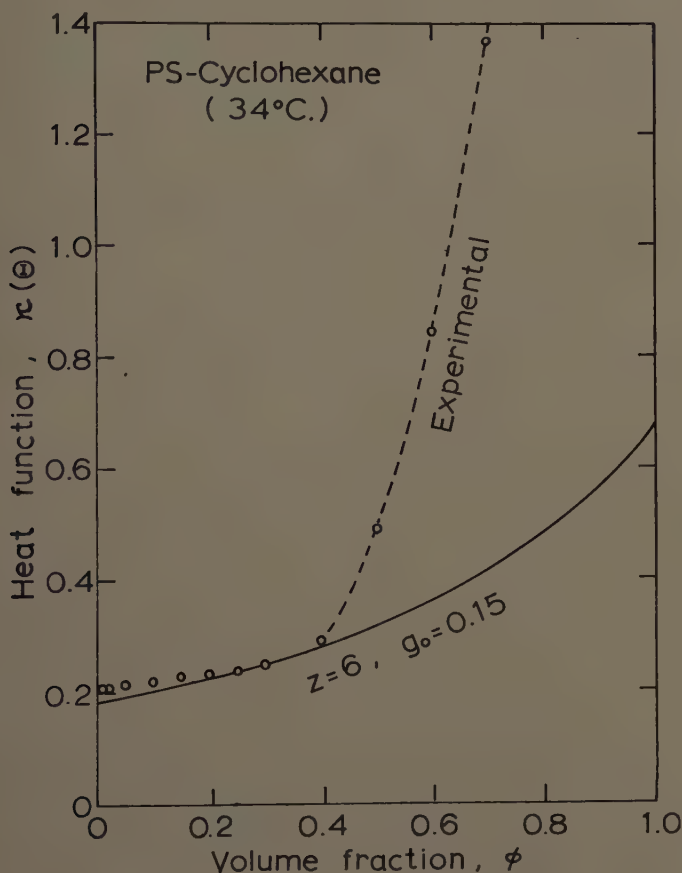


FIGURE 5. Heat function  $\kappa$  for polystyrene-cyclohexane system at 34° C. and its theoretical values.

#### Nature of the Coiling Probability

*Short-range coiling and long-range coiling.* Let us now investigate the nature of the coiling probability  $g(T, M, \phi)$ . As may be easily understood from FIGURE 6, the coiling of chain occurs in two different modes, the short-range mode and the long-range one. The short-range coiling corresponds to contacts between two neighbor segments, as shown in FIGURE 6a and b, and this may be determined chiefly by such short-range effects as the restriction on bond angle and the steric hindrance for rotation around bond axis. On the other hand, the long-range coiling corresponds to contacts between

far distant segments, as shown in FIGURE 6c, and this must be closely connected with the problem of excluded volume effect. Thus it may be expected that these two modes of coiling are considerably different from each other in their dependence on  $M$ ,  $T$ , and  $\phi$ .

Let us first consider the molecular weight dependence of these coiling probabilities. Denote by  $\gamma'$  the probability that a sequence of four segments finds a coiled form or square as given in FIGURE 6a. This probability

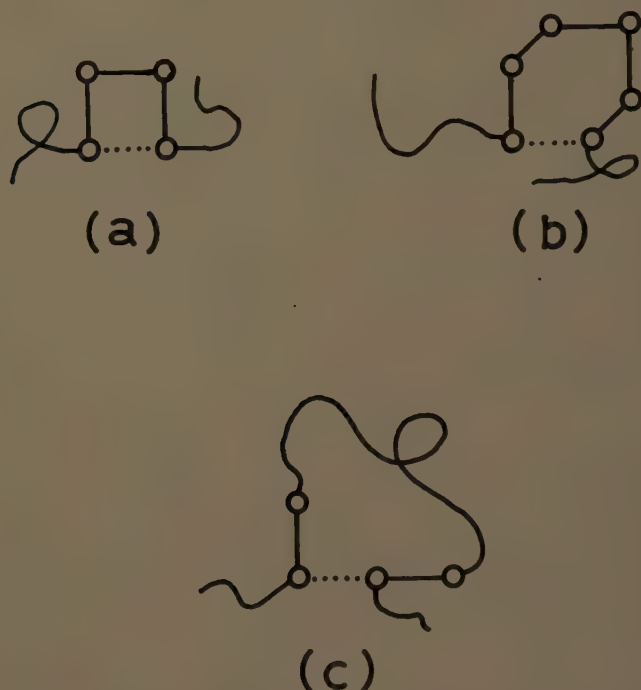


FIGURE 6. Short-range and long-range modes of chain coiling.

$\gamma'$  is essentially identical with the probability of appearance of *cis* configuration in the usual *cis-trans* rotational problem and may be independent of the molecular weight of chain. As there are  $n - 3$  four-segment sequences in a linear chain, we have

$$\frac{1}{2}zng_s' = \gamma'(n - 3) \approx \gamma'n \quad (65)$$

Similarly, for the six-segment sequences shown in FIGURE 6b we have

$$\frac{1}{2}zng_s'' = \gamma''(n - 5) \approx \gamma''n \quad (66)$$

and so on. Therefore, adding up all these contributions, we obtain

$$\frac{1}{2}zng_s = (\gamma' + \gamma'' + \dots)n = \gamma n \quad (67)$$

Equation 67 indicates that the coiling probability corresponding to the short-range mode,  $g_s$ , is approximately independent of the molecular weight.

On the contrary, the coiling probability corresponding to the long-range mode,  $g_l$ , can be calculated in the following way. Assume an equivalent sphere model, for instance, in which the polymer chain is replaced by a uniform distribution of unconnected segments within a sphere whose dimension is chosen to give the correct radius of gyration. This is, of course,

$$\langle S^2 \rangle = na^2/6 \quad (68)$$

where  $a$  is the bond length or, more precisely, an *effective* bond length, which is determined by the short-range interferences. As the volume of the equivalent sphere is

$$V^* = (4\pi/3)(5/18)^{3/2}(n^{1/2}a)^3 \quad (69)$$

the number of segment contacts in this sphere can be obtained as

$$\frac{1}{2}zn g_l = \tau n^2/V^* = (\frac{3}{4}\pi)(18/5)^{3/2}(\tau/a^3)n^{1/2} \quad (70)$$

where  $\tau$  represents the volume of an effective segment. This calculation can be refined by using a segment distribution of Gaussian form instead of the uniform distribution<sup>22</sup> or by using an equivalent ellipsoid instead of a sphere, or both.<sup>31</sup> Such modifications, however, do not alter the proportionality of  $g_l$  to  $n^{-1/2}$ .

According to the theory of random chain statistics,<sup>32,33</sup> the probability of finding a segment, such as  $j$ , in a volume element  $dv$  neighboring another given segment, such as  $i$ , is written as

$$P(O_{ij})dv = (\frac{3}{2}\pi)^{3/2}a^{-3}(j-i)^{-3/2}dv \quad (71)$$

The total number of segment contacts in a molecule is then approximately evaluated by integrating 71 over all possible pairs of segments, that is,

$$\begin{aligned} \frac{1}{2}zn g &= \int_{\text{neighbor cells}} dv \cdot \int_1^n \int_{i+2}^n P(O_{ij}) di dj \\ &= (z-2)v_0 \cdot (\frac{3}{2}\pi a^2)^{3/2} \int_2^n \frac{n-x}{x^{3/2}} dx \end{aligned} \quad (72)$$

where  $v_0$  is the volume of a lattice point (or the volume of a solvent molecule). Hence we have

$$g = \left( \frac{z-2}{z} \right) \left( \frac{3}{2\pi} \right)^{3/2} \frac{4v_0}{a^3} \left( \frac{1}{\sqrt{2}} - \frac{2}{\sqrt{n}} \right) \quad (73)$$

The first term in the last parentheses represents the short-range mode of coiling, while the second term proportional to  $n^{-1/2}$  represents the long-range one. Accordingly, we may conclude that the method of coupling of two



modes of coiling,  $g_s$  and  $g_l$ , is not addition but subtraction, in contrast to simple presumption. This indicates that the segment contact counted as the long-range mode, **70**, is a correction for an overevaluation of the contact number in the short-range-type calculation, **67**.

In the presence of the excluded volume effect the polymer chain takes a more or less expanded form from its unperturbed dimension, depending on temperature and concentration. We define a linear expansion factor  $\alpha$  by

$$\alpha^2 = \langle L^2 \rangle / \langle L^2 \rangle_0 = \langle L^2 \rangle / na^2 \quad (74)$$

where  $\langle L^2 \rangle$  represents the mean square end-to-end distance of real molecule. If a uniform expansion of the polymer coil is assumed for simplicity, we obtain

$$\frac{1}{2}zng_l = \text{const} \times (v_0/a^3)\alpha^{-3}n^{1/2} \quad (75)$$

instead of **70** for the long-range mode of coiling. On the other hand, the short-range mode of coiling is essentially independent of this kind of chain expansion. Accordingly, we obtain

$$g(T, M, \phi) = c(z - 2/z)(v_0/a^3)[1 - (c'/\alpha^3 n^{1/2})] \quad (76)$$

instead of **73**. Here  $c$  and  $c'$  are numerical constants. The coiling probability  $g(T, M, \phi)$  is thus expected to increase as  $n$  and  $\alpha$  are increased.

*Second virial coefficient,  $A_2$ .* Substituting **57** and **58** into **9** and neglecting a term of order of  $g^2$  we obtain

$$A_2 = \frac{\bar{v}^2}{2V_0} \left(1 - \frac{2}{z} - 2g\right) \left(1 - \frac{\Theta}{T}\right) \quad (77)$$

where  $\bar{v}$  is the specific volume of polymer and  $V_0$  is the molar volume of solvent. As the coiling probability  $g$  is an increasing function of  $n$ , as mentioned above, the second virial coefficient  $A_2$  is decreased as the molecular weight of polymer is increased. Similarly, the quantity  $A_2/(1 - T^{-1}\Theta)$  is also a decreasing function of  $\alpha$ . This behavior of **77** is favorably compared with that of Equation **78**, which is obtained by the distribution function theory of dilute solutions:<sup>34-37</sup>

$$A_2 = \frac{N_A \tau}{2m_0^2} h(z) \left(1 - \frac{\Theta}{T}\right) \quad (78)$$

with

$$h(z) = 1 - 2.865z + 18.51z^2 - \dots \quad (79)$$

$$z = (\frac{3}{2}\pi)^{3/2}(\tau/a^3)[1 - (\Theta/T)]n^{1/2} \quad (80)$$

Here  $\tau$  and  $m_0$  represent the volume and the molar weight of effective segment, and  $N_A$  is the Avogadro number. In this formalism (**78**), the

function  $h(z)$  is unity at theta temperature, which monotonously decreases with increasing temperature, or  $\alpha(z)$ .

*Zimm's clustering function,  $G_{00}$ .* As mentioned earlier, the coiling probability  $g$  consists of two parts, and the long-range part diminishes with increasing  $n$ . In a crude approximation, therefore, we may neglect the long-range mode of coiling and assume the quantity  $g$  to be a constant parameter independent of  $T$ ,  $M$ , and  $\phi$ .

With this assumption we can easily calculate Zimm's clustering function  $G_{00}$  of an athermal solution<sup>11</sup> by using **13** and **56**. The result is

$$\frac{G_{00}}{V_0} = \frac{2 + 2zg - g(2 + zg)\phi}{z - 2 - 2zg + g(2 + zg)\phi} \quad (81)$$

which yields

$$\lim_{\phi=0} \frac{G_{00}}{V_0} = \frac{2 + 2zg}{z - 2 - 2zg} \quad (82)$$

at infinite dilution. The substitution of the parameter values,  $z = 6$  and  $g = 0.15$ , into **81** predicts the following values for  $G_{00}/V_0$ :

$$G_{00}/V_0 = 1.72 \quad (\text{at } \phi = 0); \quad 1.48 \quad (\text{at } \phi = 1) \quad (83)$$

The quantity  $G_{00}/V_0$  is slightly decreased with increasing concentration, but still kept above unity even at  $\phi = 1$ . This result is in good accordance with Zimm and Lundberg's observation.<sup>12</sup>

For a more complete description of the solution properties we shall need to investigate the concentration dependence of the coiling probability in detail. This is the problem of the excluded volume effect in concentrated solutions; it will be a subject of the next step of the present work.

Finally, a theory similar to mine has been presented by Staverman,<sup>38</sup> which leads to

$$\sigma_0 = \frac{1}{z} \left( 1 - \frac{1}{n} + \frac{C}{n} \right)^2 \quad (84)$$

corresponding to **53**. However, the Staverman equation (**84**) also stands an overestimation of  $\sigma_0$ , as well as the present theory (**53**) does.

#### Acknowledgment

I thank Walter H. Stockmayer for his stimulating discussions and kind hospitality at Massachusetts Institute of Technology, Cambridge, Mass.

#### References

1. FLORY, P. J. 1942. *J. Chem. Phys.* **10**: 51.
2. LONGUET-HIGGINS, H. C. 1953. *Discussions Faraday Soc.* **15**: 73.
3. BUFF, F. P. & R. BROUT. 1955. *J. Chem. Phys.* **23**: 458.

4. FLORY, P. J. 1953. Principles of Polymer Chemistry. Cornell Univ. Press. Ithaca, N. Y.
5. TOMPA, H. 1956. Polymer Solutions. Butterworths Scientific Publications. London, England.
6. HUGGINS, M. L. 1942. Ann. New York Acad. Sci. **43**(1): 1.
7. MILLER, A. R. 1943. Proc. Cambridge Phil. Soc. **39**: 54, 131. See also, MILLER, A. R. 1948. The Theory of Solutions of High Polymers. Oxford Univ. Press. London, England; GUGGENHEIM, E. A. 1952. Mixtures. Oxford Univ. Press. London, England.
8. MCINTYRE, D., J. H. O'MARA & B. C. KONOUCK. 1959. J. Am. Chem. Soc. **81**: 3498.
9. KRIGBAUM, W. R. & D. O. GEYMER. 1959. J. Am. Chem. Soc. **81**: 1859.
10. FLORY, P. J. & H. DAOUST. 1957. J. Polymer Sci. **25**: 429.
11. ZIMM, B. H. 1953. J. Chem. Phys. **21**: 934.
12. ZIMM, B. H. & J. L. LUNDBERG. 1956. J. Phys. Chem. **60**: 425. See also ZIMM, B. H. 1959. Revs. Modern Phys. **31**: 123.
13. KIRKWOOD, J. G. & F. P. BUFF. 1951. J. Chem. Phys. **19**: 774.
14. KIRKWOOD, J. G. 1950. J. Chem. Phys. **18**: 380.
15. HILL, T. L. 1956. Statistical Mechanics. Chap. 8. McGraw-Hill. New York, N. Y.
16. PRIGOGINE, I. 1957. The Molecular Theory of Solutions. North-Holland.
17. KIKUCHI, R. 1951. Phys. Rev. **81**: 988.
18. KURATA, M., R. KIKUCHI & T. WATARI. 1953. J. Chem. Phys. **21**: 434.
19. KURATA, M., M. TAMURA & T. WATARI. 1955. J. Chem. Phys. **23**: 991.
20. ZIMM, B. H. 1947. ACS Meeting. Sept. 1947. See, HILDEBRAND, J. L. & R. L. SCOTT. 1950. The Solubility of Nonelectrolytes. 3rd ed. XX: 364-365. Reinhold. New York.
21. GUGGENHEIM, E. A. & M. L. McGLASHAN. 1950. Proc. Roy. Soc. (London). **A203**: 435.
22. FLORY, P. J. 1949. J. Chem. Phys. **17**: 303.
23. ZIMM, B. H., W. H. STOCKMAYER & M. FIXMAN. 1953. J. Chem. Phys. **21**: 1716.
24. TERAMOTO, E. 1951. Busseiron Kenkyu (in Japanese). **39**: 1.
- 24a. KURATA, M., H. YAMAKAWA & E. TERAMOTO. 1958. J. Chem. Phys. **28**: 785.
25. OUTER, P., C. I. CARR & B. H. ZIMM. 1950. J. Chem. Phys. **18**: 830.
26. KRIGBAUM, W. R. 1954. J. Am. Chem. Soc. **76**: 3758.
27. KRIGBAUM, W. R. & D. K. CARPENTER. 1955. J. Phys. Chem. **59**: 1166.
28. CANTOW, H. J. 1956. Z. physik. Chem. Frankfurt. **7**: 58.
29. KURATA, M., H. YAMAKAWA & H. UTIYAMA. 1959. Makromol. Chem. **34**: 139.
30. FUJITA, H., A. M. LINKLATER & J. W. WILLIAMS. 1960. J. Am. Chem. Soc. **82**: 379.
31. KURATA, M., W. H. STOCKMAYER & A. ROIG. 1960. J. Chem. Phys. **33**: 151.
32. JAMES, H. M. 1953. J. Chem. Phys. **21**: 1628.
33. FIXMAN, M. 1955. J. Chem. Phys. **23**: 1656.
34. ZIMM, B. H. 1946. J. Chem. Phys. **14**: 164.
35. ALBRECHT, A. C. 1957. J. Chem. Phys. **27**: 1002.
36. YAMAKAWA, H. 1958. J. Phys. Soc. Japan. **13**: 87. See also KURATA, M. & H. YAMAKAWA. 1958. J. Chem. Phys. **29**: 311.
37. CASASSA, E. F. & H. MARKOVITZ. 1958. J. Chem. Phys. **29**: 493.
- 37a. CASASSA, E. F. 1959. J. Chem. Phys. **31**: 800.
38. STAVERMAN, A. J. 1950. Rec. trav. chim. **69**: 163.

# CONCENTRATION DEPENDENCE OF POLYMER DIMENSIONS

Marshall Fixman  
*Mellon Institute, Pittsburgh, Pa.*

## *Introduction*

Although several attempts have been made to generalize the theory of the excluded volume effect<sup>1,2</sup> to include the dependence of the excluded volume factor  $\alpha$  on polymer concentration,<sup>3-6</sup> none has been free of such gross oversimplifications as, for example, a complete severing of the links of the polymer chain or the limitations of a perturbation calculation.

A calculation of the radial distribution function on the basis of the realistic, if approximate, model of Flory and Krigbaum<sup>7</sup> was previously used to compute the osmotic pressure.<sup>8</sup> The hope was expressed that the use of the osmotic pressure to compute a free energy and the minimization of the free energy with respect to  $\alpha$  could yield the concentration dependence of  $\alpha$ . The method has not been pursued to completion, at least not for high-polymer concentrations in "good" solvents, but such progress as has been made is here reported. Alternative calculations that avoid some of the present defects will be suggested.

## *The Model*

The physical model is a slight generalization of that used previously in discussions of the osmotic pressure.<sup>7,8</sup> A particular polymer molecule is represented as a continuous distribution of segments, such that the number of segments in a unit volume is a Gaussian function of the distance to the center of mass of the molecule. The total interaction energy of a pair of molecules is obtained by integrating the interaction energy *density* over all space. The energy density is assumed to be proportional to the product of the two segment densities at the given point. The assumptions result in an intermolecular potential that is a Gaussian function of intermolecular separation. This essentially completes the specification of the model previously used, inasmuch as the parameters that enter into the potential were taken to be the same for all molecules and configurations of the system. Now, however, it is desired that the size of a polymer molecule be subject to fluctuations; the possibility is introduced that the mean dimensions can vary with polymer concentrations. A rather simple mechanism is at once available for the description of size fluctuations. In the Gaussian function that gives the segment density distribution of each molecule, there is a single parameter proportional to the square of the radius of gyration or the end-to-end distance. This parameter can then be taken equal to its mean or most probable value multiplied by an expansion factor  $\alpha_i$ , for the  $i$ th molecule.

The probability distribution of the parameters of the system is readily given, in a purely formal way, as a Boltzmann distribution of the energy. The total interaction energy of the system is a sum of intermolecular energies  $V_{ij} = V(R_{ij}, \alpha_i, \alpha_j)$  and intramolecular energies  $V_i(\alpha_i)$ . The parameter  $\alpha_i$  may be taken, for concreteness, as the ratio of the actual radius of gyration of molecule  $i$  to the most probable radius, and  $R_{ij}$  is the distance from  $i$  to  $j$ . It follows from the hypothesis of Gaussian segment densities that<sup>1,7</sup>

$$V_{ij} = K_1(\alpha_i^2 + \alpha_j^2)^{-3/2} \exp [-K_2 R_{ij}^2 (\alpha_i^2 + \alpha_j^2)^{-1}] \quad (1)$$

$$V_i = K_3 \alpha_i^{-3} \quad (2)$$

The parameters  $K_1$ ,  $K_2$ , and  $K_3$  are independent of configuration, although they may depend on molecular weight,  $T$ ,  $P$ , and the chemical composition of polymer and solvent. With 1 and 2 and an a priori probability factor

$$\prod_i \exp [-K_4 \alpha_i^2] d\alpha_i \quad (3)$$

$$d\alpha_i = 4\pi \alpha_i^2 d\alpha_i \quad (4)$$

arising from the entropy of expansion of the molecule, the probability density of a given configuration is

$$\begin{aligned} f(\mathbf{R}_1 \cdots \mathbf{R}_N, \alpha_1 \cdots \alpha_N) \\ = Q^{-1} \exp [-K_4 \sum_i \alpha_i^2 - (\sum_{i>j} V_{ij} + \sum_i V_i)/kT] \end{aligned} \quad (5)$$

where  $Q$  is a normalizing factor.

It is hardly necessary to state that 5, although it already involves a considerable oversimplification of the internal structure of a polymer molecule, provides no easy access to  $f(\alpha_1)$ . If the polymer concentration is low, a cluster expansion of  $\alpha^2$  would be useful and no doubt could be carried out through the first power of concentration. An approximate method of calculation will be sketched, which is feasible at all concentrations; however, it has not been carried through because so much more numerical work would be required than in the method actually used. The *proposed* method is to isolate one molecule from the collection of  $N$ , say 1, and to suppose that, in the calculation of the probability of  $\alpha_1$ , all the other  $(N - 1)$  molecules may be assigned the same  $\alpha$ , the mean or most probable value. Evidently this assumption would be most reasonable at high polymer concentrations. A further approximation, reasonable in the same spirit, gives for the probability of  $\alpha_1$

$$f(\alpha_1) = Q' \exp \left\{ -K_4 \alpha_1^2 - \left[ \left\langle \frac{1}{2} \sum_{i \neq 1} V_{i1} \right\rangle + V_1(\alpha_1) \right] / kT \right\} \quad (6)$$



where

$$\left\langle \sum_{i \neq 1} V_{i1} \right\rangle = \rho \int V(R_{12}, \alpha_1, \alpha) g(R_{12}, \alpha_1, \alpha) d\mathbf{R}_2. \quad (7)$$

Here  $\rho$  is the number density of polymer molecules, and  $g(R_{12}, \alpha_1, \alpha)$  is the radial distribution function of molecules of expansion factor  $\alpha$  around the center molecule, which has a different expansion factor  $\alpha_1$ . It could be obtained from the Born-Green-Kirkwood equations by much the same method as we have previously used<sup>8</sup> to obtain  $g(R_{12}, \alpha, \alpha)$ . A maximization of  $\alpha_1^2 f(\alpha_1)$  with respect to  $\alpha_1$  then gives an equation for  $\alpha$ , in  $g(R_{12}, \alpha_1, \alpha)$ , and therefore  $f(\alpha_1)$  would be completely known. This method can be carried through when molecule 1 is a chemical species different from the other polymer molecules and does not require the integration over  $\rho$  that is required to compute a free energy (see under *The Free Energy*, below). Moreover, it should be stated that only the two-polymer one-solvent mixture is likely to yield unambiguous light-scattering determinations of dimensional changes ( $\langle \alpha_1^2 \rangle$  versus  $\rho_2$ ).

A somewhat different point of view is *actually taken* here. Only one  $\alpha$  will enter into the calculation, and it is used to characterize the ensemble rather than a particular molecule. Fluctuations of the dimensions of individual molecules will be suppressed during the calculation of the free energy of a fictitious system, namely, a system of polymer molecules all of which have the same Gaussian segment density. The scale factor  $\alpha$  that enters into the density distribution appears also in the intermolecular potential (Equation 1), and thereby in the free energy. After the free energy of interaction per molecule is computed, there is added to it the intramolecular free energy, and the whole is minimized with respect to  $\alpha$ .

### *The Free Energy*

A few equations will be required to establish the free energy of the solution in terms of the osmotic pressure of the solute, the latter being known from a previous calculation.<sup>8</sup> By assumption,  $\alpha$  is to be adjusted to its most probable value at constant  $T$  and atmospheric pressure. Consequently, the Gibbs free energy  $G$  rather than the Helmholtz free energy is to be minimized.

$$G(T, P) = N_1 \mu_1 + N_2 \mu_2 \quad (8)$$

where  $\mu_1$  and  $\mu_2$  are the chemical potentials of solvent and solute, respectively. Let  $P = P_0 + \pi$ , where  $P_0$  is the fixed atmospheric pressure and  $\pi$  the osmotic pressure.  $G(T, P_0)$  is required for the minimization with respect to  $\alpha$ . From the definition of  $\pi$  it follows that  $\mu_1 = \mu_1^0$ , the potential of pure solvent at 1 atmosphere.

Now a change in  $\pi$  may be imagined to result from a change in the num-

ber density of polymer molecules. The Gibbs-Duhem equation, which states in general that

$$N_1 d\mu_1 + N_2 d\mu_2 = -SdT + VdP \quad (9)$$

reduces under osmotic conditions to

$$N_2 d\mu_2 = Vd\pi \quad (10)$$

Therefore

$$\mu_2(T, P_0, \rho) = \int_{\rho_0}^{\rho} \rho^{-1} d\pi + \mu_2(T, P_0, \rho_0) \quad (11)$$

where  $\rho_0$  is a concentration so small that the interaction energy of polymer molecules becomes negligible. Equation 8 becomes, with 11,

$$G(T, P) = N_1 \mu_1^0 + N_2 \mu_2(T, P_0, \rho_0) + N_2 \int_{\rho_0}^{\rho} \rho^{-1} d\pi \quad (12)$$

$$P = P_0 + \pi$$

Suppose now that the osmotic conditions are removed (the semipermeable membrane is sealed) and the closed system is expanded at constant  $T$  to the pressure  $P_0$ .

$$\begin{aligned} dG &= -SdT + VdP + \sum \mu_i dN_i \\ &= VdP \end{aligned} \quad (13)$$

Therefore

$$G(T, P) - G(T, P_0) = V\pi \quad (14)$$

if the compressibility of the system be neglected. Equations 14 and 12 give

$$\begin{aligned} G(T, P_0) &= N_1 \mu_1^0 + N_2 \mu_2(T, P_0, \rho_0) + N_2 [\rho^{-1} \pi - \rho_0^{-1} \pi(\rho_0)] \\ &\quad + N_2 \int_{\rho_0}^{\rho} \rho^{-2} \pi d\rho - V\pi \end{aligned} \quad (15)$$

after a partial integration of  $\int \rho^{-1} d\pi$ . That part of  $G(T, P_0)$  which depends on the intermolecular potential is, per molecule,

$$G_2 \equiv \int_{\rho_0}^{\rho} \rho^{-2} \pi d\rho \quad (16)$$

This is the result one might have expected since, were  $\pi$  the hydrostatic pressure of a one-component system,  $G_2$  would be the *Helmholtz* free energy.

The intramolecular part of the free energy per molecule is, according to Flory,<sup>1</sup>

$$G_i = kT[K\alpha^{-3}Z - 3 \ln \alpha + \frac{3}{2}(\alpha^2 - 1)] \quad (17)$$

where  $K$  is a numerical constant (to be taken as 134/105 when  $\alpha$  determines the radius of gyration, in order to gain agreement with the perturbation theory<sup>2,9</sup> of  $\alpha$ ), and

$$Z = (3/2\pi R_0^2)^{3/2} \beta n^2 \quad (18)$$

for a polymer chain of  $n$  segments, mean square end-to-end distance  $R_0^2$  in the random flight approximation, and segment-segment excluded volume  $\beta$ . Thus the quantity to be minimized with respect to  $\alpha$  is  $\Delta G = G_2 + G_i$ .

$$\Delta G = \int_{\rho_0}^{\rho} \rho^{-2} \pi d\rho + kT \left[ K\alpha^{-3}Z - 3 \ln \alpha + \frac{3}{2}(\alpha^2 - 1) \right] \quad (19)$$

#### The Osmotic Pressure\*

The osmotic pressure has been computed,<sup>8</sup> approximately, on the basis of a potential of form 1:

$$V(R) = kT(4/\pi^{1/2})A \exp(-BR^2) \quad (20)$$

$$A = 7.18\alpha^{-3}Z \quad (21)$$

$$B = 9.61(\alpha^2 R_0^2)^{-1}$$

where the numerical constants in 21 have been chosen to agree with perturbation calculations<sup>10-12</sup> of the osmotic second virial coefficient. An approximate radial distribution function was used

$$g(R) = 1 - a \exp(-\delta BR^2) \quad (22)$$

and, by a variational procedure, the parameters  $a$  and  $\delta$  determined in terms of  $A$ ,  $B$ , and  $\rho$ . Equations 20 and 22 gave an osmotic pressure

$$\pi = \rho kT - (\rho^2/6) \int R V'(R) g(R) dR \quad (23a)$$

or

$$\pi = \rho kT + 2\pi kT \rho^2 A B^{-3/2} [1 - a(1 + \delta)^{-5/2}] \quad (23)$$

Substitution of 23 into 19 gives

$$\begin{aligned} (kT)^{-1} \Delta G = \int_{\rho_0}^{\rho} \rho^{-1} d\rho + 2\pi A B^{-3/2} \int_{\rho_0}^{\rho} [1 - a(1 + \delta)^{-5/2}] d\rho \\ + \left[ K\alpha^{-3}Z - 3 \ln \alpha + \frac{3}{2}(\alpha^2 - 1) \right] \end{aligned} \quad (24)$$

\* In this section,  $\pi$  designates the osmotic pressure only on the left-hand sides of Equations 23 and 23a. Elsewhere  $\pi$  is the pure number.

The equation of  $\partial(\Delta G)/\partial\alpha$  to zero now determines  $\alpha$ . Note that  $AB^{-3/2}$  is, according to **21**, independent of  $\alpha$ .

$$\begin{aligned} (kT)^{-1} \frac{\partial(\Delta G)}{\partial\alpha} &= -2\pi AB^{-3/2} \frac{\partial}{\partial\alpha} \int_0^\infty a(1+\delta)^{-5/2} d\rho \\ &\quad - 3[KZ\alpha^{-4} + \alpha^{-1} - \alpha] \\ &= 0 \end{aligned} \quad (25)$$

where  $\rho_0$  has been allowed to approach zero.

The procedure that has been used here will naturally raise several questions as to self-consistency. In part, this doubt results from the approximations' being lumped together and thereby obscured, relative to the procedure suggested above under *The Model*. Some of the difficulties and, occasionally, a resolution of them can be pointed out. Equation **23a** requires the assumption of pairwise additivity of the potential  $V(R)$  of average force between solute molecules. It also requires, almost as a matter of definition of the potentials, that  $V(R)$  not depend on concentration, as here it eventually will, through  $\alpha$ . It nevertheless turns out that the basic question of self-consistency is favorably resolved for a very simple reason. The reason is that  $\alpha$  is not treated as a function of concentration, but rather as an arbitrary parameter, up to the point where  $\Delta G$  is fully known, **24**. This means that the  $\alpha$  that occurs in **24** explicitly, and implicitly in  $A$ ,  $B$ , etc., will contribute nothing to the first derivative of  $\Delta G$  with respect to  $\rho$  ( $\partial\Delta G/\partial\alpha = 0$ ). Therefore the (osmotic) pressure obtained from  $\Delta G$  by differentiation with respect to  $\rho$  will agree with the virial theorem pressure, **23a** and **23**. For a more detailed discussion of a similar problem, see Mayer and Careri.<sup>13</sup>

A solution of **25** is quite difficult to obtain. Only for the case of weak interactions ( $A < 0.2$ ) is the solution reasonably straightforward and the result for every  $A$  accessible with one calculation. Only one other situation will be investigated, namely, the case of fairly large  $A$  ( $A > 1.2$ ), at not too large  $\rho$ . It turned out here<sup>8</sup> that  $a \cong 1$  up to such large  $\rho$  as to yield considerable changes in  $\alpha$  or, for very large  $A$ , to exceed the a priori limits of the chosen potential  $V(R)$  (a polymer volume fraction of ca. 0.1).

### Small $A$

When  $A$  is small,  $a$  is small and becomes smaller as  $\rho$  increases. The equations previously given<sup>8</sup> for  $a$  and  $\delta$  may then be linearized with respect to  $a$ , and take the form

$$\begin{aligned} ai_2 + \phi f_2 - \rho ah_2 &= 0 \\ ai_4 + \phi f_4 - \rho ah_4 &= 0 \end{aligned} \quad (26)$$

where  $\phi = \alpha^{-3}$  and

$$i_n = - \int_0^\infty x^n \exp(-2x^2) dx \quad (27)$$

$$f_2 = A'(\delta/1 + \delta)^{3/2}; \quad f_4 = \frac{3}{2}(\delta/1 + \delta)f_2 \quad (28)$$

$$h_2 = \pi^{3/2} A' B'^{-3/2} (2 + \delta)^{-3/2}; \quad h_4 = \frac{3}{2} (1 + \delta) (2 + \delta)^{-1} h_2 \quad (29)$$

$$A' = \alpha^3 A; \quad B' = \alpha^2 B \quad (30)$$

The definitions of  $A'$  and  $B'$  make them independent of variations in  $\alpha$ .

Although **25** apparently requires  $a$  and  $\delta$  in terms of  $\alpha$  and  $\rho$ , it turns out to be simpler to obtain  $a$  and  $\rho$  in terms of  $\delta$  and  $\alpha$ , and change the  $\rho$  integration to a  $\delta$  integration. From **26**

$$\rho = i_2 B'^{3/2} (2\pi^{3/2} A')^{-1} (1 - \delta) (2 + \delta)^{5/2} \quad (31)$$

$$a = -2f_2 \phi [i_2 \delta (1 + \delta)]^{-1} \quad (32)$$

and therefore

$$\eta \equiv a(1 + \delta)^{-5/2} = (-2A'/i_2) \phi \delta^{1/2} (1 + \delta)^{-5} \quad (33)$$

Notice that the dependence of  $\eta$  on  $\alpha$  is a simple proportionality to  $\phi = \alpha^{-3}$ , as follows from **33** and **31**. That is, **31** shows that  $\delta$  is independent of  $\alpha$ ; for a given polymer ( $A'$ ,  $B'$ ),  $\delta$  is a function only of  $\rho$ .

Equation **33** gives in **25**

$$\alpha^5 - \alpha^3 = KZ - 4\pi i_2^{-1} A'^2 B'^{-3/2} \int_0^\rho \delta^{1/2} (1 + \delta)^{-5} d\rho \quad (34)$$

A transformation of variables  $\rho \rightarrow \delta$ , through **31**, gives

$$\alpha^5 - \alpha^3 = 0.1777 A' - A' \pi^{-1/2} \int_1^{\delta(\rho)} \delta^{1/2} (2 + \delta)^{3/2} \cdot (7\delta - 1) (1 + \delta)^{-5} d\delta \quad (35)$$

where  $A' = 7.18Z$  (Equation **21**) and  $K = 134/105$  have been introduced. It proves convenient to tabulate the solution for  $\alpha$  not against  $\rho$  but against the dimensionless concentration

$$\nu' \equiv \pi^{3/2} B'^{-3/2} \rho \quad (36)$$

or

$$\nu' = (\pi/2)^{1/2} (16A')^{-1} (\delta - 1) (2 + \delta)^{5/2} \quad (37)$$

as follows from **31**. The integration in **35** was performed numerically, and then a simultaneous tabulation of  $(\alpha^5 - \alpha^3)/A'$  and  $\nu'A'$  against  $\delta$ , **35** and **37** respectively, gave as a result a tabulation of  $(\alpha^5 - \alpha^3)/A'$  against  $\nu'A'$ . To an order of approximation consistent with the previous lineariza-



tion with respect to  $a$ ,  $(\alpha^5 - \alpha^3)/A' \cong 2(\alpha - 1)/A'$ , and FIGURE 1 is so computed.

Although the actual dependence of  $\alpha$  on  $\rho$  will be governed by the scale factors  $A'$  and  $B'$ , one may conclude from FIGURE 1 that as  $\rho$  increases from zero,  $\alpha$  at first decreases rapidly, and then more and more slowly. It is also clear from FIGURE 1 and Equations 35 and 37 that  $\alpha$  approaches asymptotically a value less than unity, as  $\rho \rightarrow \infty$ . This was originally a rather

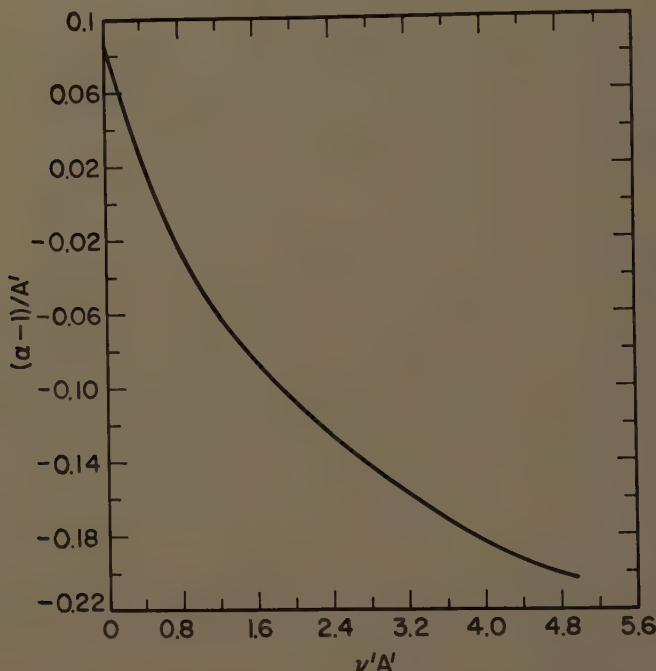


FIGURE 1. The expansion factor  $\alpha$  plotted against the dimensionless measure of concentration  $\nu'$ . The scale factor  $A'$  is an intermolecular potential parameter;  $A' \lesssim 0.2$ .

surprising result, as we interpreted the behavior of  $g(R)$  at high concentrations—namely,  $g(R) \rightarrow 1$ , all  $R$ , as  $\rho \rightarrow \infty$ —to mean that the effect of segment-segment interactions on  $\alpha$  would become unimportant. That is, we expected the Flory result,  $\alpha \rightarrow 1$  as  $\rho \rightarrow \infty$ , to be confirmed. However, some pondering over the details of the calculation will make it clear that only by a rather fortuitous cancellation of two tendencies could the result be  $\alpha \rightarrow 1$ . The intramolecular forces expand the molecule, and the intermolecular forces cause the molecule to contract. Furthermore it is not true that  $g(R) \rightarrow 1$  implies unambiguously a random distribution of segments. If the center of one molecule is held at a fixed position, it is implied by  $g(R) \rightarrow 1$  that the segment density contributed by other mole-

cules becomes uniform in space as  $\rho \rightarrow \infty$ ; nevertheless, the fixed molecule still maintains its Gaussian density distribution. Although the fixed central molecule contributes only a small part of the total segment density at large  $\rho$ , that small part may and evidently does play a disproportionately large role in the determination of its own degree of expansion.

A reminder is in order that the Flory-Krigbaum derivation<sup>7</sup> of  $V(R)$  did not include, in the local energy density, entropy of mixing terms beyond the second power of volume fraction. Quite possibly these higher terms will make  $\alpha \rightarrow 1$  as  $\rho \rightarrow \infty$ , in a more complete theory.

### Large $A$

Another and different simplification of the equations that determine  $a$  and  $\delta$  is possible if the solvent is very good. For large  $A$  (roughly  $A > 1.2$ ), the value of  $a$  was shown to be essentially unity for values of  $\rho$  as large as need be considered. However, it turns out that quite large changes in  $\alpha$  occur as the concentration is increased, and the intermolecular potential energy, through its dependence on  $\alpha$ , becomes concentration dependent to an extent that cannot be taken as a small perturbation. The process of compensating for these changes in  $\alpha$  requires considerable although straightforward numerical labor. Only a few results are available at present; a more extensive tabulation of  $\alpha$  (and  $\delta$ ) against  $\nu'$ , for a sequence of values of  $A'$ , will in due course be submitted elsewhere.

For  $a \equiv 1$ ,  $\delta$  satisfies<sup>8</sup>

$$I_4 + \phi f_4 - \rho g = 0 \quad (38)$$

where

$$I_4 \equiv \int_0^\infty \ln(1 - e^{-x^2}) x^4 e^{-x^2} dx \cong -0.1450 \quad (39)$$

$$g \equiv \frac{3}{2} A' B'^{-3/2} \pi^{3/2} [(1 + \delta)(2 + \delta)^{-5/2} - (1 + 2\delta)(1 + \delta)^{-1} \cdot (2 + 3\delta)^{-5/2}] \quad (40)$$

and  $f_4$  is given in 28.

As before, the  $\rho$  integration in 25 will be converted to a  $\delta$  integration. The derivative with respect to  $\alpha$  or  $\phi$  in 25 requires

$$\left( \frac{\partial \delta}{\partial \phi} \right)_\rho = f_4 [\rho (\partial g / \partial \delta) - \phi (\partial f_4 / \partial \delta)]^{-1} \quad (41)$$

from 38. Also from 38,

$$\left( \frac{\partial \delta}{\partial \rho} \right)_\phi = -g [\rho (\partial g / \partial \delta) - \phi (\partial f_4 / \partial \delta)]^{-1} \quad (42)$$

and therefore

$$\left(\frac{\partial \delta}{\partial \phi}\right)_\rho = (-f_4/g) \left(\frac{\partial \delta}{\partial \rho}\right)_\phi \quad (43)$$

The derivative with respect to  $\alpha$  in **25** may be eliminated with **43**, and then the  $\rho$  integration converted to a  $\delta$  integration with  $(\partial \delta / \partial \rho)_\phi d\rho = d\delta$ . The result is

$$\alpha^5 - \alpha^3 = (134Z/105) - 5\pi^{-1/2} A' \int_{\delta(\alpha, 0)}^{\delta(\alpha, \rho)} I(\delta) d\delta \quad (44)$$

where

$$I(\delta) = \frac{(1 + \delta)^{-6} \delta^{5/2}}{[(1 + \delta)(2 + \delta)^{-5/2} - (1 + 2\delta)(1 + \delta)^{-1}(2 + 3\delta)^{-5/2}]} \quad (45)$$

The limits on the  $\delta$  integral are determined as functions of  $\rho$  and  $\alpha$  from **38**. In principle, the method of solution would be to choose  $A'$  and  $B'$ , and the concentration  $\rho$  at which  $\alpha$  is desired. Then **38** would provide the values  $\delta(\alpha, 0)$  and  $\delta(\alpha, \rho)$  if  $\alpha$  were known. One could then guess at  $\alpha$  until the proper solution of **44** were found, for the given  $A'$ ,  $B'$ , and  $\rho$ . In practice the procedure has been to cast **38** into a form that gives  $\delta$  as a function of  $A = A'/\alpha^3$  and  $\nu = \nu'\alpha^3$ . A division of **44** by  $\alpha^3$ , and the substitution  $Z = A'/7.18$  gives

$$\alpha^2 - 1 = 0.1777A \left(1 - 15.87 \int_{\delta(A, 0)}^{\delta(A, \nu)} I(\delta) d\delta\right) \quad (46)$$

For a sequence of given  $A$ 's, there were tabulated (1)  $\nu$  versus  $\delta$ , from **38** and (2)  $\alpha$  versus  $\delta(A, \nu)$  from **46**. The result is a tabulation of  $\alpha$  and  $\delta$  versus  $\nu$  for a given  $A$ . It is easily seen that to keep  $A$  fixed as  $\delta(A, \nu)$  and  $\nu$  change means that  $A' = \alpha^3 A$  is changing. In principle this creates no problem; one need only tabulate  $A'$  alongside  $(A, \delta, \nu, \alpha)$ , and then search the tables, interpolating where necessary, for a preassigned value of  $A'$ . The result will be a series of entries  $(A', \delta, \nu, \alpha)$ , all having the same value of  $A'$  but successively increasing values of  $\delta$  and  $\nu$  and successively decreasing values of  $\alpha$ . The computation of  $\nu' = \nu/\alpha^3$  is then readily made for each entry, and one finally has for an assigned  $A'$ ,  $\delta$  and  $\alpha$  tabulated against the good measure of concentration  $\nu'$ . Unfortunately, as I indicated, my initial tables were not extensive enough to carry  $\nu'$  to adequately large values. However, even the fragmentary results here given are quite sufficient to permit qualitative inferences of the concentration dependence of  $\alpha$  in "good" solvents.

I have tabulated  $\alpha$  against  $\nu$  for a sequence of  $A$ 's; some of the results are given in **FIGURE 2**. They probably are reliable only for small  $\nu$  or small decreases in  $\alpha$ . That is, the abscissa could be related to  $\rho$  by taking  $B$  equal to its value at infinite dilution, if  $\rho$  is small.

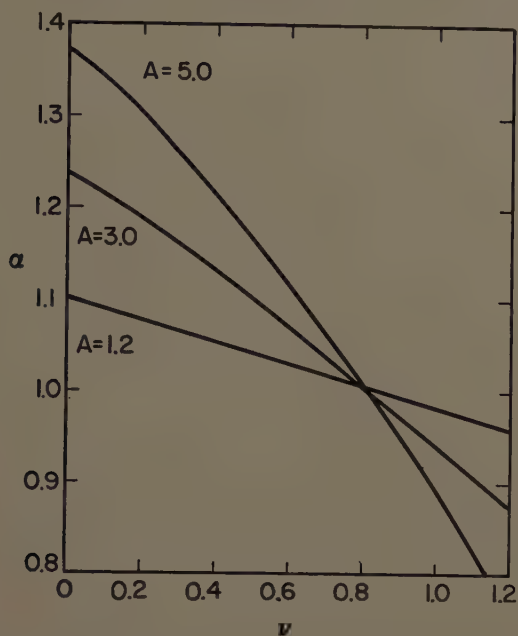


FIGURE 2. Alpha plotted against  $\nu = \alpha^3 \nu'$  for various values of  $A = A'/\alpha^3$ .

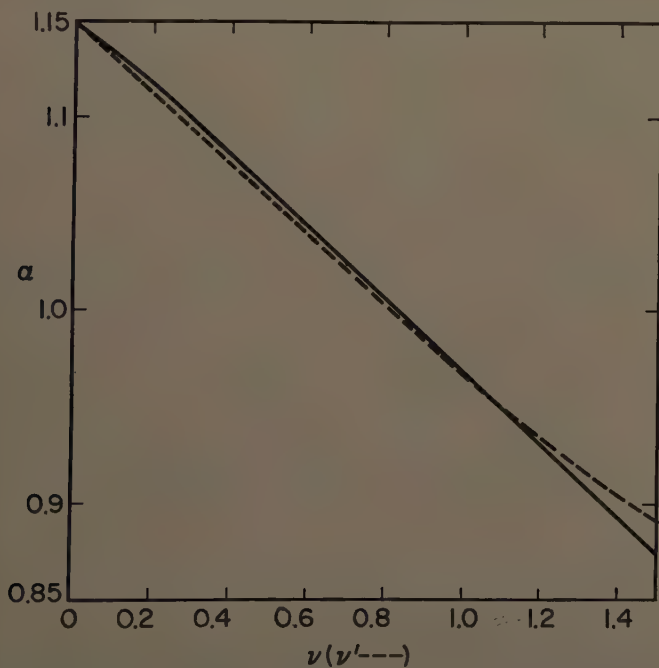


FIGURE 3. Solid curve:  $\alpha$  plotted against  $\nu$  for  $A = 1.8$  held constant. Dashed curve:  $\alpha$  plotted against  $\nu'$  for  $A' = 1.8 \times [\alpha(\nu = 0)]^3$  held constant.

For one value of  $A$ ,  $A = 1.8$ , I have gone through the procedure of "renormalizing" the  $A$  and  $\nu$  arguments to  $A'$  and  $\nu'$ , to as large a  $\nu'$  as was possible. Every point on the dashed curve in FIGURE 3 refers to a single polymer-solvent system (fixed  $A' = 1.8 \times [\alpha(0)]^3$ ) and the ordinate  $\nu'$  is proportional to  $\rho$  with a fixed proportionality constant. It is seen that only very small changes in the curve are induced by this "renormalization" other than a simple reinterpretation of the abscissa. Evidently, for qualitatively unknown reasons, the two changes in  $A$  and  $\nu$  tend to cancel each other. There is, however, one very significant effect at the higher concentrations. The renormalized curve begins to flatten out, and it is to be expected that  $\alpha$  will asymptotically approach a limiting value at high concentrations. The qualitative behavior of  $\alpha$  is, accordingly, the same in poor (small  $A'$ ) or good (large  $A'$ ) solvents: an initially rapid decrease to values *below unity* and a subsequent leveling off at high concentrations.

There is one very useful although tentative conclusion that may be drawn from the dashed curve of FIGURE 3. Up to concentrations in which appreciable overlapping of polymer domains is forced to occur ( $\nu' \sim 1$ ) and  $\alpha$  is significantly lowered, the dashed curve is quite close to a straight line. This means that a virial expansion of  $\alpha$  in powers of  $\rho$  could also give information about experimentally detectable decreases in  $\alpha$ .

### Summary

The mean dimensions of chain polymer molecules in dilute solution will usually be expanded beyond their random flight values because of the mutual repulsive forces exerted by chain segments. These repulsive forces may, however, be screened by the presence of other polymer molecules in solution, and accordingly the mean dimensions depend on polymer concentration. I have discussed the evaluation of this concentration dependence by a minimization of the total free energy of the solution. To the free energy of expansion of an isolated polymer molecule is added the free energy of interaction with other polymer molecules. The latter part of the free energy is known from a theoretical expression for the osmotic pressure and its dependence on polymer dimensions. The well-known dimensional expansion factor  $\alpha$ , which is greater than unity for a polymer molecule in dilute solution in a good solvent, will dip below unity when the concentration is increased. At a sufficiently high concentration beyond the reach of the present theory,  $\alpha$  may again approach unity.

### References

1. FLORY, P. J. 1949. J. Chem. Phys. **17**: 303.
2. FIXMAN, M. 1955. J. Chem. Phys. **23**: 1656.
3. KOTIN, L. 1960. Doctoral thesis. Harvard Univ. Cambridge, Mass.
4. KAWAI, T. & K. SAITO. 1957. J. Polymer Sci. **26**: 213.



5. FLORY, P. J. 1953. Principles of Polymer Chemistry. Cornell Univ. Press. Ithaca, N. Y.
6. KAWAI, T. 1955. Bull. Chem. Soc. Japan. **28**: 679.
7. FLORY, P. J. & W. R. KRIGBAUM. 1950. J. Chem. Phys. **18**: 1086.
8. FIXMAN, M. 1960. J. Chem. Phys. **33**: 370.
9. STOCKMAYER, W. H. 1955. J. Polymer Sci. **15**: 595.
10. ZIMM, B. 1946. J. Chem. Phys. **14**: 164.
11. ALBRECHT, A. C. 1957. J. Chem. Phys. **27**: 1002.
12. STOCKMAYER, W. H. 1960. Makromolekulare Chem. **35**: 1960.
13. MAYER, J. E. & G. CARERI. 1952. J. Chem. Phys. **20**: 1001.

# THEORY OF THE NON-NEWTONIAN VISCOSITY OF HIGH POLYMER SOLUTIONS

Bruno H. Zimm\*

*School of Science and Engineering, University of California, La Jolla, Calif.*

Peterlin in an earlier paper in this monograph has already discussed the possible theoretical sources for the non-Newtonian viscosity of high polymer solutions. I, too, have been investigating methods for calculating numerically the non-Newtonian effect of the hydrodynamic interaction. Since the calculations are still in progress, this note attempts merely to summarize some of the more striking preliminary results.

The exact form of the hydrodynamic interaction tensor, which gives the velocity of flow of the solvent produced at point  $j$  by the application of a unit force at point  $i$ , is

$$(1/|r|)(1 - rr/r^2),$$

where  $r$  is the vector from  $i$  to  $j$ . This form, originally used by Burgers<sup>1</sup> for the case of simple single particles, raises serious algebraic obstacles in the way of a solution of the equations of motion of any system of more than two or three centers. Kirkwood and Riseman<sup>2</sup> introduced a simple approximation to avoid the difficulty. They replaced the tensor with its average value in the molecule at rest, which depends only on the average distances in the molecule, a constant for any pair of chain segments. With this approximation the viscosity of high polymer solutions turns out to be Newtonian.<sup>3</sup>

I have tried two different ways of improving this approximation. Neither leads to exact results, but one seems much more promising than the other. The first and less promising method is also the more obvious; it is to use the Kirkwood-Riseman approximation, but with the average distances pertaining to the molecule in its steady state at a given rate of shear rather than at rest. In shear the molecule is anisotropically expanded, so that different averages are needed for the different components of the tensor. The result of the rather involved calculation is puzzling. At low-to-moderate shear rates the viscosity drops, as in the experiments, as a result of a complicated interplay of different terms; as the shear rate rises further, however, a monotonic rise in the viscosity occurs. This rise is due to a general weakening of the interaction as the molecule expands and as its interior becomes more and more exposed to the flow of solvent. In so far as I know, this rise has no counterpart in experiment.

\* This work was done in part while the author was associated with the General Electric Research Laboratory, and in part while he held a Visiting Professorship at Yale University, New Haven, Conn.

It therefore seems in order to search for another method of improving the Kirkwood-Riseman approximation, and the following approach has led to encouraging progress. We seek to represent the interaction tensor as a polynomial in  $r$  and its components. In principle the representation could be made as exact as desired by using a sufficient number of terms in the polynomial, but the computational difficulties increase rapidly, so that we are forced to limit the number drastically. From this point of view, the Kirkwood-Riseman approximation consists of using a one-term (constant) polynomial; I have now extended the polynomial to two terms, including one in  $r^2$ , as well as a constant. This form of interaction can be expressed in terms of the normal coordinates of the problem, and the equations of motion can be solved.

The result is gratifyingly simple, and it has at least the qualitative features of the experimental data. The viscosity is found to drop from its initial value as the shear rate is increased, at first falling rapidly, then more and more slowly, but never rising again as in the first method of approximation. The drop in viscosity first becomes appreciable, about 5 percent, when the shear rate reaches the reciprocal of the longest relaxation time of the chain;<sup>3</sup> something like this might have been anticipated on physical grounds.

This apparent agreement with experiment is encouraging, and it indicates that further refinements of this method should be examined. The obvious next step is to include anisotropic terms in the polynomial, and then higher powers of  $r$ . While the amount of labor involved in carrying out these steps may be considerable, there do not appear to be any fundamental difficulties.

### References

1. BURGERS, J. M. 1938. Second Report on Viscosity and Plasticity of the Amsterdam Academy of Sciences. Nordemann. New York, N. Y.
2. KIRKWOOD, J. G. & J. R. RISEMAN. 1948. *J. Chem. Phys.* **16**: 565.
3. ZIMM, B. H. 1956. *J. Chem. Phys.* **24**: 269.

# RECENT RESULTS IN THE CONTINUUM THEORY OF VISCOELASTIC FLUIDS\*

Bernard D. Coleman  
*Mellon Institute, Pittsburgh, Pa.*

Walter Noll  
*Mathematics Department, Carnegie Institute of Technology, Pittsburgh, Pa.*

## INTRODUCTION

This article is concerned with phenomenological aspects of the mechanical behavior of viscoelastic† fluids. The discussion is limited to those special circumstances in which all nonmechanical influences can be neglected; that is, no consideration is given to thermal, chemical, and electromagnetic phenomena.

Our procedure is as follows. After reviewing in Section 1 some kinematical prerequisites, we give in Section 2 a mathematical definition of the concept of a simple fluid. This definition is sufficiently general to include perfect fluids, Newtonian fluids, and viscoelastic fluids as special cases. In Section 3 we discuss the behavior of a simple fluid in steady simple shearing flow. It turns out that for incompressible fluids several steady flow problems can be solved by direct appeal to the definition. Some properties of these solutions that may be of interest to experimenters are discussed in Section 4. Recent results on the behavior of simple fluids in periodic motions are given in Section 5. In Section 6 we formulate a general "smoothness assumption," which makes it possible to prove a theorem that seems to justify the intuitive notion that for most fluids the theory of the Newtonian fluid should be a first-order correction to the theory of perfect fluids in the limit of "slow motions." A rigorous procedure for determining the form of higher-order corrections is sketched in Section 7.

It is not our intention to supply here formal mathematical proofs of all our assertions, for this article is not intended primarily for mathematicians working in continuum mechanics. Our goal is to summarize in an article of reasonable length certain recent results in the mechanics of fluids that may be of interest to polymer physicists. The omitted proofs not already published elsewhere will appear shortly in the *Archive for Rational Mechanics and Analysis*.

\* The work reported in this paper was supported in part by grants from the Air Force Office of Scientific Research, Washington, D.C., under Contract AF 49(638)541 with the Mellon Institute, Pittsburgh, Pa., and from the National Science Foundation, Washington, D.C., under Grant NSF-G 5250 to Carnegie Institute of Technology, Pittsburgh, Pa.

† The term viscoelastic does not have a precise meaning except in linearized theories. Here we use the word to indicate that we are dealing with materials that do not obey the classical laws of fluid mechanics or elasticity.

Although we omit some proofs, we endeavor not only to state each result precisely but also to make explicit the mathematical hypotheses from which it was deduced.

Before proceeding to our main topics and becoming involved in mathematical symbolism, we first try to give in this introduction a rough idea as to what we mean by a simple fluid.

The word fluid, as used in everyday speech, does not have a precise meaning. It might be said that an essential property of fluids is absence of preferred configurations; thus a fluid may be defined as a substance with the property that every configuration is an undistorted configuration. Physicists sometimes say that a fluid is a substance that cannot support a shearing traction without giving way to it. Some dictionaries define fluid as a substance capable of flowing. In order to give these definitions exact meaning and to see whether they are related, a general mathematical theory of the mechanical behavior of continuous media must be presumed. Such a general theory now exists.

Since the days of Euler and Cauchy,\* almost all phenomenological theories of the mechanical behavior of continuous media have rested on constitutive assumptions that may be seen to fall as special cases within a general hypothesis framed only much later and called the principle of determinism for the stress. The stress  $S(t)$  at a material point  $X$  at time  $t$  is determined by the past history of the motion in an arbitrarily small neighborhood of  $X$ .

For many materials† the principle of determinism is not needed in such a general form; in most theories that have been proposed,  $S(t)$  is determined at  $X$  by the history, up to time  $t$ , of only the first spatial gradient  $F$  at  $X$  of the displacement function.  $F$  is called, for short, the deformation gradient.

The deformation gradient  $F(\tau)$  for  $X$  at time  $\tau$  is a second-order tensor; it is defined as the gradient of the position vector  $\xi = \{\xi^1, \xi^2, \xi^3\}$ , at time  $\tau$  of  $X$  with respect to the position vector,  $\mathbf{q} = \{q^1, q^2, q^3\}$ , of  $X$  in whatever configuration we have taken as reference. If we are using a Cartesian coordinate system, the components  $F^i_j$  of  $F(\tau)$  are given by

$$F^i_j = \frac{\partial \xi^i}{\partial q^j}. \quad (1)$$

Of course,  $F(\tau)$  depends not only on the configuration at time  $\tau$ , but also on the configuration taken as a reference. By the history of the displacement gradient up to time  $t$  we mean a specification of  $F(\tau)$  for all  $\tau$ ,  $-\infty <$

\* For an excellent review of the work done up to 1952 see Truesdell.<sup>1,2</sup> A comprehensive article by W. Noll and C. Truesdell entitled "The Non-linear Field Theories of Mechanics" will appear soon in Flügge's *Encyclopedia of Physics*.

† Among the materials excepted are dilute gases with large velocity gradients<sup>3,4</sup> and fluids with very large density gradients<sup>5</sup> (for example, fluids in situations in which capillarity effects cannot be neglected).



$\tau \leq t$ . In rough terms we can say that the information contained in the history of the displacement gradient at a material point consists in a specification of all the rotations and stretches (both their magnitudes and directions) experienced by the material point in the past and, furthermore, the specification of the times at which these rotations and stretches occurred. Substances for which the history of the deformation gradient determines the stress have been called simple materials,<sup>6</sup> and the general phenomenological theory of their mechanical behavior has been developed considerably in recent years.<sup>6-11</sup>

The functional\*  $\mathfrak{R}_M$  which establishes the correspondence between the history of the deformation gradient and the stress tensor will in general depend on which configuration  $M$  is taken as a reference in computing the deformation gradient. For certain materials such as diamond and cross-linked rubber† there are certain special configurations which, when taken as reference configurations, will give the functional  $\mathfrak{R}_M$  a particularly simple form. These special configurations have the property that if a material point  $X$  has been held in one of these configurations for all times  $\tau$ ,  $-\infty < \tau \leq t$ , then  $S(t)$  at  $X$  must be a hydrostatic pressure. We call such configurations undistorted.

For those materials for which only certain special configurations are undistorted, the functionals  $\mathfrak{R}_M$  have the following property: Suppose we are given the history up to time  $t$  of the deformation gradient  $F$  relative to some general configuration  $M'$  which may not be undistorted. Then we cannot use  $\mathfrak{R}_M$  to compute  $S(t)$  unless we also know the displacement gradient of  $M'$  computed with the configuration  $M$  taken as a reference. This is not the case for all materials, however. For some substances a knowledge of the history of the deformation gradient  $F$ , computed relative to an arbitrary configuration  $M'$ , completely determines the stress, provided that we know merely the mass density corresponding to  $M'$  or, equivalently, provided that we know merely the determinant of the deformation gradient relating  $M'$  to  $M$ .‡ For such a material there exists a single functional  $\mathfrak{R}$ , which gives  $S(t)$  as a function of the density  $\rho$  of a configuration  $M'$  and the history of the deformation gradient  $F$  relative to  $M'$ :

$$S(t) = \mathfrak{R}_{\tau=-\infty}^t (F(\tau); \rho). \quad (2)$$

Here  $F$  is a tensor-valued function of  $\tau$ ,  $-\infty < \tau \leq t$ , and  $\rho$  is a number.

\* A functional here is simply a function whose arguments are functions and whose values are tensors; the stress tensor at time  $t$  is taken as a functional of the history of the deformation gradient up to time  $t$ , which may in turn be regarded as a tensor-valued function of a time variable  $\tau$ ,  $-\infty < \tau \leq t$ .

† We assume here that the temperature and our time scale are such that a negligible fraction of chemical bonds can break during any mechanical experiment.

‡ It turns out that such a substance must be isotropic; the condition on  $\mathfrak{R}_M$  stated here is, however, much stronger than isotropy. In the language of Noll,<sup>6</sup> our condition is equivalent to the assertion that the isotropy group of  $\mathfrak{R}_M$  is the full unimodular group.

If Equation 2 holds at the material point  $X$ , then we say that  $X$  is a material point of a simple fluid.\*

Since the functional  $\mathfrak{R}$  in 2 does not change if the configuration  $M'$  is changed, any configuration may be used as a reference. In certain problems it may be convenient to take the present state as a reference, then  $\rho$  is just the density at  $X$  at time  $t$ , and  $F$  is a function which has the value  $I$  (the identity tensor) at time  $t$ .

If a simple fluid has remained in a single configuration  $M$  for all times  $\tau$ ,  $-\infty < \tau \leq t$ , then the stress  $S(t)$  is a function of only the density corresponding to  $M$ . Furthermore, it can be shown by appeal to the principle of material objectivity† that  $S(t)$  must then reduce to a hydrostatic pressure. Since this result holds for *any* configuration  $M$ , it follows that every configuration of a simple fluid is undistorted. A simple fluid that has been at rest forever obeys the laws of classic hydrostatics. It follows from these remarks that if the stress in a simple fluid is not a hydrostatic pressure, then the fluid cannot have always been at rest in one configuration. Thus a simple fluid cannot support a shearing stress indefinitely without flowing.

The concept of a simple fluid is a very general one. Simple fluids can exhibit those phenomena that are now attracting the main attention of experimental rheologists: stress relaxation, non-Newtonian viscosity, and normal stress effects. In particular, we believe that the theory of simple fluids can be successfully applied to rationalize the treatment of mechanical data on pure amorphous, not cross-linked, polymers and polymer solutions.‡

We do not wish to give the impression that the theory of the simple fluid is so general that it is the only theory that can give precise meaning to the intuitive notion of fluidity. Consider the dictionary definition of a fluid as "a substance which is capable of flowing." There is, of course, no unique way of making this definition precise. We can suppose that what is really meant by the condition of being "capable of flowing" is the condition of sustaining a steady simple shearing flow in at least one direction when subjected to appropriate shearing tractions of bounded magnitude.§ A

\* The materials that we call here simple fluids were defined by Noll,<sup>6</sup> and were then called fluids. That article contains a rigorous presentation of the ideas roughly sketched in this introduction. What we now call simple fluids have also been called general fluids<sup>10,11</sup> because they not only include perfect fluids, Newtonian fluids, the Reiner-Rivlin fluids,<sup>12,13</sup> and the Rivlin-Ericksen fluids<sup>14,15</sup> as special cases, but because they are also much more general than all these special fluids in that they are capable of representing long-range hereditary effects such as stress relaxation.

† This principle,<sup>6</sup> which is also called the principle of material indifference, is a mathematical statement of the idea that the response of materials is independent of the observer, that is, invariant under changes of frame.

‡ It is possible that the theory of simple fluids cannot be successfully applied to the physics of liquid crystals. My colleague and I, however, are not sufficiently familiar with the mechanical behavior of such substances to hazard a categorical statement on this.

§ Note that we do not require that the shearing tractions be constant in time.

substance that meets this condition might be called a hypofluid. Every simple fluid is a hypofluid but not vice versa. One can even imagine hypofluids that may remain at rest indefinitely without obeying the laws of classical hydrostatics.\*

The materials defined by Ericksen in his recent articles<sup>16,17</sup> on anisotropic fluids are special hypofluids. Ericksen calls these substances anisotropic fluids because they have the property that the stress at a point  $X$  depends on a vector  $\mathbf{n}$ , which can be interpreted as determining a preferred direction at  $X$ . In each case, the vector  $\mathbf{n}$  depends in a specified way upon the history of the motion of  $X$ . In some of these fluids,  $\mathbf{n}$  reduces to the zero vector when the fluid has been at rest forever.† Depending on the choice of values for the material constants occurring in Ericksen's constitutive equations, the hypofluids considered by him may or may not be simple fluids. Ericksen's work illustrates the kind of behavior that hypofluids may exhibit when they do not reduce to simple fluids.

*Notation.* We denote vectors and points in Euclidean space by boldface Latin or Greek miniscules:  $\mathbf{v}$ ,  $\mathbf{x}$ ,  $\xi$ ,  $\dots$ . Second-order tensors are denoted by lightface Latin majuscules:  $A$ ,  $B$ ,  $Q$ ,  $I$ ,  $F$ ,  $C_t(\tau)$ ,  $\dots$ . For the trace of a tensor  $F$  we write  $\text{tr}F$  and for the determinant of  $F$  we write  $\det F$ . The transpose of  $F$  is denoted by  $F^T$ . We say that a tensor  $S$  is symmetric if  $S = S^T$ . The identity or unit tensor is written  $I$ . The symbol  $Q$  is used only for orthogonal tensors; that is, tensors such that  $QQ^T = Q^TQ = I$ . The physical components of the tensor  $T$  are denoted by  $T_{ij}$ . We use both  $\|F_t(\tau)\|$  and  $\|F_{(i)}{}^j(\tau)\|$  to denote the matrix of components of the tensor  $F_t(\tau)$  relative to a preassigned basis. The gradient operator and divergence operator are denoted by  $\nabla$  and  $\text{div}$ , respectively; we sometimes add a subscript to  $\nabla$  to emphasize the independent variable with respect to which we differentiate:  $\nabla_{\mathbf{x}}$ .

### 1. SOME ELEMENTARY KINEMATICS

Consider the material point  $X$  which occupies the position  $\mathbf{x}$  (in Euclidean space  $\mathcal{E}$ ) at time  $t$ . Let us suppose that at time  $\tau$ ,  $X$  occupied‡ the position  $\xi$  in  $\mathcal{E}$ . For the dependence of  $\xi$  on  $\mathbf{x}$ ,  $t$ , and  $\tau$  we write

$$\xi = \chi_t(\mathbf{x}, \tau). \quad (1.1)$$

The function  $\chi_t$  may be called the displacement function relative to the configuration at time  $t$ .

If the velocity field  $\mathbf{v}$  is given as a function of the position  $\xi$  in  $\mathcal{E}$  and the time  $\tau$ ,

$$\mathbf{v} = \mathbf{v}(\xi, \tau), \quad (1.2)$$

\* Furthermore, a hypofluid need not be isotropic; that is, for a hypofluid there need not exist a reference configuration  $M$  such that the isotropy group<sup>6</sup> of  $\mathfrak{R}_M$  contains the full orthogonal group.

† Ericksen's use of the word anisotropic is not the direct antithesis of the use of the word isotropic by Noll.<sup>6</sup>

‡ The letter  $t$  will be regarded as the present time and  $\tau$  a time earlier than  $t$ .

then the position  $\xi(\tau)$  of each particle at time  $\tau$ ,

$$\xi(\tau) = \chi_t(\mathbf{x}, \tau), \quad (1.3)$$

can be found if its position  $\mathbf{x}$  at time  $t$  is known. For  $\xi(\tau)$  is simply that solution of differential equation

$$\frac{d\xi(\tau)}{d\tau} = \mathbf{v}[\xi(\tau), \tau] \quad (1.4)$$

which satisfies the end condition

$$\xi(\tau) |_{\tau=t} = \chi_t(\mathbf{x}, t) = \mathbf{x}. \quad (1.5)$$

Thus a knowledge of the position  $\mathbf{x}$  of each material point at time  $t$  and the velocity field (1.2) for all  $\tau$  is equivalent to a knowledge of the displacement function defined in 1.1.\*

The gradient  $F_t(\tau)$  of  $\chi_t(\mathbf{x}, \tau)$  with respect to  $\mathbf{x}$ ,

$$F_t(\tau) = \nabla_{\mathbf{x}} \chi_t(\mathbf{x}, \tau), \quad (1.6)$$

is the *deformation gradient at time  $\tau$  relative to the configuration at time  $t$* . This second-order tensor  $F_t(\tau)$  can also be called the deformation gradient at time  $\tau$  computed with the present state taken as reference. The following equation follows from 1.5:

$$F_t(t) = I. \quad (1.7)$$

Here  $I$  is the unit or "metric" tensor.

Let  $\rho(\tau)$  and  $\rho(t)$  be the mass densities at the material point  $X$  at times  $\tau$  and  $t$ , respectively. It follows from a well-known result† in kinematics that these densities are connected by the formula

$$\det F_t(\tau) = \frac{\rho(t)}{\rho(\tau)}. \quad (1.8)$$

We now define a tensor  $C_t(\tau)$ , which is called the *right Cauchy-Green tensor at time  $\tau$  relative to the configuration at time  $t$* :

$$C_t(\tau) = F_t^T(\tau) F_t(\tau). \quad (1.9)$$

It follows from its definition that the right Cauchy-Green tensor is symmetric. Furthermore, since we always assume that  $F_t(\tau)$  is invertible,‡ it also follows that  $C_t(\tau)$  is positive definite.

It follows from 1.7 and 1.9 that

$$C_t(t) = I. \quad (1.10)$$

\* We make these remarks because flow problems are usually defined in terms of properties of the velocity field, whereas in the theory to be presented here the stress is regarded as being determined by the history of the spatial gradient of the displacement function.

† See Truesdell,<sup>1</sup> p. 140, Equation 13.5.

‡ That is,  $\det(F_t) \neq 0$ .



We shall often find it convenient to regard  $C_t(\tau)$  as a function of the time lapse  $r$  between  $\tau$  and  $t$ :

$$r = t - \tau. \quad (1.11)$$

We shall then assume that  $r \geq 0$  (that is, that  $\tau \leq t$ ).

The derivatives  $A_n$  of  $C_t(\tau)$  at  $\tau = t$ ,

$$\left. \frac{d^n}{d\tau^n} C_t(\tau) \right|_{\tau=t} = (-1)^n \left. \frac{d^n}{dr^n} C_t(t-r) \right|_{r=0} = A_n, \quad (1.12)$$

are the Rivlin-Ericksen tensors.\* The tensor  $A_1$  is familiar in classical hydrodynamics. It is simply twice the symmetric part  $D$  of the velocity gradient tensor  $\nabla_{\mathbf{x}}\mathbf{v}(\mathbf{x}, t)$ . To see this we write

$$A_1 = \left. \frac{d}{d\tau} C_t(\tau) \right|_{\tau=t} = \left. \frac{d}{d\tau} F_t^T(\tau) F_t(\tau) \right|_{\tau=t} \quad (1.13)$$

$$= L_1^T(t) F_t(t) + L_1(t) F_t^T(t) = L_1^T(t) + L_1(t) \quad (1.14)$$

where  $L_1(t)$  is defined to be the time derivative of the displacement gradient  $F_t(\tau)$  at time  $t$ :

$$L_1(t) = \left. \frac{d}{d\tau} F_t(\tau) \right|_{\tau=t}. \quad (1.15)$$

By 1.6 we have

$$L_1(t) = \left. \frac{d}{d\tau} \nabla_{\mathbf{x}} \mathbf{x}_t(\mathbf{x}, \tau) \right|_{\tau=t}. \quad (1.16)$$

Assuming  $\mathbf{x}_t$  is smooth in  $\mathbf{x}$  and  $\tau$ , we can interchange the order of differentiation in 1.16, and we get

$$L_1(t) = \nabla_{\mathbf{x}} \left. \frac{d\mathbf{x}_t}{d\tau}(\mathbf{x}, \tau) \right|_{\tau=t} = \nabla_{\mathbf{x}} \mathbf{v}(\mathbf{x}, t). \quad (1.17)$$

Thus 1.14 becomes

$$A_1 = (\nabla_{\mathbf{x}} \mathbf{v}(\mathbf{x}, t))^T + \nabla_{\mathbf{x}} \mathbf{v}(\mathbf{x}, t) = 2D. \quad (1.18)$$

To compute  $A_n$  for arbitrary  $n$  one can differentiate  $F_t^T(\tau) F_t(\tau)$   $n$  times with respect to  $\tau$  and then put  $\tau = t$ . In this way we get

$$A_n = \sum_{k=0}^n \binom{n}{k} L_k^T L_{n-k} \quad (1.19)$$

\* See Noll,<sup>6</sup> Sections 8 and 9. Rivlin and Ericksen<sup>14</sup> were the first to recognize the importance of the tensors  $A_n$  for  $n > 1$  and used them extensively in their theory of isotropic materials.



where

$$\begin{aligned} L_n(t) &= \left. \frac{d^n F_t(\tau)}{d\tau^n} \right|_{\tau=t} \quad n = 1, 2, \dots \\ L_0(t) &= I. \end{aligned} \quad (1.20)$$

For example

$$A_2 = L_2 + L_2^T + 2L_1^T L_1. \quad (1.21)$$

From 1.6 and 1.20 we have

$$L_2 = \left. \frac{d^2}{d\tau^2} \nabla_{\mathbf{x}} \kappa_t(\mathbf{x}, \tau) \right|_{\tau=t}. \quad (1.22)$$

We assume the velocity field to be smooth in  $\mathbf{x}$  and  $\tau$ . Then,

$$L_2 = \nabla_{\mathbf{x}} \left. \frac{d^2}{d\tau^2} \kappa_t(\mathbf{x}, \tau) \right|_{\tau=t} = \nabla \dot{\mathbf{v}} \quad (1.23)$$

and, if we remember 1.17, it follows that  $A_2$  is determined by the spatial gradients  $L_1$  and  $L_2$  of the velocity field  $\mathbf{v}(\mathbf{x}, t)$  and the acceleration field  $\dot{\mathbf{v}}(\mathbf{x}, t)$  at  $\mathbf{x}$  at time  $t$ .

The function  $C_t$  plays a central role in the theory of simple fluids, and the two tensors  $A_1$  and  $A_2$  occur frequently in special applications.

## 2. SIMPLE FLUIDS

### *Compressible Fluids*

For the purposes of the present article we can define a simple fluid as follows.

*Definition.* The material at  $X$  is a *simple fluid* if the stress tensor  $S(t)$  at  $X$  at time  $t$  depends on the history of the motion through an equation of the form

$$S(t) = \mathfrak{F}_{r=0}^{\infty} [C_t(t-r); \rho(t)]. \quad (2.1)$$

Here,  $\mathfrak{F}$  is a functional which has for its argument the history of the right Cauchy-Green tensor relative to the configuration at time  $t$  and the density at time  $t$ .  $\mathfrak{F}$  is assumed to obey the following identity for all histories  $C_t(t-r)$  and for all constant orthogonal tensors  $Q$ :

$$Q \mathfrak{F}_{r=0}^{\infty} [C_t(t-r); \rho(t)] Q^T = \mathfrak{F}_{r=0}^{\infty} [Q C_t(t-r) Q^T; \rho(t)]. \quad (2.2)$$

In general,  $\mathfrak{F}$  will depend on the material point  $X$ , but we do not make this dependence explicit since our present discussion is limited to homogeneous

bodies, that is, bodies that have the same constitutive equation at each material point.

Although this definition looks different in form from that given by Noll<sup>6</sup> and discussed in our introduction, it has been shown\* to be equivalent to the original definition.

Let us temporarily restrict our attention to situations in which the simple fluid has been at rest for all times  $\tau$ ,  $-\infty < \tau \leq t$ . Then,

$$C_i(t - r) \equiv I, \quad 0 \leq r < \infty, \quad (2.3)$$

and the functional  $\mathfrak{S}_{r=0}^{\infty} [C_i(t - r); \rho(t)]$  reduces to a function of  $\rho(t)$ :

$$\begin{aligned} S(t) &= \mathfrak{S}_{r=0}^{\infty} [C_i(t - r); \rho(t)] = \mathfrak{S}_{r=0}^{\infty} [I; \rho(t)] \\ &= H[\rho(t)]. \end{aligned} \quad (2.4)$$

Furthermore, since for all orthogonal  $Q$

$$I = QIQ^T, \quad (2.5)$$

Equation 2.2 becomes

$$Q \mathfrak{S}_{r=0}^{\infty} [I; \rho(t)] Q^T = \mathfrak{S}_{r=0}^{\infty} [I; \rho(t)]; \quad (2.6)$$

that is,

$$QS(t)Q^T = S(t). \quad (2.7)$$

Now, when a tensor  $S(t)$  obeys an identity of the form 2.7 for *all* orthogonal  $Q$ , then  $S(t)$  must be a scalar multiple of the identity. Hence we have proved the following: If a simple fluid has been at rest for all times in the past, then the stress in the fluid is given by a hydrostatic pressure  $p$ , which depends only on the density, that is,

$$S = -p(\rho)I. \quad (2.8)$$

### *Incompressible Fluids*

If the homogeneous body under consideration consists of an incompressible fluid, then we need not make the dependence of  $S(t)$  on the density  $\rho(t) = \rho_0 = \text{const.}$  explicit. Furthermore the stress in an incompressible fluid is determined by the history of the motion only up to a scalar pressure  $p$ . Thus in the incompressible case we replace 2.1 by

$$T(t) = \mathfrak{S}_{r=0}^{\infty} [C_i(t - r)], \quad (2.9)$$

\* See Noll<sup>6</sup> (Sections 21 and 22). Equation 2.2 follows from the isotropy of simple fluids and the principle of material objectivity. A functional  $\mathfrak{S}$  that obeys Equation 2.2 for all orthogonal  $Q$  is said to be *isotropic*.

where

$$T = S + pI \quad (2.10)$$

is called the *extra stress*. The tensor-valued functional  $\mathfrak{S}$  is now determined only up to an arbitrary scalar-valued functional of  $C_t(t-r)$ . We remove this indeterminacy by the normalization

$$\text{tr} T(t) = \text{tr} \mathfrak{S}_{r=0}^{\infty} [C_t(t-r)] = 0. \quad (2.11)$$

It follows from 2.10 and 2.11 that  $p$  reduces to the mean pressure:

$$p = -\frac{1}{3} \text{tr} S, \quad (2.12)$$

and  $T$  is the deviatoric part of  $S$ . The functional  $\mathfrak{S}$  is of course still isotropic in the incompressible case; that is,

$$Q \mathfrak{S}_{r=0}^{\infty} [C_t(t-r)] Q^T = \mathfrak{S}_{r=0}^{\infty} [Q C_t(t-r) Q^T], \quad (2.13)$$

for all histories  $C_t(t-r)$  and all constant orthogonal tensors  $Q$ .

By the same argument used in the compressible case, it follows from 2.13 that when the motion reduces to a state of rest, that is, when  $C_t(t-r) \equiv I$ ,

$$T(t) = \mathfrak{S}_{r=0}^{\infty} [C_t(t-r)] = \mathfrak{S}_{r=0}^{\infty} (I) \quad (2.14)$$

and thus reduces to a scalar  $b$  times the identity,

$$T(t) = bI. \quad (2.15)$$

In the present case, however, it follows from 2.11 that  $\text{tr} T = 3b = 0$ . Hence,

$$\mathfrak{S}_{r=0}^{\infty} (I) = 0. \quad (2.16)$$

Since the motion of an incompressible fluid is always isochoric (volume preserving) it follows from 1.8, 1.7, and 1.9 that

$$\det C_t(\tau) \equiv 1, \quad -\infty < \tau \leq t. \quad (2.17)$$

Hence for an incompressible fluid the functional  $\mathfrak{S}$  need only be defined over a domain of functions whose values are unimodular\* symmetric positive definite tensors.

We remark that a useful, necessary and sufficient condition for the motion of a fluid body to be isochoric is that

$$\text{div } \mathbf{v} = 0 \quad (2.18)$$

throughout the body at all times  $t$ .

\* That is, with unit determinant.

When we consider special flow problems in incompressible fluids we shall always assume that the body forces  $\mathbf{g}$  (per unit mass) have a single-valued potential  $\psi$ :

$$\mathbf{g} = -\text{grad } \psi. \quad (2.19)$$

We shall also make use of the *modified pressure*  $\phi$ :

$$\phi = p + \rho\psi. \quad (2.20)$$

It coincides with the ordinary pressure  $p$  if there are no body forces. The dynamical equations will then take the form

$$\text{div } T - \text{grad } \phi = \rho \dot{\mathbf{v}}. \quad (2.21)$$

### 3. SIMPLE SHEARING FLOW

We now illustrate some of the concepts introduced in the previous sections by considering a simple shearing flow of an incompressible fluid. We define this flow by postulating that in some Cartesian coordinate system  $x^1, x^2, x^3$  the velocity field  $\mathbf{v}(\mathbf{x}) = \{v^1, v^2, v^3\}$  has the form

$$\begin{aligned} v^1 &= 0, \\ v^2 &= v(x^1), \\ v^3 &= 0. \end{aligned} \quad (3.1)$$

Since  $\mathbf{v}$  is assumed to be independent of  $t$ , simple shearing flow, as we have defined it, is a steady flow. Furthermore, since  $\mathbf{v}$  clearly satisfies Equation 2.18, simple shearing flow is isochoric and thus compatible with incompressibility.

Let  $\xi^i(\tau)$  be the coordinates of the position at time  $\tau$  of the material point whose position at time  $t$  has coordinates  $x^i$ . Then

$$\xi^i(t) = x^i. \quad (3.2)$$

On substituting 3.1 into 1.4 we get

$$\begin{aligned} \frac{d\xi^1}{d\tau} &= 0, \\ \frac{d\xi^2}{d\tau} &= v(\xi^1), \\ \frac{d\xi^3}{d\tau} &= 0. \end{aligned} \quad (3.3)$$

It is easily seen that the solution of the system 3.3 subject to the end condition 3.2 is

$$\begin{aligned} \xi^1(\tau) &= x^1, \\ \xi^2(\tau) &= x^2 + (\tau - t)v(x^1), \\ \xi^3(\tau) &= x^3. \end{aligned} \quad (3.4)$$

It follows from the definition **1.6** that, in our present Cartesian coordinate system, the components  $F_{(t)j}^i(\tau)$  of the deformation gradient tensor  $F_t(\tau)$  are given by

$$F_{(t)j}^i = \frac{\partial \xi^i}{\partial x^j}. \quad (3.5)$$

Equations **3.4** and **3.5** yield the following expression for the matrix of the components  $F_{(t)j}^i(\tau)$  of  $F_t(\tau)$ :

$$\| F_t(\tau) \| = \| F_{(t)j}^i(\tau) \| = \begin{vmatrix} 1 & 0 & 0 \\ (\tau - t)\kappa & 1 & 0 \\ 0 & 0 & 1 \end{vmatrix}, \quad (3.6)$$

where

$$\kappa = \frac{dv(x^1)}{dx^1}. \quad (3.7)$$

Equations **1.9** and **3.6** yield

$$\| C_t(t - r) \| = \begin{vmatrix} 1 + r^2\kappa^2 & -r\kappa & 0 \\ -r\kappa & 1 & 0 \\ 0 & 0 & 1 \end{vmatrix} \quad (3.8)$$

for the matrix of the components of  $C_t(t - r)$ . Hence, in simple shearing flow,  $C_t(t - r)$  is quadratic in  $r$  and has the form

$$C_t(t - r) = I - rA_1 + \frac{1}{2}r^2A_2, \quad (3.9)$$

where  $I$  is the unit tensor and  $A_1$  and  $A_2$  are the first two Rivlin-Ericksen tensors defined in **1.12**. By **3.8** the matrices of the components of  $A_1$  and  $A_2$  are

$$\| A_1 \| = \kappa \begin{vmatrix} 0 & 1 & 0 \\ 1 & 0 & 0 \\ 0 & 0 & 0 \end{vmatrix}, \quad \| A_2 \| = 2\kappa^2 \begin{vmatrix} 1 & 0 & 0 \\ 0 & 0 & 0 \\ 0 & 0 & 0 \end{vmatrix}. \quad (3.10)$$

Whenever  $C_t(t - r)$  has the form **3.9**,\*  $C_t(t - r)$  is completely determined by  $A_1$  and  $A_2$ . When this is the case in an incompressible simple fluid, the functional  $\mathfrak{F}$  of **2.9** must reduce to a function  $\mathfrak{h}$  of the two tensors  $A_1$  and  $A_2$ :

$$T(t) = \mathfrak{F}_{r=0}^{\infty} [C_t(t - r)] = \mathfrak{h}(A_1, A_2). \quad (3.11)$$

Furthermore,  $T(t)$  must be independent of  $t$ . It follows from **2.13** that

\* There is a large class of steady flows, including Poiseuille flow, concentric pipe flow, and Couette flow, for which **3.9** holds.



the tensor function  $\mathfrak{h}$  must be isotropic; that is,

$$\mathfrak{h}(QA_1Q^T, QA_2Q^T) = Q\mathfrak{h}(A_1, A_2)Q^T \quad (3.12)$$

must hold identically in  $A_1, A_2$ , and  $Q$ , where  $Q$  is orthogonal. From 2.11 and 2.16 we have

$$\text{tr}[\mathfrak{h}(A_1, A_2)] = 0, \quad (3.13)$$

$$\mathfrak{h}(0, 0) = 0. \quad (3.14)$$

It follows from 3.11 and 3.12 that whenever  $C_i(t - r)$  is quadratic in  $r$  and the matrices of the physical components of  $A_1$  and  $A_2$  have the special form shown in 3.10, the matrix of the physical components of  $T(t)$  must have the form\*

$$\|T(t)\| = \begin{bmatrix} T_{11} & T_{12} & 0 \\ T_{21} & T_{22} & 0 \\ 0 & 0 & T_{33} \end{bmatrix}, \quad T_{12} = T_{21} \quad (3.15)$$

where the  $T_{ij}$  are functions of  $\kappa$  alone. By 3.13 we have

$$T_{11} + T_{22} + T_{33} = 0. \quad (3.16)$$

It is clear from 3.15 and 3.16 that the components  $T_{ij}$  of the extra stress may be expressed in terms of three independent functions of  $\kappa$ :

$$T_{12} = \tau(\kappa), \quad T_{11} - T_{33} = \sigma_1(\kappa), \quad T_{22} - T_{33} = \sigma_2(\kappa). \quad (3.17)$$

From 2.10 we see that for the components  $S_{ij}$  of the stress tensor  $S(t)$  we also have

$$S_{12} = S_{21} = \tau(\kappa) \quad (3.18)$$

$$S_{11} - S_{33} = \sigma_1(\kappa) \quad S_{22} - S_{33} = \sigma_2(\kappa).$$

Because of the isotropy relation 3.12, the functions  $\tau$ ,  $\sigma_1$ , and  $\sigma_2$  do not depend on which Cartesian coordinate system is used to obtain the simple form 3.1 for the velocity field. In other words, these three functions depend on only the material and not on the direction in which the material is being sheared. For this reason,  $\tau$ ,  $\sigma_1$ , and  $\sigma_2$  are called *material functions*.

The functions  $\tau$ ,  $\sigma_1$ , and  $\sigma_2$  are not completely arbitrary. It follows from 3.12 that†

$$\tau(-\kappa) = -\tau(\kappa), \quad \sigma_i(\kappa) = \sigma_i(-\kappa), \quad (3.19)$$

\* See Coleman and Noll<sup>10</sup> p. 294; the proof given therein is the same as the proof of 5.20 in Section 5. That 3.15 follows from 3.11, the isotropy of  $\mathfrak{h}$ , and 3.10 can also be proved using the Rivlin-Ericksen representation theorems for isotropic functions.<sup>14</sup>

† Coleman and Noll<sup>10</sup> pp. 294, 295; the proof is the same as the proof of 5.26 in Section 5. Equation 3.19 can also be proved using the Rivlin-Ericksen representation theorems.

that is, that  $\tau$  must be an odd function, while  $\sigma_1$  and  $\sigma_2$  are even functions. No further restrictions are imposed on  $\tau$ ,  $\sigma_1$ , and  $\sigma_2$  by the isotropy condition **2.13**.

Equation **3.14** implies that the material functions  $\tau$ ,  $\sigma_1$ , and  $\sigma_2$  must vanish for  $\kappa = 0$ :

$$\tau(0) = \sigma_1(0) = \sigma_2(0) = 0. \quad (3.20)$$

A further restrictive condition on  $\tau$  follows from the assumption that the dissipation of energy must be positive. This condition is

$$\kappa\tau(\kappa) > 0, \quad \text{if } \kappa \neq 0; \quad (3.21)$$

that is,  $\tau(\kappa)$  must have the same sign as  $\kappa$ . If it is assumed that  $\tau$  is twice continuously differentiable, then **3.20** and **3.21** imply that  $\tau(\kappa)$  must be a strictly increasing function of  $\kappa$  in some interval  $-\kappa_0 \leq \kappa \leq +\kappa_0$  around  $\kappa = 0$ . In this interval  $\tau$  will have a strictly increasing odd inverse  $\bar{\tau}^1$ . Whenever  $\bar{\tau}^1$  occurs in the remainder of this article we assume that we are in the range in which  $\tau$  has a single-valued inverse.

The "shear-dependent viscosity," used in the rheological literature can be identified with  $\tau(\kappa)/\kappa$ :

$$\eta(\kappa) = \frac{\tau(\kappa)}{\kappa}. \quad (3.22)$$

It follows from **3.19** that  $\eta$  must be an even function. Since  $\tau(0) = 0$ , if we assume that  $\tau$  is twice differentiable at  $\kappa = 0$ , then  $\eta$  is differentiable at  $\kappa = 0$  and

$$\eta'(0) = 0. \quad (3.23)$$

If we assume that  $\sigma_1$  and  $\sigma_2$  are differentiable then

$$\sigma_1'(0) = \sigma_2'(0) = 0. \quad (3.24)$$

If approximations based on Taylor expansions of  $\eta$ ,  $\sigma_1$ , and  $\sigma_2$  in a neighborhood of  $\kappa = 0$  are used to fit experimental data, only even powers of  $\kappa$  can occur.

Let us examine the special forms taken by the material functions  $\tau$ ,  $\sigma_1$ , and  $\sigma_2$  for some of those particular materials whose behavior is covered by the theory of incompressible simple fluids.

For incompressible perfect fluids

$$\tau(\kappa) = \sigma_1(\kappa) = \sigma_2(\kappa) \equiv 0 \quad (3.25)$$

for all  $\kappa$ .

For incompressible Newtonian fluids

$$\begin{aligned} \tau(\kappa) &= \kappa\eta, & \eta &= \text{const.} > 0 \\ \sigma_1(\kappa) &= \sigma_2(\kappa) \equiv 0, \end{aligned} \quad (3.26)$$

for all  $\kappa$ ; that is, the viscosity function **3.22** is a constant and the normal stress differences shown in **3.18** are zero.

In the incompressible case the theory of the Reiner-Rivlin fluids<sup>12,13</sup> places no restrictions on  $\tau$  other than those which hold for all simple fluids. When we consider the normal stresses in simple shearing flow, however, it turns out that the Reiner-Rivlin theory yields the result

$$S_{11} = S_{22}. \quad (3.27)$$

Thus by **3.18**, Reiner-Rivlin fluids have the special property

$$\sigma_1(\kappa) \equiv \sigma_2(\kappa). \quad (3.28)$$

The theory of incompressible fluids of the differential type<sup>6</sup> which was first considered by Rivlin and Ericksen,<sup>14</sup> yields results in simple shearing flow<sup>15</sup> that are equivalent to those obtained in the theory of simple fluids; that is, there are no restrictions on the material functions  $\tau$ ,  $\sigma_1$ , and  $\sigma_2$  for Rivlin-Ericksen fluids beyond those which we have stated for simple fluids. The greater generality of the theory of simple fluids over that of fluids of the differential type is not exhibited in either simple shearing flow or in the steady flows which we shall consider in Section 4.\*

There is a famous conjecture, due to Weissenberg,<sup>18</sup> to the effect that in simple shearing flow one should have

$$S_{11} = S_{33}, \quad (3.29)$$

which, by **3.18**, is equivalent to

$$\sigma_1(\kappa) \equiv 0. \quad (3.30)$$

No such result follows from the theory of simple fluids without the addition of new special hypotheses.

We complete our discussion of simple shearing flow by illustrating the solution of an elementary boundary value problem in terms of the material functions  $\tau$ ,  $\sigma_1$ , and  $\sigma_2$ . Let us consider a simple shearing flow between an infinite plate I at rest and an infinite plate II moving with constant speed  $V$  parallel to plate I. We denote the distance between the plates by  $d$ . The  $x^2$  and  $x^3$  axes are chosen to be in the plane of plate I and such that plate II moves in the  $x^2$  direction. The  $x^1$  axis is then perpendicular to the plates with  $x^1 = 0$  at plate I. Assuming that the fluid adheres to the walls, we have the boundary conditions

$$v(0) = 0, \quad v(d) = V. \quad (3.31)$$

\* It is indeed a remarkable fact that each of the steady flow solutions obtained by Rivlin<sup>14</sup> for Rivlin-Ericksen fluids are valid for all simple fluids. The greater generality of the theory of simple fluids is best seen by considering not steady flows but rather stress relaxation experiments.

We further assume that the modified pressure  $\phi$ , defined in 2.20, has no gradient in the direction of the flow:

$$\frac{\partial \phi}{\partial x^2} = 0. \quad (3.32)$$

We have pointed out that for simple shearing flow the extra stresses  $T_{ij}$  are functions of  $\kappa$  alone. Thus by 3.7, the  $T_{ij}$  can vary with the  $x^1$  coordinate only. It follows directly from this observation that for simple shearing flow the dynamical Equations 2.21 must reduce to

$$\begin{aligned} \frac{\partial T_{11}}{\partial x^1} + \frac{\partial \phi}{\partial x^1} &= 0, \\ \frac{\partial T_{12}}{\partial x^1} + \frac{\partial \phi}{\partial x^2} &= 0, \\ \frac{\partial \phi}{\partial x^3} &= 0. \end{aligned} \quad (3.33)$$

A simple analysis of 3.32 and 3.33 shows that these differential equations are satisfied only if

$$T_{12} = b \quad (3.34)$$

$$\phi = T_{11} - c, \quad (3.35)$$

where  $b$  and  $c$  are constants.

From 3.34 and 3.17 we observe that  $\kappa$  must be independent of  $\mathbf{x}$ :

$$\kappa = \bar{\tau}^1(b) = \text{const.} \quad (3.36)$$

Equation 3.7 and the conditions 3.31 then imply that

$$v(x^1) = \frac{V}{d} x^1, \quad (3.37)$$

$$\kappa = V/d. \quad (3.38)$$

According to 3.18 the shearing stress is

$$S_{12} = \tau(V/d). \quad (3.39)$$

Since  $S_{12}$  is equal to the tangential force per unit area that must be applied to the moving plate II in order to produce the flow, Equation 3.39 gives an easily grasped physical meaning to the material function  $\tau$ .

It follows from 3.38, 3.17, and 3.16 that all the components  $T_{ij}$  of  $T$  must be constant. Hence by 3.35, the modified pressure  $\phi$  is a constant. Using 2.20 and 2.10 we find

$$S_{11} = c - \rho\psi. \quad (3.40)$$

Hence if the potential  $\psi$  of the body forces is known, then a measurement of the normal force per unit area on the moving plate determines the value of the constant  $c$ .

Equations 3.38 and 3.18 yield

$$S_{11} - S_{33} = \sigma_1(V/d), \quad S_{22} - S_{33} = \sigma_3(V/d), \quad (3.41)$$

and thus give a physical meaning to the material functions  $\sigma_1$  and  $\sigma_2$ .

On combining Equations 3.39 through 3.41 we find the following expression for the matrix of the stress tensor:

$$\| S \| = \begin{vmatrix} c - \rho\psi & \tau(V/d) & 0 \\ \tau(V/d) & c - \rho\psi + \sigma_2(V/d) - \sigma_1(V/d) & 0 \\ 0 & 0 & c - \rho\psi - \sigma_1(V/d) \end{vmatrix}. \quad (3.42)$$

#### 4. SOME OTHER STEADY FLOWS

In the previous section we introduced three material functions  $\tau$ ,  $\sigma_1$ , and  $\sigma_2$ , which determine the extra stress  $T$  in simple shearing flow. It is clear from Equations 3.39 and 3.41 that if one could carry out in the laboratory a simple shearing flow between two parallel infinite plates then, by observing the relative speed of the plates and making appropriate force measurements, one could experimentally determine  $\tau$ ,  $\sigma_1$ , and  $\sigma_2$ . Of course, such an experimental program does not appear practicable at the present time. It is a noteworthy fact, however, that in addition to simple shearing flow, there are several other steady flow problems that can be solved exactly for incompressible simple fluids, and the resulting stress and velocity profiles are related by the same three material functions,  $\tau$ ,  $\sigma_1$ , and  $\sigma_2$ . This class of solvable flow problems contains\* Poiseuille flow<sup>10</sup> and also helical flow,<sup>11</sup> of which concentric pipe flow and Couette flow are special cases. If experimental measurements are combined with any one of the solutions to determine  $\tau$ ,  $\sigma_1$ , and  $\sigma_2$ , then complete stress and velocity profiles can be predicted for the other flows. Experimental rheologists do believe that they can achieve in the laboratory and can experimentally study flows that are a close approximation to Poiseuille flow, concentric pipe flow, and Couette flow. In this section we list, without complete derivation, some results of the theory of simple fluids that bear on experimental studies of these flows.

\* Other steady flow problems whose solutions for incompressible simple fluids involve only  $\tau$ ,  $\sigma_1$ , and  $\sigma_2$  are torsional flow, circular flow between concentric spheres, and circular flow between a cone and plate. We do not go into details on these flows because they are not compatible, under reasonable body forces, with the dynamical equations unless inertia is neglected. For the reader who is interested in these particular flows, we remark that the solutions of Rivlin,<sup>15</sup> Langlois,<sup>19</sup> and Markovitz and Williamson<sup>20</sup> for Rivlin-Ericksen fluids, and the statements made by Markovitz<sup>21</sup> about his "theories of class  $H$ ," are just as valid for simple fluids.



*Poiseuille Flow*

We consider a steady flow of an incompressible simple fluid in an infinite circular pipe of radius  $R$  and use cylindrical coordinates\*  $r$ ,  $z$ , and  $\theta$  with the  $z$ -axis coincident with the axis of the pipe. We say that we have Poiseuille flow if in such a coordinate system the contravariant components† of the velocity field  $\mathbf{v}(\mathbf{x}) = \{v^r, v^z, v^\theta\}$  have the form

$$\begin{aligned}v^r &= 0, \\v^z &= v(r), \\v^\theta &= 0,\end{aligned}\tag{4.1}$$

and if the fluid adheres to the walls of the pipe:

$$v(R) = 0.\tag{4.2}$$

An important measurable quantity in the experimental approximations to Poiseuille flow is the applied force  $a$  per unit volume in the direction of flow. This quantity  $a$ , which is also called the *driving force*, may be precisely defined as follows. Consider the total applied force  $f$  in the direction of flow exerted on the column of fluid with radius  $R$ , cross section  $\alpha$ , and lying between two planes  $z = z_I$  and  $z = z_{II}$ :

$$f = \left[ \int_{\alpha} S_{zz} dA \right]_{z=z_{II}} - \left[ \int_{\alpha} S_{zz} dA \right]_{z=z_I} - \int_{z_I}^{z_{II}} \int_{\alpha} \frac{\partial \psi}{\partial z} \rho dA dz, \tag{4.3}$$

that is,

$$f = \int_{\alpha} [(S_{zz} - \rho\psi)_{z=z_{II}} - (S_{zz} - \rho\psi)_{z=z_I}] dA; \tag{4.4}$$

$a$  is then defined as

$$a = \frac{f}{\pi R^2(z_{II} - z_I)}.\tag{4.5}$$

It can be proved that  $a$  is a constant; that is,  $a$  is independent of the choice of  $z_{II}$  and  $z_I$ . If there are no body forces, then  $\psi = \text{const.}$  and  $a$  reduces to the pressure head per unit length. If the only body force is gravity acting in the direction of flow, and if there is no pressure head, then  $a$  is simply the specific weight of the fluid.

We shall express the other measurable quantities in terms of the driving force  $a$ , the radius  $R$ , the body force potential  $\psi$ , and the material functions  $\tau$ ,  $\sigma_1$ , and  $\sigma_2$ .

\* Throughout this section (Section 4) the symbol  $r$  always refers to the radial coordinate of a cylindrical coordinate system; in all the other sections of the paper  $r$  denotes a time lapse. No confusion should arise.

† The form of 4.1 is such that the contravariant components of  $\mathbf{v}(\mathbf{x})$  are the same as the physical components, although this is not true for an arbitrary velocity field in cylindrical coordinates.

It can be shown that in Poiseuille flow the velocity profile is given by

$$v(r) = \int_r^R \tau^{-1}(\tfrac{1}{2}av) dv, \quad (4.6)$$

and from this it follows that the volume discharge  $\Lambda$  per unit time through a cross section of the pipe,

$$\Lambda = 2\pi \int_0^R v(r)r dr, \quad (4.7)$$

is given by

$$\Lambda = \frac{8\pi}{a^3} \int_0^{aR/2} v^2 \tau^{-1}(v) dv. \quad (4.8)$$

The rheological literature contains several derivations, based on special assumptions, of formulas equivalent to 4.8;\* the point of interest here is that 4.8 can be shown to be valid for *all* incompressible simple fluids.

It can also be shown that in our cylindrical coordinate system the matrix of the physical components of the stress tensor has the form

$$\| S \| = \begin{vmatrix} S_{rr} & S_{rz} & 0 \\ S_{zr} & S_{zz} & 0 \\ 0 & 0 & S_{\theta\theta} \end{vmatrix}, \quad (4.9)$$

where

$$\begin{aligned} S_{rz} &= S_{zr} = -\tfrac{1}{2}ar, \\ S_{rr} &= az + \rho\psi + \int_r^R \frac{1}{v} \sigma_1[\tau^{-1}(\tfrac{1}{2}av)] dv + c, \\ S_{rr} - S_{\theta\theta} &= \sigma_1[\tau^{-1}(\tfrac{1}{2}ar)], \\ S_{zz} - S_{\theta\theta} &= \sigma_2[\tau^{-1}(\tfrac{1}{2}ar)]. \end{aligned} \quad (4.10)$$

Because of the assumed incompressibility of the fluid, when only  $a$ ,  $R$ , and  $\psi$  are given, the normal pressures are determined only up to a constant hydrostatic pressure of magnitude  $c$ . Assuming  $\psi$  to be known, a single measurement of  $S_{rr}$  fixes the value of this constant  $c$ .

It is worth remarking that according to these equations the normal thrust  $S_{zz}$  in the axial direction

$$S_{zz} = S_{rr} + \sigma_2[\tau^{-1}(\tfrac{1}{2}ar)] - \sigma_1[\tau^{-1}(\tfrac{1}{2}ar)] \quad (4.11)$$

depends, in general, on  $r$ . On comparing 4.11 and 3.28, we see that for

\* See Hermans,<sup>22</sup> pp. 249 and 250.

Reiner-Rivlin fluids  $S_{rr} = S_{zz}$ . The tendency of a stream of an incompressible viscoelastic fluid to swell upon efflux from a pipe is most likely related to both a dependence of  $S_{rr}$  on  $r$  and a lack of equality between  $S_{rr}$  and  $S_{zz}$ . Either effect can be used to make the swelling plausible.

### *Special Cases of Helical Flow*

*Flow between concentric pipes.* We consider a steady flow of an incompressible simple fluid between two fixed coaxial circular cylinders of radii  $R_1$  and  $R_2$  ( $R_1 < R_2$ ). We again use cylindrical coordinates  $r$ ,  $z$ , and  $\theta$ , with the  $z$ -axis parallel to the axis of the pipes, and again assume that the velocity field has the form 4.1. However, we now impose the following boundary conditions:

$$v(R_1) = v(R_2) = 0. \quad (4.12)$$

We again use the symbol  $a$  for the applied force per unit volume in the axial direction:

$$a = \frac{f}{\pi(R_2^2 - R_1^2)(z_{II} - z_I)}. \quad (4.13)^*$$

Here  $f$  is the total applied force in the  $z$  direction exerted on the annulus of fluid which lies between two planes  $z = z_I$  and  $z = z_{II}$ . It can be shown that  $a$  is independent of  $z_I$  and  $z_{II}$ .

We wish to express the other measurable quantities in terms of the variables  $a$ ,  $R_1$ , and  $R_2$ ,  $\psi$  and the functions  $\tau$ ,  $\sigma_1$ , and  $\sigma_2$ . To this end we define a function  $\alpha$  as follows:

$$\alpha(r) = br^{-1} - \frac{1}{2}ar^2; \quad (4.14)$$

the constant  $b$  is chosen so that

$$\int_{R_1}^{R_2} \bar{\tau}^{-1}[\alpha(r)] dr = 0. \quad (4.15)$$

It follows from the known solution to the problem of helical flow<sup>11</sup> that the velocity profile in concentric pipe flow is given by

$$v(r) = \int_{R_1}^r \bar{\tau}^{-1}[\alpha(v)] dv, \quad (4.16)$$

and from this it follows that the volume discharge  $\Lambda$  per unit time,

$$\Lambda = 2\pi \int_{R_1}^{R_2} v(r)r dr, \quad (4.17)$$

\* Equation 3.7 of Coleman and Noll<sup>11</sup> contains misprints; it should read as our Equation 4.13.

is given by

$$\Lambda = -\pi \int_{R_1}^{R_2} \bar{\tau}[\alpha(r)] r^2 dr. \quad (4.18)$$

It can also be shown that in our cylindrical coordinate system the matrix of the physical components, the stress tensor for concentric pipe flow, has the form 4.9, but now instead of 4.10 we have

$$\begin{aligned} S_{rz} &= S_{zr} = \alpha(r), \\ S_{rr} &= az + \rho\psi - \int_{R_1}^r \frac{1}{\nu} \sigma_1 \{ \bar{\tau}[\alpha(\nu)] \} d\nu + c, \\ S_{rr} - S_{\theta\theta} &= \sigma_1 \{ \bar{\tau}[\alpha(r)] \}, \\ S_{zz} - S_{\theta\theta} &= \sigma_2 \{ \bar{\tau}[\alpha(r)] \}. \end{aligned} \quad (4.19)$$

When there are no body forces in the radial direction,  $\psi$  is independent of  $r$  and the second of the equations 4.19 yields an interesting formula for the difference in the radial thrusts per unit area on the inner and outer cylinders:

$$S_{rr}(R_2) - S_{rr}(R_1) = - \int_{R_1}^{R_2} \frac{1}{\nu} \sigma_1 \{ \bar{\tau}[\alpha(\nu)] \} d\nu. \quad (4.20)$$

This difference  $S_{rr}(R_2) - S_{rr}(R_1)$  in the normal stresses on the two cylinders should certainly be measurable. We note that according to 4.20,  $S_{rr}(R_2) = S_{rr}(R_1)$  if and only if the Weissenberg relation 3.30 holds. It appears to us that the measurement of  $S_{rr}(R_2) - S_{rr}(R_1)$  in concentric pipe flow furnishes the most direct and convenient way available for experimenters to check Weissenberg's conjecture for particular substances. We emphasize that there has been no "neglect of inertia" in the derivation of 4.20.

*Couette flow.* We again consider a steady flow of an incompressible simple fluid between two coaxial cylinders of radii  $R_1$  and  $R_2$ , ( $R_1 < R_2$ ), and we use the same cylindrical coordinate system as before. Instead of assuming that the cylinders are at rest, we now postulate that the inner and outer cylinders rotate with constant angular velocities  $\Omega_1$  and  $\Omega_2$ , respectively. The contravariant components of the velocity field  $\mathbf{v}(\mathbf{x}) = \{v^r, v^\theta, v^z\}$  are assumed to have the form

$$\begin{aligned} v^r &= 0, \\ v^\theta &= 0, \\ v^z &= \omega(r); \end{aligned} \quad (4.21)$$

that is, for Couette flow the motion is in circles. In 4.21  $\omega$  has the dimen-

sions of angular velocity.\* Since we assume that the fluid adheres to the walls, we have the boundary conditions

$$\omega(R_1) = \Omega_1, \quad \omega(R_2) = \Omega_2. \quad (4.22)$$

An important measurable variable in the experimental approximations to Couette flow is the torque  $M$  per unit height required to maintain the relative motion of the bounding cylinders.

It can be shown<sup>10</sup> that in Couette flow the velocity profile obeys the equation

$$\frac{d\omega(r)}{dr} = \frac{1}{r} \frac{1}{\tau} \left( \frac{M}{2\pi r^2} \right); \quad (4.23)$$

thus for this flow, a knowledge of  $M$  and the angular velocity of one of the bounding cylinders completely determines the velocity profile. Integration of 4.23 with the boundary conditions 4.22 yields the following formula† relating the observable angular velocity difference  $\Omega_2 - \Omega_1$  to the torque  $M$  through the material function  $\tau$ :

$$\Omega_2 - \Omega_1 = \frac{1}{2} \int_{M/(2\pi R_2^2)}^{M/(2\pi R_1^2)} \frac{1}{\nu} \frac{1}{\tau}(\nu) d\nu. \quad (4.24)$$

The matrix of the physical components of the stress tensor for Couette flow has the following form in our present coordinate system:

$$\| S \| = \begin{vmatrix} S_{rr} & 0 & S_{r\theta} \\ 0 & S_{zz} & 0 \\ S_{\theta r} & 0 & S_{\theta\theta} \end{vmatrix}, \quad (4.25)$$

where

$$\begin{aligned} S_{\theta r} = S_{r\theta} &= \frac{M}{2\pi r^2}, \\ S_{rr} &= \rho\psi - \int_{R_1}^r \left\{ \rho\nu\omega^2(\nu) + \frac{1}{\nu} \sigma_1 \left[ \frac{1}{\tau} \left( \frac{M}{2\pi\nu^2} \right) \right] \right. \\ &\quad \left. - \frac{1}{\nu} \sigma_2 \left[ \frac{1}{\tau} \left( \frac{M}{2\pi\nu^2} \right) \right] \right\} d\nu + c, \\ S_{rr} - S_{zz} &= \sigma_1 \left[ \frac{1}{\tau} \left( \frac{M}{2\pi r^2} \right) \right], \\ S_{\theta\theta} - S_{zz} &= \sigma_2 \left[ \frac{1}{\tau} \left( \frac{M}{2\pi r^2} \right) \right]. \end{aligned} \quad (4.26)$$

$$c = \text{const.}$$

\* The physical components  $\bar{v}^i$  of  $\mathbf{v}(\mathbf{x})$  are  $\bar{v}^z = \bar{v}^r = 0$ ,  $\bar{v}^\theta = r\omega$ .

† Derivations, based on special assumptions, of formulas equivalent to 4.23 have been known for some time (Mooney,<sup>23</sup> Section 3).



If the potential  $\psi$  of the body forces is independent of  $r$ , the second equation of 4.26 yields the following expression for the difference of the normal stresses at the outer and inner cylinders:\*

$$S_{rr}(R_2) - S_{rr}(R_1) = - \int_{R_1}^{R_2} \left\{ \rho r \omega^2(r) - \frac{1}{r} \sigma_1 \left[ \frac{-1}{\tau} \left( \frac{M}{2\pi r^2} \right) \right] - \frac{1}{r} \sigma_2 \left[ \frac{-1}{\tau} \left( \frac{M}{2\pi r^2} \right) \right] \right\} dr. \quad (4.27)$$

When  $(R_2 - R_1)/R_1 \ll 1$ , this formula is approximated by

$$S_{rr}(R_2) - S_{rr}(R_1) \approx \frac{R_2 - R_1}{R_1} \left\{ \sigma_2 \left[ \frac{-1}{\tau} \left( \frac{M}{2\pi R_2^2} \right) \right] - \sigma_1 \left[ \frac{-1}{\tau} \left( \frac{M}{2\pi R_2^2} \right) \right] \right\}. \quad (4.28)$$

The error in this approximation is of the order of  $[(R_2 - R_1)/R_1]^2$ . The inertial term  $\rho r \omega^2(r)$  in the integral on the right side of 4.27 makes a contribution to  $S_{rr}(R_2) - S_{rr}(R_1)$  of the order of  $[(R_2 - R_1)/R_1]^3$ , and therefore does not appear in 4.28.

Padden and DeWitt<sup>24</sup> have described an apparatus for measuring  $S_{rr}(R_2) - S_{rr}(R_1)$  in Couette flow. On comparing 4.27 and 3.28 we see that for Reiner-Rivlin fluids only the centrifugal forces contribute to  $S_{rr}(R_2) - S_{rr}(R_1)$ .† Markovitz,<sup>21</sup> in his analysis of available normal stress data on concentrated polyisobutylene solutions of high molecular weight, has remarked that the results of Padden and DeWitt<sup>24</sup> show that solutions of that polymer do not obey the Reiner-Rivlin theory. In fact Padden and DeWitt found that  $S_{rr}(R_2) > S_{rr}(R_1)$ , whereas centrifugal effects alone would yield  $S_{rr}(R_2) < S_{rr}(R_1)$ .

## 5. SOME OSCILLATORY MOTIONS

Here we consider the behavior of incompressible simple fluids in certain oscillatory motions. For simplicity, we confine our discussion to a class of flows that we call periodic shearing flows. These flows are defined to have the property that in some Cartesian coordinate system  $x^1, x^2, x^3$  the velocity field,  $\mathbf{v}(\mathbf{x}) = \{v^1, v^2, v^3\}$ , has the form

$$\begin{aligned} v^1 &= 0, \\ v^2 &= v(x^1, t), \\ v^3 &= 0, \end{aligned} \quad (5.1)$$

where  $v$  is periodic in  $t$  with period  $\theta$ ; that is, we assume that there exists a finite positive number  $\theta$  such that

$$v(x^1, t + \theta) = v(x^1, t) \quad (5.2)$$

\* A result equivalent to 4.27 was obtained by Rivlin for Rivlin-Ericksen fluids (Rivlin,<sup>16</sup> p. 186).

† This fact was pointed out by Rivlin in his early work on Reiner-Rivlin fluids (Rivlin,<sup>13</sup> p. 279).

for all  $x^1$  and all  $t$ . This flow clearly satisfies Equation 2.18 and hence is compatible with incompressibility.

For a periodic shearing flow, Equations 1.4 and 1.5 take the form

$$\frac{d\xi^1}{dt} = 0, \quad \frac{d\xi^2}{d\tau} = v(\xi^1, \tau), \quad \frac{d\xi^3}{d\tau} = 0; \quad (5.3)$$

$$\xi^i(t) = x^i. \quad (5.4)$$

Here the  $\xi^i(\tau)$  are the coordinates of the position at time  $\tau$  of the material point whose position at time  $t$  has coordinates  $x^i$ .

The solution of the system 5.3 with the end condition 5.4 is

$$\begin{aligned} \xi^1(\tau) &= x^1, \\ \xi^2(\tau) &= x^2 - u_{(t)}(x^1, t - \tau), \\ \xi^3(\tau) &= x^3, \end{aligned} \quad (5.5)$$

where the function  $u_{(t)}(x^1, r)$  is defined by

$$u_{(t)}(x^1, r) = \int_0^r v(x^1, t - s) ds. \quad (5.6)$$

It follows from 1.6 and 5.5 that, in our present coordinate system, the matrix of the components  $F_{(t)}^i{}_j(t - r)$  of the deformation gradient tensor  $F_{(t)}(t - r)$  is

$$\| F_{(t)}(t - r) \| = \| F_{(t)}^i{}_j(t - r) \| = \begin{vmatrix} 1 & 0 & 0 \\ \lambda_{(t)}(r) & 1 & 0 \\ 0 & 0 & 1 \end{vmatrix}, \quad (5.7)$$

$$\lambda_{(t)}(r) = \frac{\partial u_{(t)}(x^1, r)}{\partial x^1}. \quad (5.8)$$

Since we shall henceforth keep our attention on a particular point in space, we do not need to make explicit the dependence of  $\lambda_{(t)}(r)$  on  $\mathbf{x}$ .

We note, for future use, that 5.2 implies that the following equation holds for all  $r$  and  $t$ :

$$\lambda_{(t+\theta)}(r) = \lambda_{(t)}(r); \quad (5.9)$$

that is, for each  $r$ ,  $\lambda_{(t)}(r)$ , regarded as a function of  $t$ , is periodic with period  $\theta$ .

By 5.7 and 1.9 the matrix of the components of  $C_t(t - r)$  is

$$\| C_t(t - r) \| = \begin{vmatrix} 1 + \lambda_{(t)}^2(r) & \lambda_{(t)}(r) & 0 \\ \lambda_{(t)}(r) & 1 & 0 \\ 0 & 0 & 1 \end{vmatrix}. \quad (5.10)$$

Hence in all periodic shearing flows,  $C_t(t - r)$  has the form

$$C_t(t - r) = I + E_t(r) + G_t(r) \quad (5.11)$$

where  $I$  is again the unit tensor and the matrices of the components of  $E_t(r)$  and  $G_t(r)$  are

$$E_t(r) = \lambda_{(t)}(r) \begin{vmatrix} 0 & 1 & 0 \\ 1 & 0 & 0 \\ 0 & 0 & 0 \end{vmatrix}, \quad (5.12)$$

$$G_t(r) = \lambda_{(t)}^2(r) \begin{vmatrix} 1 & 0 & 0 \\ 0 & 0 & 0 \\ 0 & 0 & 0 \end{vmatrix}.$$

It is obvious that whenever the history  $C_t(t - r)$  has the form **5.11**,  $C_t(t - r)$  is determined by two functions of  $r$ ,  $E_t$  and  $G_t$ . When this is the case, it follows from **2.9** that we may regard the extra stress at time  $t$  as given by a functional  $\mathfrak{G}$  whose arguments are the functions  $E_t$  and  $G_t$ .

$$T(t) = \mathfrak{G}_{r=0}^{\infty} [E_t(r), G_t(r)]. \quad (5.13)$$

Furthermore, it follows from **2.13** and **5.11** that  $\mathfrak{G}$  must be an isotropic functional; that is, the following identity must hold for all functions  $E_t$ ,  $G_t$  and all constant orthogonal tensors  $Q$ :

$$Q \mathfrak{G}_{r=0}^{\infty} [E_t(r), G_t(r)] Q^T = \mathfrak{G}_{r=0}^{\infty} [QE_t(r)Q^T, QG_t(r)Q^T]. \quad (5.14)$$

Let us consider the particular orthogonal tensor  $Q$  whose components, in our present Cartesian coordinate system, are given by the matrix

$$\| Q \| = \begin{vmatrix} 1 & 0 & 0 \\ 0 & 1 & 0 \\ 0 & 0 & -1 \end{vmatrix}. \quad (5.15)$$

Then **5.12** yields

$$QE_t(r)Q^T = E_t(r), \quad QG_t(r)Q^T = G_t(r). \quad (5.16)$$

Hence, from **5.13** and **5.14** we get

$$QT(t)Q^T = T(t). \quad (5.17)$$

Denoting the matrix of the components of  $T$  by

$$\| T \| = \begin{vmatrix} T_{11} & T_{12} & T_{13} \\ T_{21} & T_{22} & T_{23} \\ T_{31} & T_{32} & T_{33} \end{vmatrix}, \quad (5.18)$$

we find that the matrix of the components of  $QTQ^T$  is given by

$$\| QTQ^T \| = \begin{vmatrix} T_{11} & T_{12} & -T_{13} \\ T_{21} & T_{22} & -T_{23} \\ -T_{31} & -T_{32} & T_{33} \end{vmatrix}. \quad (5.19)$$

According to 5.17, the matrices exhibited in 5.18 and 5.19 must coincide; this is possible only if  $T_{13} = T_{31} = T_{23} = T_{32} = 0$ . Hence we have proved that in periodic shearing flow the matrix of the components of the extra stress has the form

$$T(t) = \begin{vmatrix} T_{11}(t) & T_{12}(t) & 0 \\ T_{21}(t) & T_{22}(t) & 0 \\ 0 & 0 & T_{33}(t) \end{vmatrix}. \quad (5.20)$$

From 2.11 we have

$$T_{11}(t) + T_{22}(t) + T_{33}(t) = 0. \quad (5.21)$$

It follows from 5.12 and 5.13 that the components  $T_{ij}(t)$  of  $T(t)$  depend on only the function  $\lambda_{(t)}$ . Furthermore, it is clear from 5.20 and 5.21 that these components  $T_{ij}(t)$  may be expressed in terms of three independent functionals with argument  $\lambda_{(t)}$ . We choose

$$\begin{aligned} T_{12}(t) &= \mathfrak{t} \int_{r=0}^{\infty} [\lambda_{(t)}(r)], \\ T_{11}(t) - T_{33}(t) &= \mathfrak{s}_1 \int_{r=0}^{\infty} [\lambda_{(t)}(r)], \\ T_{22}(t) - T_{33}(t) &= \mathfrak{s}_2 \int_{r=0}^{\infty} [\lambda_{(t)}(r)]. \end{aligned} \quad (5.22)$$

In consequence of 5.14 the three functionals  $\mathfrak{t}$ ,  $\mathfrak{s}_1$ , and  $\mathfrak{s}_2$  are independent of the orientation of our Cartesian coordinate system and depend only on the material under consideration. We call  $\mathfrak{t}$ ,  $\mathfrak{s}_1$ , and  $\mathfrak{s}_2$  *material functionals*.

The isotropy relation 5.14 places restrictions on  $\mathfrak{t}$ ,  $\mathfrak{s}_1$ , and  $\mathfrak{s}_2$ . To find these restrictions we take

$$\| Q \| = \begin{vmatrix} 1 & 0 & 0 \\ 0 & -1 & 0 \\ 0 & 0 & 1 \end{vmatrix} \quad (5.23)$$

as a second choice of  $Q$  in 5.14. The Equations 5.12 then yield

$$QE_t(r)Q^T = -E_t(r), \quad QG_t(r)Q^T = G_t(r), \quad (5.24)$$

and from 5.20 we get

$$\|QT(t)Q^T\| = \left\| \begin{array}{ccc} T_{11}(t) & -T_{12}(t) & 0 \\ -T_{12}(t) & T_{22}(t) & 0 \\ 0 & 0 & T_{33}(t) \end{array} \right\|. \quad (5.25)$$

It is clear from 5.12 that the conjugation operation 5.24 is equivalent to replacing  $\lambda_{(t)}(r)$  by  $-\lambda_{(t)}(r)$ . Thus by 5.14 and 5.13, when we replace the function  $\lambda_{(t)}$  by the function  $-\lambda_{(t)}$ , the matrix  $\|T(t)\|$  of Equation 5.20 goes over into the matrix  $\|QT(t)Q^T\|$  of Equation 5.25. This is equivalent to saying that the material functionals of 5.22 obey the following identities:

$$\int_{r=0}^{\infty} t [-\lambda_{(t)}(r)] = - \int_{r=0}^{\infty} t [\lambda_{(t)}(r)], \quad \mathfrak{z}_i[-\lambda_{(t)}(r)] = \mathfrak{z}_i[\lambda_{(t)}(r)]; \quad (5.26)$$

that is, that  $t$  is an odd functional, while  $\mathfrak{z}_1$  and  $\mathfrak{z}_2$  are even functionals.

Whenever the matrix of the Cartesian components of the history  $C_t(t-r)$  has the form shown in 5.10, the Equations 5.20, 5.22, and 5.26 are not only necessary, but are also sufficient, for the validity of Equation 2.13 for all constant orthogonal tensors  $Q$ . Hence the isotropy condition 2.13 (or 5.14) yields no further restrictions on the functionals  $t$ ,  $\mathfrak{z}_1$ , and  $\mathfrak{z}_2$  beyond those exhibited in Equations 5.26.

The results obtained so far are valid for arbitrary, not necessarily periodic, flows of the type 5.1. We can now examine the consequences of the periodicity 5.2 of the velocity field.

For definiteness, let us assume that  $\theta$  is the smallest positive number such that 5.2 is true for all  $x^1$  and all  $t$ . Equations 5.9 and 5.12 then yield  $E_{t+\theta}(r) = E_t(r)$  and  $G_{t+\theta}(r) = G_t(r)$  for all  $r$  and  $t$ , and it then follows from 5.13 that

$$T(t+\theta) = T(t) \quad (5.27)$$

for all  $t$ . Thus we have the not unexpected result that the extra stress is periodic with period  $\theta$ . This does not mean, however, that  $\theta$  need be the minimum period for each of the components of  $T(t)$ . It turns out that by adding to 5.2 an assumption that is usually met in experimental approximations to periodic shearing flow and that by using 5.26, we get a result much stronger than 5.27. The assumption is that

$$v(x^1, t) = -v(x^1, t + \theta/2); \quad (5.28)$$

for all  $x^1$  and  $t$ ; that is, that the absolute value of  $v$  has a period equal to one half the minimum period of  $v$ .\*

\* This assumption is obeyed, for example, by  $v(x^1, t) = b(x^1) \sin \left[ \frac{2\pi t}{\theta} + \epsilon(x^1) \right]$ .



It follows from **5.28** and the definition of  $\lambda_{(t)}(r)$  that

$$\lambda_{(t)}(r) = -\lambda_{(t+\theta/2)}(r) \quad (5.29)$$

for all  $r$  and all  $t$ . Equations **5.29** and **5.26** yield

$$\begin{aligned} \int_{r=0}^{\infty} [\lambda_{(t+\theta/2)}(r)] &= \int_{r=0}^{\infty} [-\lambda_{(t)}(r)] = - \int_{r=0}^{\infty} [\lambda_{(t)}(r)], \\ \oint_{r=0}^{\infty} [\lambda_{(t+\theta/2)}(r)] &= \oint_{r=0}^{\infty} [-\lambda_{(t)}(r)] = \oint_{r=0}^{\infty} [\lambda_{(t)}(r)], \end{aligned} \quad (5.30)$$

$i = 1, 2$ ; these equations hold identically in  $t$ . It immediately follows from **5.30**, **5.22**, and **5.21** that the following equations hold for all  $t$ :

$$\begin{aligned} T_{12}(t + \theta/2) &= -T_{12}(t), \\ T_{11}(t + \theta/2) &= T_{11}(t), \\ T_{22}(t + \theta/2) &= T_{22}(t), \\ T_{33}(t + \theta/2) &= T_{33}(t). \end{aligned} \quad (5.31)$$

Hence we have proved that if the velocity has the property **5.28** then the shearing stress  $T_{12}$  also has this property and, furthermore, the normal extra stresses  $T_{11}$ ,  $T_{22}$ , and  $T_{33}$  oscillate with a frequency that is twice the frequency of oscillation of the velocity field and the displacement field.\*

## 6. SLOW MOTIONS AND NEWTONIAN FLUIDS

We fix the present time  $t$  and use the abbreviation  $C(r) = C_t(t - r)$  to emphasize the fact that the history of the right Cauchy-Green tensor is a function of  $r$ . Only the dependence on  $r$  matters in determining the value of the functional  $\mathfrak{S}$  which gives the stress.

In Section 2† we pointed out that if a simple fluid has been at rest for all times  $\tau$ ,  $-\infty < \tau \leq t$ , then the history  $C(r) = C_t(t - r)$ , regarded as a function of  $r$ , reduces to that function whose value for each  $r$  is the identity tensor  $I$ :

$$C(r) = C_t(t - r) \equiv I, \quad 0 \leq r < \infty. \quad (6.1)$$

\* We remark that the only essential constitutive assumption required for the proof of **5.26**, and thus **5.31**, is the isotropy condition **2.13**. In fact, results similar to **5.31** can be derived for the Cartesian components of the stress tensor  $S$  in a periodic shearing motion in an arbitrary isotropic body that is not necessarily either a fluid or incompressible, provided only that the motion is a symmetric oscillation about an undistorted configuration. We further remark that just as the results of Section 3 for simple shearing flow can be shown to hold for flows that have a similar form in other orthogonal coordinate systems,<sup>10</sup> so can our results on periodic shearing flow be extended to flows which have the form **5.1** and **5.2** in these coordinate systems. However, the treatment of boundary value problems for periodic flows is a much more complicated matter than the treatment of such problems for steady flows.

† See Equations **2.3** through **2.8**. We now drop the assumption of incompressibility made in Sections 3 through 5.

We then showed that when **6.1** holds the stress must reduce to a hydrostatic pressure which depends on the density alone:

$$S = -p(\rho)I. \quad (6.2)$$

The dynamical theory of perfect fluids deals with those special examples of simple fluids that have the property that Equation **6.2** holds for all histories  $C(r) = C_t(t - r)$ ; that is, for perfect fluids the stress is always a hydrostatic pressure, even if the fluid has been sheared in the past or is being sheared at present.

Since we know that **6.2** holds with exactitude for all simple fluids that have been eternally at rest, we feel that it must be possible to make precise the intuitive notion that if we restrict our considerations to histories that do not differ too much from that exhibited in **6.1**, then the theory of perfect fluids should be, in some sense, an approximation to the general theory of simple fluids.

The theory of Newtonian fluids is based on the following constitutive equation for the stress:

$$S = -p(\rho)I + [\lambda(\rho)\text{tr}D]I + 2\eta(\rho)D \quad (6.3)$$

here  $D$  is one half of the first Rivlin-Ericksen tensor  $A_1$  or, by **1.18**, the symmetric part of the velocity gradient tensor;\*  $\eta$  and  $\lambda$  are functions of  $\rho$  alone and are called coefficients of viscosity;†  $\lambda$  plays no role in isochoric motions, for in such motions  $\text{tr}D = 0$ . When a fluid is at rest we have  $D = 0$ . Thus **6.3** reduces to **6.2** whenever the fluid is at rest, and the physical significance of the material function  $p$  in **6.3** is clear:  $p(\rho)$  is the hydrostatic pressure the fluid would be supporting if it were at rest at its present density.

It is clear that all materials obeying Equation **6.3** are simple fluids. Furthermore it can be shown, using the isotropy condition **2.2**, that Equation **6.3** holds for any simple fluid for which the stress depends only on  $\rho$  and the velocity gradient, with a linear dependence on the latter.‡

For some substances, such as water, the theory of Newtonian fluids accounts remarkably well for experimental measurements over a very wide range of conditions. Other substances, such as molten polymers and polymer solutions, definitely do not obey Equation **6.3** exactly. However, our intuition and a host of rheological measurements suggest that the theory of Newtonian fluids should approximate the behavior of nearly all real fluids in the limit of slow motions. In other words, our physical

\*  $D$  is also called the rate of deformation tensor. Truesdell,<sup>1</sup> p. 126, calls **6.3** the Newton-Cauchy-Poisson law and gives a brief summary of its history.

†  $\eta(\rho)$  is sometimes called the shear viscosity and  $\frac{3\lambda(\rho) + 2\eta(\rho)}{3}$  the bulk viscosity.

‡ In essence this was first shown by Stokes; it is in fact an immediate consequence of the now famous representation theorem for isotropic tensor functions of one tensor variable. For a recent direct proof the reader is referred to Serrin's encyclopedia article.<sup>25</sup>

prejudice indicates that the logical status of the theory of Newtonian fluids in the theory of simple fluids should be this: when the kinematical history does not differ too much from the "rest history" shown in **6.1**, the theory of Newtonian fluids should be a first-order correction to the theory of perfect fluids.

There is more than one possible mathematical interpretation for the statement that the theories of perfect and Newtonian fluids are "approximations" to the more general theory of simple fluids. The particular interpretation that interests us here may be roughly outlined as follows. We first characterize the various possible local kinematical histories at a material point by the tensor functions  $C(r) = C_t(t - r)$ , regarded as functions of  $r$ , and the densities  $\rho = \rho(t)$ , for these are the only variables that enter the theory of simple fluids. We restrict our attention to a particular class of the functions  $C(r)$ ; this is the class of functions that are, in some sense to be made precise later, "close to" the function shown in **6.1**. We assume that for each  $\rho(t)$  the functional  $\mathfrak{S}$  in the general constitutive Equation **2.1** is, again in some sense to be made precise later, a "smooth" functional at the function **6.1**. We then show that if for any  $\rho(t)$  we consider functions  $C(r)$  that "approach" the identity function  $C(r) \equiv I$ , then the values of the stress  $S(t)$  computed using the functional  $\mathfrak{S}$  will approach those computed using the constitutive equations of perfect and Newtonian fluids. To show that the Newtonian fluid is a complete first-order correction to the theory of perfect fluids we must show that as the functions  $C(r)$  approach the identity function  $C(r) \equiv I$  the error made in using **6.3** in place of **2.1** goes to zero faster than the term  $\lambda(\rho)\text{tr}D + 2\eta D$  that appears in **6.3** but not in **6.2**.\*

The crucial issue to be settled before we can develop these ideas is that of making precise what we mean by the distance between two histories of Cauchy-Green tensors. We must somehow introduce a notion of distance, or a metric, into a space  $\mathcal{S}$  of functions  $C(r)$  whose values are symmetric tensors and whose arguments are numbers  $r$ ,  $0 \leq r < \infty$ . We shall do this by defining a norm for the functions in  $\mathcal{S}$ ; the norm of each function can be thought of as its "magnitude" or "length." The distance between two functions  $C^{(1)}(r)$  and  $C^{(2)}(r)$  will then be the norm, or length, of their difference  $C^{(1)}(r) - C^{(2)}(r)$ .

There is one essential property that we demand of this norm. It must be compatible with the fact that all real materials have an imperfect memory: in any experiment we expect the events that happened in the recent past to be more important than those that happened in the very distant

\* The reader will notice that we have picked the simplest possible interpretation that can be given to the notion that one physical theory approximates another. Our discussion is limited to constitutive equations. We do not ask whether the solutions of given boundary value problems are similar in the different theories, for this at present appears to be an extremely difficult question. Except for extremely trivial cases, we do not even know what is a well-put boundary value problem for simple fluids.

past. Indeed if this were not the case it would be exceedingly difficult to design experiments, because the experimenter, not being in control of events that happened before he was born, would never be sure that he had adequate knowledge of the history of the materials he was testing. Since physical prejudice suggests that there is a wide variation in the memories exhibited by different substances, we might expect the actual recipe to be used for computing the norm of a function  $C(r)$  should vary with the substance under consideration. Any recipe used, however, must be compatible with the statement that all memories are imperfect and must, therefore, place greater emphasis on the values of  $C(r)$  for small  $r$  than the values for very large  $r$ . In the remainder of this section we shall consider a class of norms with such a property. By assuming that for the metric generated by some norm in this class the constitutive functional  $\mathfrak{S}$  of each simple fluid is differentiable at the identity function **6.1**, we shall be able to obtain theorems that tend to justify our speculations about the approximate behavior of simple fluids in slow motions.

### *An Approximation Theorem*

We deal here with symmetric tensors only. We follow standard practice and define the norm  $|A|$  of a symmetric tensor  $A$  to be

$$|A| = \sqrt{\text{tr}(A^2)}. \quad (6.4)$$

It is easily verified that

$$\text{if } A = 0, \text{ then } |A| = 0; \quad (6.5)$$

$$\text{if } A \neq 0, \text{ then } |A| > 0; \quad (6.6)$$

and

$$|A + B| \leq |A| + |B| \quad (6.7)$$

for all symmetric tensors  $A$  and  $B$ . Equations **6.5** to **6.7** justify our use of the word norm.

Let us suppose that we can associate with any simple fluid a real-valued function  $h$  of a real variable  $r$ ,  $0 \leq r < \infty$ . We call  $h(r)$  the *influence function* for the fluid. We shall assume that  $h(r)$  obeys the following three conditions: (a)  $h(r) > 0$  for all  $r$ ; (b)  $h(r)$  is continuous over its entire domain; and (c) for all positive numbers  $c$  the function

$$g(\alpha, c) = \sup_{r > c} \frac{h(r/\alpha)}{h(r)}, \quad \alpha > 0, \quad (6.8)^*$$

satisfies

$$\lim_{\alpha \rightarrow 0} \frac{g(\alpha, c)}{\alpha} = 0. \quad (6.9)$$

\* The term sup stands for supremum of, that is, least upper bound of.

In rough language, we can say that the condition (c) states that  $h(r)$  approaches zero very rapidly as  $r$  approaches infinity. For example, the condition (c) is not obeyed by functions of the form

$$h(r) = (1 + r)^{-m} \quad (6.10)$$

if  $m \leq 1$ , but is obeyed by such functions if  $m > 1$ . The condition is also obeyed by all functions of the form

$$h(r) = (1 + r)^m e^{-\beta r}, \quad \beta > 0, \quad m \text{ arbitrary.} \quad (6.11)$$

In fact, it can be proved that our hypotheses on  $h(r)$  are obeyed by any positive continuous function which for some  $\epsilon > 0$  obeys the limit relation

$$\lim_{r \rightarrow \infty} r^{1+\epsilon} h(r) = 0.$$

monotonically for large  $r$ .

Let  $A(r)$  be a (symmetric) tensor-valued function of the real variable  $r$ ,  $0 \leq r < \infty$ . We define the *norm*  $|A(r)|_h$  of the function  $A(r)$  to be

$$|A(r)|_h = \sup_{r \geq 0} \{ |A(r)|_h(r) \}. \quad (6.12)^*$$

We restrict our attention to the set  $S_h$  of tensor-valued functions  $A(r)$  such that

$$|A(r)|_h < \infty. \quad (6.13)$$

The set  $S_h$  obviously depends on the choice of the function  $h(r)$ . It follows from Equations 6.5 to 6.7 and the definition 6.12 that

$$\text{if } A(r) \equiv 0, \quad \text{then } |A(r)|_h = 0; \quad (6.14)$$

$$\text{if } A(r) \neq 0 \text{ for some value of } r, \quad \text{then } |A(r)|_h > 0; \quad (6.15)$$

and

$$|A(r) + B(r)|_h \leq |A(r)|_h + |B(r)|_h \quad (6.16)$$

for all functions  $A(r)$ ,  $B(r)$  in  $S_h$ . Thus  $S_h$  is a normed function space and has a metric  $d_h$  defined by

$$d_h\{A(r), B(r)\} = |A(r) - B(r)|_h; \quad (6.17)$$

$d_h\{A(r), B(r)\}$  may be called the distance between the functions  $A(r)$  and  $B(r)$ .

Let  $\mathfrak{F}$  be a functional whose domain is the normed function space  $S_h$  and whose range is the set of all symmetric tensors. We say that the

\* The subscript  $h$  on  $|A(r)|_h$  is a reminder that the norm is defined over a function space and that the norm depends on the influence function  $h$ .



functional  $\mathfrak{F}$  possesses a *Fréchet differential*\*  $\delta\mathfrak{F}$  at the function  $A(r)$  if there exists a functional  $\delta\mathfrak{F}$  such that the following equation holds for all functions  $B(r)$  in  $\mathcal{S}_h$ :

$$\begin{aligned} \mathfrak{F}_{r=0}^\infty [A(r) + B(r)] &= \mathfrak{F}_{r=0}^\infty [A(r)] \\ &+ \delta\mathfrak{F}_{r=0}^\infty [A(r); B(r)] + |B(r)|_h \mathfrak{R}_{r=0}^\infty [B(r)] \end{aligned} \quad (6.18)$$

where, when  $|B(r)|_h$  goes to zero, the remainder term  $|B(r)|_h \mathfrak{R}_{r=0}^\infty [B(r)]$  approaches zero faster than  $|B(r)|_h$ , that is,

$$\lim_{|B(r)|_h \rightarrow 0} \mathfrak{R}_{r=0}^\infty [B(r)] = 0; \quad (6.19)$$

the functional  $\delta\mathfrak{F}$  is assumed to be both linear and continuous in its second variable. Here, linearity means that

$$\begin{aligned} \delta\mathfrak{F}_{r=0}^\infty [A(r); \alpha^{(1)} B^{(1)}(r) + \alpha^{(2)} B^{(2)}(r)] \\ = \alpha^{(1)} \delta\mathfrak{F}_{r=0}^\infty [A(r); B^{(1)}(r)] + \alpha^{(2)} \delta\mathfrak{F}_{r=0}^\infty [A(r); B^{(2)}(r)] \end{aligned} \quad (6.20)$$

holds for all numbers  $\alpha^{(1)}$ ,  $\alpha^{(2)}$  and for all functions  $B^{(1)}(r)$ ,  $B^{(2)}(r)$  in  $\mathcal{S}_h$ ; continuity means that

$$\lim_{d_h\{B^{(i)}(r), B(r)\} \rightarrow 0} \left| \delta\mathfrak{F}_{r=0}^\infty [A(r); B^{(i)}(r)] - \delta\mathfrak{F}_{r=0}^\infty [A(r); B(r)] \right| = 0 \quad (6.21)$$

for all functions  $B(r)$  in  $\mathcal{S}_h$  and for all sequences  $B^{(i)}(r)$  (of functions in  $\mathcal{S}_h$ ) that approach  $B(r)$ .

We are now ready to lay down our *fundamental smoothness assumption* about the constitutive functionals  $\mathfrak{S}$  occurring in the definition of a simple fluid. We assume that for each simple fluid there is an influence function  $h(r)$  obeying the conditions (a), (b), and (c) and such that in the normed function space  $\mathcal{S}_h$  the constitutive functional  $\mathfrak{S}$  possesses a Fréchet differential  $\delta\mathfrak{S}$  at the identity function 6.1. This means that we can put for any history  $C_t(t-r)$  in  $\mathcal{S}_h$

$$B(r) = I - C_t(t-r), \quad (6.22)$$

and the stress  $S(t)$  corresponding to  $C_t(t-r)$  will be given by

$$\begin{aligned} S(t) = \mathfrak{S}_{r=0}^\infty [C_t(t-r); \rho(t)] &= \mathfrak{S}_{r=0}^\infty [I; \rho(t)] + \delta\mathfrak{S}_{r=0}^\infty [I; B(r); \rho(t)] \\ &+ |B(r)|_h \mathfrak{R}_{r=0}^\infty [B(r); \rho(t)] \end{aligned} \quad (6.23)$$

\* The theory of Fréchet differentials of functionals is developed in detail in Hille and Phillips.<sup>24</sup>

where the functional  $\mathfrak{R}$  obeys **6.19** and the functional  $\delta\mathfrak{S}$  is linear and continuous in its second variable,  $B(r)$ .

From the discussion of the paragraph containing Equations **2.3** through **2.8**, we see that the tensor  $\mathfrak{S}_{r=0}^{\infty} [I; \rho(t)]$  has the form

$$\mathfrak{S}_{r=0}^{\infty} [I; \rho(t)] = -p[\rho(t)]I \quad (6.24)$$

where  $p[\rho(t)]$  is the hydrostatic pressure that the material point under consideration would now be sustaining if it had been at rest with the density  $\rho(t)$  at all times  $\tau$ ,  $-\infty < \tau \leq t$ . The term in **6.23** involving the Fréchet differential  $\delta\mathfrak{S}$  gives, in a certain sense, a continuous linear correction to the value of  $\mathfrak{S}$  at the function **6.1**.

Suppose we are given a history  $C(r)$  in  $\mathcal{S}_h$ ; we wish to have for comparison a set of other histories that may be regarded as being "essentially the same" as  $C(r)$  yet having been "carried out at a slower rate." Perhaps the simplest way to do this is to replace the variable  $r$  by a new variable  $\alpha r$ , where the range of the parameter  $\alpha$  is  $0 \leq \alpha \leq 1$ . We shall denote the new functions of  $r$  generated this way by  $C(\alpha r)$ :

$$C(\alpha r) = C_t(t - r\alpha). \quad (6.25)$$

We call the functions  $C(\alpha r)$  the *retarded histories* corresponding to  $C(r) = C_t(t - r)$ .

It is evident from **1.10** that for  $\alpha = 0$ ,  $C(\alpha r)$  reduces to the identity function **6.1**. We are here interested in the way the retarded histories approach the identity function as  $\alpha$  approaches zero. We assume that  $C(r)$  is differentiable at  $r = 0$ . It can then be proved, using the conditions on the influence function  $h$ , that for small  $\alpha$  the retarded histories  $C(\alpha r)$ , corresponding to  $C(r) = C_t(t - r)$ , are "close to" the function **6.1** in the following sense:

$$C(\alpha r) = I - 2\alpha D + o(\alpha, r), \quad (6.26)$$

where  $o(\alpha, r)$  is a tensor-valued function of  $r$  in the space  $\mathcal{S}_h$ , and

$$\lim_{\alpha \rightarrow 0} \frac{|o(\alpha; r)|_h}{\alpha} = 0. \quad (6.27)$$

In **6.26**  $D$  is the symmetric part of the velocity gradient tensor **1.18**, **1.13**:

$$2D = - \left. \frac{d}{dr} C(r) \right|_{r=0} = - \left. \frac{d}{dr} C_t(t - r) \right|_{r=0}. \quad (6.28)$$

Although the result shown in **6.26** is not unexpected, its proof (which we do not go into here) is nontrivial and depends very heavily on our assumption of condition (c) on  $h(r)$ : Equation **6.26** would not hold if the influence function  $h(r)$  did not go to zero rapidly enough as  $r \rightarrow \infty$ .

Once **6.26** is established it is relatively easy to prove the following theorem, which is a direct consequence of the definition of a simple fluid **2.1**, **2.2**, the smoothness assumption **6.23**, and the "lemma" **6.26**.

*Theorem.* Let  $C(r)$  be a function in  $\mathcal{S}_h$  that is differentiable at  $r = 0$ . For the retarded histories  $C(\alpha r)$ , corresponding to  $C(r) = C_t(t - r)$ , the functional  $\mathfrak{S}$ , which gives the stress in a simple fluid, takes the following form:

$$\lim_{r=0}^{\infty} [C(\alpha r); \rho] = -p(\rho)I + G(\alpha D; \rho) + o(\alpha). \quad (6.29)$$

Here  $p(\rho)$  is given by **6.24**;  $\alpha D$  is given by

$$\alpha D = -\frac{1}{2} \frac{dC(t - \alpha r)}{dr} \Big|_{r=0} = -\frac{\alpha}{2} \frac{dC_t(t - r)}{dr} \Big|_{r=0}; \quad (6.30)$$

$G(\alpha D; \rho)$  is a (symmetric) tensor-valued function that is linear and isotropic in  $\alpha D$ ; and  $o(\alpha)$  is a tensor-valued function of  $\alpha$  with the property that

$$\lim_{\alpha \rightarrow 0} \frac{|o(\alpha)|}{\alpha} = 0. \quad (6.31)$$

The statement that the function  $G(\alpha D; \rho)$  is linear in  $\alpha D$  means that for all numbers  $\alpha^{(1)}$  and  $\alpha^{(2)}$  and for all symmetric tensors  $D^{(1)}$  and  $D^{(2)}$ ,

$$G(\alpha^{(1)} D^{(1)} + \alpha^{(2)} D^{(2)}; \rho) = \alpha^{(1)} G(D^{(1)}; \rho) + \alpha^{(2)} G(D^{(2)}; \rho). \quad (6.32)$$

The isotropy of  $G(\alpha D; \rho)$  in  $\alpha D$  means that

$$G(\alpha Q D Q^T; \rho) = Q G(\alpha D; \rho) Q^T \quad (6.33)$$

for all symmetric tensors  $D$  and all orthogonal tensors  $Q$ . It can be shown\* that these conditions of linearity and isotropy are equivalent to the assertion that  $G(\alpha D; \rho)$  has the form

$$G(\alpha D; \rho) = [\lambda(\rho) \text{tr}(\alpha D)]I + 2\eta(\rho)\alpha D. \quad (6.34)$$

Hence our theorem states that the stress at time  $t$  in a simple fluid with a history of the form  $C_t(t - \alpha r)$  is given to within terms of order  $\alpha$  by

$$S(t) = -p[\rho(t)]I + \{\lambda[\rho(t)]\text{tr}(\alpha D)\}I + \eta[\rho(t)]\alpha D + o(\alpha). \quad (6.35)$$

The first term on the right in **6.35**,  $-p[\rho(t)]I$ , gives the stress that the fluid would be bearing at time  $t$  if it were a perfect fluid. We note that by **6.30** and **1.13**,  $\alpha D$  is one half the first Rivlin-Ericksen tensor (or, by **1.18**, the symmetric part of the velocity gradient at time  $t$ ) corresponding to the history  $C_t(t - \alpha r)$ . Hence on comparing **6.35** with **6.3** we see that

\* See, for example, the proof in Serrin,<sup>26</sup> which we have previously mentioned.

the first three terms on the right in 6.35 give the stress the fluid would be bearing if it were a Newtonian fluid. The remaining term  $o(\alpha)$  is of higher order in  $\alpha$  than the first three terms. Since  $\alpha$  is a measure of the "rate of motion" with "slow motions" corresponding to small  $\alpha$ , these observations show that the theory of the Newtonian fluid is indeed a complete first-order correction to the theory of perfect fluids in the limit of slow motions.

## 7. HIGHER-ORDER CORRECTIONS TO THE THEORY OF PERFECT FLUIDS

In the previous section we showed that if we replace a given history of the Cauchy-Green tensor  $C_t(t - r)$  by a retarded history  $C(\alpha r) = C_t(t - \alpha r)$ ,  $0 \leq \alpha \leq 1$ , then in the limit as  $\alpha$  approaches zero the constitutive equation for the stress in a simple fluid agrees, to within terms of order one in  $\alpha$ , with the constitutive equation of Newtonian fluids. Here we shall sketch a rigorous procedure for ascertaining the form of terms of higher order in  $\alpha$ . At the outset we remark that it appears to us that any approximation theorem exhibiting these higher-order terms must rest on hypotheses that are stronger than the smoothness assumption laid down in Section 6. First, it turns out that we need a condition on the influence function that is stronger than our previous condition (c); second, it is obvious that we must now work with Fréchet differentials of order higher than one.

### *Approximations of Order $n$ , $n > 1$*

We again restrict our considerations to symmetric tensors and use Equation 6.4 as the definition of the norm of a tensor.

We continue to suppose that we can associate with any simple fluid a real-valued function  $h$  of the real variable  $r$ ,  $0 \leq r < \infty$ . We now assume that this influence function  $h(r)$  obeys the following three conditions: (a')  $h(r) > 0$  for all  $r$ ; (b')  $h(r)$  is continuous over its entire domain; and (c') for all positive numbers  $c$  the function

$$g(\alpha, c) = \sup_{r > c} \frac{h(r/\alpha)}{h(r)}, \quad \alpha > 0, \quad (7.1)$$

satisfies

$$\lim_{\alpha \rightarrow 0} \frac{g(\alpha, c)}{\alpha^n} = 0. \quad (7.2)$$

The conditions (a') and (b') are repetitions of the conditions (a) and (b) assumed for  $h(r)$  in Section 6; however, since  $n$  is here a positive integer greater than 1, the condition (c') is stronger than the condition (c) of Section 6. We note that the condition (c') is still obeyed by all functions of the form 6.11 and by those functions of the form 6.10 for which  $m > n$ . Our new hypotheses on  $h(r)$ , though obeyed by a smaller class of functions

$h(r)$  than the hypotheses made in Section 6, are still obeyed for a given  $n$  by any positive continuous function for which there exists an  $\epsilon > 0$  such that the limit relation

$$\lim_{r \rightarrow \infty} r^{n+\epsilon} h(r) = 0$$

holds monotonically for large  $r$ . Furthermore, condition (c') is obeyed for all  $n$  if  $h(r)$  approaches zero exponentially fast as  $r \rightarrow \infty$ .

We again use Equation 6.12 to define the norm of tensor-valued functions of  $r$ , and we restrict our attention to the set  $S_h$  of functions for which this norm is finite.

Consider a functional  $\mathfrak{F}$  whose domain is  $S_h$  and whose range is the set of all symmetric tensors. We say that  $\mathfrak{F}$  has an  $n$ th order Fréchet differential at the function  $A(r)$  if there exist  $n$  functionals  $\delta^j \mathfrak{F}$  (of  $j + 1$  function variables) such that the following equation holds for all functions  $B(r)$  in  $S_h$ :

$$\begin{aligned} \mathfrak{F}_{r=0} [A(r) + B(r)] &= \mathfrak{F}_{r=0} [A(r)] + \sum_{j=1}^n \frac{1}{j!} \delta^j \mathfrak{F}_{r=0} [A(r); B(r), \dots B(r)] \\ &\quad + [ [B(r)]_h ]^n \mathfrak{R}_{r=0} [B(r)], \end{aligned} \quad (7.3)$$

where the functional  $\mathfrak{R}$  obeys Equation 6.19 and, in addition, the  $j$ th functional  $\delta^j \mathfrak{F}$ , when regarded as a functional of  $j + 1$  distinct function variables

$$\delta^j \mathfrak{F}_{r=0} [A(r); B_{(1)}(r), \dots B_{(j)}(r)], \quad (7.4)$$

is not only completely symmetric\* and jointly continuous in its last  $j$  variables  $B_{(1)}(r), \dots B_{(j)}(r)$ , but is also linear in each of these  $j$  variables when all of the other variables are held fixed.† It then follows that each functional  $\delta^j \mathfrak{F}$  is uniquely determined. If the  $j$  variables  $B_{(1)}(r), \dots B_{(j)}(r)$  are all the same, as they are in 7.3, that is,

$$B_{(l)}(r) \equiv B(r), \quad l = 1 \dots j,$$

then  $\delta^j \mathfrak{F}$ , regarded as a functional of  $B(r)$ , is a homogeneous functional of order  $j$ . The functional  $\delta^j \mathfrak{F}$  in 7.3 and 7.4 is called the  $j$ th order Fréchet differential of the functional  $\mathfrak{F}$ .

We now have the mathematical apparatus required for asserting a smoothness assumption about the constitutive functionals  $\mathfrak{F}$  for simple fluids that is strong enough to enable us to obtain corrections to the theory of perfect fluids that are complete up to terms of order  $n$  in  $\alpha$ . We call

\* That is, any two functions  $B_{(l)}(r), B_{(m)}(r)$ ,  $1 \leq l < m \leq j$ , may be interchanged in 7.4 without changing the value of the functional.

† For short, we say that the functional  $\delta^j \mathfrak{F}$  shown in 7.4 is multilinear in its last  $j$  variables.



this assumption the *augmented smoothness assumption* of order  $n$ . It asserts that for each simple fluid there is an influence function  $h(r)$  obeying the conditions (a'), (b'), and (c') and such that in the normed function space  $\mathcal{S}_h$  the constitutive functional  $\mathfrak{S}$  has an  $n$ th order Fréchet differential at the identity function **6.1**. In other words, our augmented smoothness assumption asserts that if, for any history  $C_t(t-r)$  in  $\mathcal{S}_h$ , we put  $C_t(t-r) = I + B(r)$  then

$$\begin{aligned} S(t) &= \mathfrak{S}_{r=0}^{\infty} [C_t(t-r); \rho(t)] = \mathfrak{S}_{r=0}^{\infty} [I; \rho(t)] \\ &+ \sum_{j=0}^n \frac{1}{j!} \delta^j \mathfrak{S}_{r=0}^{\infty} [I; B(r), \dots B(r); \rho(t)] \\ &+ [ [B(r)]_h ]^n \mathfrak{R}_{r=0}^{\infty} [B(r)] \end{aligned} \quad (7.5)$$

where the functional  $\mathfrak{R}$  obeys **6.19** and the functional  $\delta^j \mathfrak{S}$ , when regarded as a functional of  $j+1$  distinct function variables

$$\delta^j \mathfrak{S}_{r=0}^{\infty} [I; B_{(1)}(r), \dots B_{(j)}(r); \rho], \quad (7.6)$$

is multilinear, continuous, and completely symmetric in its last  $j$  variables,  $B_{(1)}(r) \dots B_{(j)}(r)$ , and is uniquely determined by  $\mathfrak{S}$ .

We are now interested again in the way retarded histories  $C(\alpha r)$ , corresponding to a given history  $C(r) \equiv C_t(t-r)$  in  $\mathcal{S}_h$ , approach the identity function **6.1** as  $\alpha$  approaches zero. The result **6.26** is not strong enough for our present purposes. The new condition (c') on the influence function  $h(r)$  now enables us, however, to prove the following statement: Assume that  $C(r)$  is  $n$  times differentiable at  $r=0$ , that is, that the  $k$ th Rivlin-Ericksen tensor corresponding to the history  $C(r)$

$$A_k = (-1)^k \frac{d^k}{dr^k} C(r) \Big|_{r=0} \quad (7.7)$$

exists for  $k=1, \dots, n$ ; it then follows that

$$C(\alpha r) = I + \sum_{k=1}^n \frac{(-\alpha r)^k}{k!} A_k + o(\alpha^n; r) \quad (7.8)$$

where  $o(\alpha^n; r)$  is a tensor-valued function of  $r$  in  $\mathcal{S}_h$  with the property

$$\lim_{\alpha \rightarrow 0} \frac{|o(\alpha^n; r)|_h}{\alpha^n} = 0. \quad (7.9)$$

We omit the proof of **7.8** but remark that it rests heavily on our assumption of condition (c') on  $h(r)$ .

The definition of a simple fluid **2.1** and **2.2**, the augmented smoothness assumption of order  $n$  **7.5**, and the new "lemma" **7.8** yield the following theorem without much difficulty.

*Theorem.* Let  $C(r)$  be a function in  $S_h$ , which is  $n$  times differentiable at  $r = 0$ . For the retarded histories  $C(\alpha r)$  the constitutive functional  $\mathfrak{S}$  takes the following form:

$$\mathfrak{S}_{r=0}^{\infty} [C(\alpha r); \rho] = -p(\rho)I + \sum_{j=1}^n \sum_{\substack{k_1 + \dots + k_j \leq n \\ k_1 \leq k_2 \leq \dots \leq k_j}} G_{j;k_1, \dots, k_j}(A_{k_1}^{\alpha}, \dots, A_{k_j}^{\alpha}; \rho) + o(\alpha^n). \quad (7.10)$$

Here  $o(\alpha^n)$  is tensor-valued function of  $\alpha$  such that

$$\lim_{\alpha \rightarrow 0} \frac{|o(\alpha^n)|}{\alpha^n} = 0; \quad (7.11)$$

$A_k^{\alpha}$  is the  $k$ th Rivlin-Ericksen tensor for the retarded history  $C(\alpha r)$ ,

$$A_k^{\alpha} = (-1)^k \frac{d^k C(\alpha r)}{dr^k} \Big|_{r=0} = (-\alpha)^k \frac{d^k C_t(t-r)}{dr^k} \Big|_{r=0} = \alpha^k A_k; \quad (7.12)$$

$G_{j;k_1, \dots, k_j}(A_{k_1}, \dots, A_{k_j}; \rho)$ , as a function of the  $j$  symmetric tensors  $A_{k_1}, \dots, A_{k_j}$ , is an isotropic, multilinear function whose values are symmetric tensors; and  $p(\rho)$  is given by 6.24.

The statement that  $G_{j;k_1, \dots, k_j}$  is an isotropic function means that the following identity holds for all orthogonal tensors  $Q$  and all sets of  $j$  symmetric tensors  $A_{k_1}, \dots, A_{k_j}$ :

$$\begin{aligned} QG_{j;k_1, \dots, k_j}(A_{k_1}, \dots, A_{k_j}; \rho)Q^T \\ = G_{j;k_1, \dots, k_j}(QA_{k_1}Q^T, \dots, QA_{k_j}Q^T; \rho). \end{aligned} \quad (7.13)$$

When we say that  $G_{j;k_1, \dots, k_j}$  is a multilinear function we mean that if any  $j-1$  of the tensor variables  $A_{k_1}, \dots, A_{k_j}$  are held fixed, then  $G_{j;k_1, \dots, k_j}$  is linear, in the sense of 6.32, in the remaining variable. It will be noticed that the term  $G_{j;k_1, \dots, k_i, \dots, k_j}(A_{k_1}^{\alpha}, \dots, A_{k_i}^{\alpha}, \dots, A_{k_j}^{\alpha})$  is, therefore, of order  $\sum_{i=1}^j k_i$  in  $\alpha$ .

Perhaps it will help clarify our notation if we write out in detail Equation 7.10 for the special case of  $n = 3$ :

$$\begin{aligned} \mathfrak{S}_{r=0}^{\infty} (C(\alpha r); \rho) = & -p(\rho)I + G_{1,1}(A_1^{\alpha}; \rho) + G_{1,2}(A_2^{\alpha}; \rho) \\ & + G_{1,3}(A_3^{\alpha}; \rho) + G_{2,1,1}(A_1^{\alpha}, A_1^{\alpha}; \rho) \\ & + G_{2,1,2}(A_1^{\alpha}, A_2^{\alpha}; \rho) + G_{3,1,1,1}(A_1^{\alpha}, A_1^{\alpha}, A_1^{\alpha}; \rho) \\ & + o(\alpha^3). \end{aligned} \quad (7.14)$$

To make clear the dependence of each term on  $\alpha$ , 7.14 may be rewritten as follows:

$$\begin{aligned}
\sum_{r=0}^{\infty} [C(\alpha r); \rho] = & -p(\rho)I + \alpha G_{1,1}(A_1; \rho) + \alpha^2 [G_{1,2}(A_2; \rho) \\
& + G_{2,1,1}(A_1, A_1; \rho)] + \alpha^3 [G_{1,3}(A_3; \rho) \\
& + G_{2,1,2}(A_1, A_2; \rho) + G_{3,1,1,1}(A_1, A_1, A_1; \rho)] \\
& + o(\alpha^3).
\end{aligned} \tag{7.15}$$

Each function  $G_{j;k_1, \dots, k_j}(A_{k_1}, \dots, A_{k_j})$ ,  $k_1 \leq k_2 \leq \dots \leq k_j$ , because it is isotropic and multilinear, may be expressed as a sum of products of the form

$$\lambda(\rho) \phi_1 \phi_2 \dots \phi_m (A_{i_1} A_{i_2} \dots A_{i_q} + A_{i_q} \dots A_{i_2} A_{i_1}) \tag{7.16}$$

where the  $\phi_i$ s are traces of products of some of the tensors  $A_{k_i}$  and are such that each  $A_{k_i}$  occurs precisely once in 7.16.\* Hence it follows from our theorem that for each finite  $n$  only a finite number of scalar material functions  $\lambda_i(\rho)$  are needed to determine the functional  $\sum$  to within terms of order  $n$  in  $\alpha$ . For incompressible materials these material functions reduce to constants. Thus a finite number of material constants fix the constitutive equation for the extra stress in an incompressible fluid to within terms of order  $n$  in  $\alpha$ . We illustrate these remarks by considering the special case of  $n = 2$ .

#### Approximations of Order 2

In this case Equation 7.10 becomes

$$\begin{aligned}
\sum_{r=0}^{\infty} [C(\alpha r); \rho] = & -p(\rho)I + G_{1,1}(A_1^\alpha; \rho) + G_{1,2}(A_2^\alpha; \rho) \\
& + G_{2,1,1}(A_1^\alpha, A_1^\alpha; \rho) + o(\alpha^2).
\end{aligned} \tag{7.17}$$

The tensor functions  $G_{1,1}(A_1; \rho)$ ,  $G_{1,2}(A_2; \rho)$  and  $G_{2,1,1}(A_1^\alpha, A_1^\alpha; \rho)$  must have the form

$$G_{1,1}(A_1; \rho) = [\lambda_1 \text{tr} A_1]I + \lambda_2 A_1 \tag{7.18}$$

$$G_{1,2}(A_2; \rho) = [\lambda_3 \text{tr} A_2]I + \lambda_4 A_2 \tag{7.19}$$

$$G_{2,1,1}(A_1, A_1; \rho) = [\lambda_5 (\text{tr} A_1)^2 + \lambda_6 \text{tr} A_1^2]I + [\lambda_7 \text{tr} A_1]A_1 + \lambda_8 A_1^2. \tag{7.20}$$

The coefficients  $\lambda_i$  in Equations 7.18 to 7.20 depend on only the density  $\rho$ . It is now clear that Equations 7.17 through 7.20 yield the following expression for the stress  $S(t)$  in a compressible simple fluid with the history  $C_i(t - r\alpha)$ :

$$\begin{aligned}
S(t) = & -pI + \mu_1 [\text{tr} A_1^\alpha]I + \mu_2 A_1^\alpha + [\mu_3 \text{tr}(A_1^\alpha)^2 + \mu_4 (\text{tr} A_1^\alpha)^2 \\
& + \mu_5 \text{tr} A_2^\alpha]I + [\mu_6 \text{tr} A_1^\alpha]A_1^\alpha + \mu_7 (A_1^\alpha)^2 + \mu_8 A_2^\alpha + o(\alpha^2)
\end{aligned} \tag{7.21}$$

\* Methods for further reduction of expressions of the form 7.16 have been developed by Spencer and Rivlin.<sup>27,28</sup>

where the coefficients  $\mu_i$ , being just the coefficients  $\lambda_i$  numbered in a more convenient order, are functions of  $\rho(t)$  alone. The terms involving  $\mu_1$  and  $\mu_2$  are of order 1 in  $\alpha$ . Since  $A_1^\alpha = 2\alpha D$ , on comparing 7.21 with 6.35 we see that

$$\mu_1 = \frac{1}{2}\lambda(\rho)$$

$$\mu_2 = \eta(\rho).$$

The terms involving  $\mu_3, \dots, \mu_8$  are of order two in  $\alpha$ .

Note: The theory of Reiner-Rivlin fluids would not yield the terms with  $\mu_5$  and  $\mu_8$ . Hence from our present point of view, the Reiner-Rivlin theory does not yield for simple fluids a complete first correction to the theory of Newtonian fluids.

The second-order approximation to the constitutive equation 2.9 of an incompressible simple fluid is obtained from 7.21 by the following modifications. First of all, we recall that in an incompressible fluid the pressure  $p$  is indeterminate and not given by 6.24. The constitutive equation gives only the extra stress  $T(t)$ . Furthermore, in the expression for the extra stress in an incompressible fluid all of the terms in 7.21 that are scalar products of the identity tensor  $I$  will be determined by the normalization 2.11:

$$\text{tr} T = 0. \quad (7.22)$$

Also, it follows from 2.18 that in any permissible motion in an incompressible fluid we must have

$$\text{tr}(A_1^\alpha) = 0; \quad (7.23)$$

this means that the constitutive equation for such a fluid will have no terms such as those involving  $\mu_1, \mu_4$ , and  $\mu_6$  in 7.21. Finally we note that the remaining coefficients (that is, those corresponding to  $\mu_2, \mu_7$ , and  $\mu_8$ ) must now be constants. In this way we obtain the following simple formula for the extra stress  $T(t)$  in an incompressible fluid with a history  $C_t(t - r\alpha)$ :

$$T(t) = \gamma I + \beta_1 A_1^\alpha + \beta_2 (A_1^\alpha)^2 + \beta_3 A_2^\alpha + o(\alpha^2), \quad (7.24)$$

where  $\beta_1, \beta_2$ , and  $\beta_3$  are material constants and  $\gamma$  is determined by 7.22,

$$\gamma = -\frac{1}{3}[\beta_2 \text{tr}(A_1^\alpha)^2 + \beta_3 \text{tr} A_2^\alpha]. \quad (7.25)$$

It is useful here to use a normalization different from 7.22 by absorbing the term  $\gamma I$  of 7.24 into the extra stress. We then have

$$T = S + pI = \beta_1 A_1^\alpha + \beta_2 (A_1^\alpha)^2 + \beta_3 A_2^\alpha + o(\alpha^2). \quad (7.26)$$

Here  $p$  is no longer the mean pressure 2.12. For an incompressible Newtonian fluid  $\beta_2 = \beta_3 = 0$ , and  $\beta_1$  is called the viscosity. For an incompressible

Reiner-Rivlin fluid  $\beta_3 = 0$ ; thus we again see that already in the first correction to the Newtonian fluid, the Reiner-Rivlin fluid yields a result less general than that obtained for simple fluids.

The material constants  $\beta_1$ ,  $\beta_2$ , and  $\beta_3$  are related by the following formulas to the three material functions  $\tau$ ,  $\sigma_1$ , and  $\sigma_2$ , defined in Section 3:

$$\begin{aligned}\beta_1 &= \lim_{\kappa \rightarrow 0} \frac{\tau(\kappa)}{\kappa} \\ \beta_2 &= \lim_{\kappa \rightarrow 0} \frac{\sigma_2(\kappa)}{\kappa^2} = \lim_{\kappa \rightarrow 0} \frac{1}{2} \frac{d^2 \sigma_2(\kappa)}{d\kappa^2}, \\ \beta_3 &= \lim_{\kappa \rightarrow 0} \frac{\sigma_1(\kappa) - \sigma_2(\kappa)}{2\kappa^2} = \lim_{\kappa \rightarrow 0} \frac{1}{4} \left\{ \frac{d^2 \sigma_1(\kappa)}{d\kappa^2} - \frac{d^2 \sigma_2(\kappa)}{d\kappa^2} \right\}.\end{aligned}\quad (7.27)$$

In the second-order approximation 7.26 the "shear dependence of the viscosity" does not yet appear; however, all the "normal stress effects" are already present.

Motivated by 7.26 we define an incompressible second-order fluid by the constitutive equation

$$T \triangleq S + pI = 2\eta D + 4\beta_2 D^2 + \beta_3 A_2. \quad (7.28)^*$$

Of course, an incompressible Newtonian fluid is a special case of 7.28 with  $\beta_2 = \beta_3 = 0$ . In many important dynamical situations† the constitutive Equation 7.28 leads to linear field equations just as in the Newtonian case. For this reason many of the problems that can be solved for Newtonian fluids can also be solved for these second-order fluids.

### Comparison with Dimensional Arguments

If the kinematics are such that  $C_t(t-r) \equiv C(r)$  is an analytic function of  $r$  for  $0 \leq r < \infty$ , then this function is determined by its derivatives at  $r = 0$ , which by 1.12 are essentially the Rivlin-Ericksen tensors  $A_n$ . Thus the restriction of the functional  $\mathfrak{S}_{r=0}^\infty[C(r)]$  to these special analytic histories may be regarded as an isotropic function of all the Rivlin-Ericksen tensors. In those special cases in which only a finite number  $m$  of the tensors  $A_n$  are important‡ we are led to a relation of the form

$$S(t) = G(A_1, \dots, A_m), \quad (7.29)$$

where  $G$  is an isotropic function of  $m$  tensor variables. Equation 7.29 is the constitutive equation of Rivlin-Ericksen fluids.<sup>14</sup> By starting from the Relation 7.29 and using dimensional analysis one can obtain approxi-

\* Langlois<sup>19</sup> used an equation of the form 7.28 to represent "slightly viscoelastic fluids." We believe our derivation of 7.26 gives 7.28 a sound physical interpretation.

† For example, unsteady shearing flows.

‡ For example, in the flow problems considered in Sections 3 and 4 all the  $A_n$  vanish except  $A_1$  and  $A_2$ .



mation formulas that are formally the same as those exhibited above. However, such a formal procedure does not elucidate the physical significance behind our equations; that is, it does not indicate the conditions under which an experimenter can expect them to be useful. The derivation we have outlined here assumes for  $C(r)$  only a finite norm and the existence of those derivatives at  $r = 0$  that occur in the approximation formulas. For  $r \neq 0$ ,  $C(r)$  need not even be continuous, much less analytic. Furthermore, our treatment shows that the crucial point is not smoothness of the history  $C(r)$  for all  $r$  but rather smoothness of the functional  $\mathcal{S}$  in a function space  $S_h$  whose norm accounts explicitly for "imperfect memory."

## REFERENCES

1. TRUESDELL, C. 1952. *J. Rational Mech. Anal.* **1**: 125-300.
2. TRUESDELL, C. 1953. *J. Rational Mech. Anal.* **2**: 593-616.
3. IKENBERRY, E. & C. TRUESDELL. 1956. *J. Rational Mech. Anal.* **5**: 1-54.
4. TRUESDELL, C. 1956. *J. Rational Mech. Anal.* **5**: 55-128.
5. KORTEWEG, D. J. 1901. *Arch. néerl. sci.* **6**: 1-24.
6. NOLL, W. 1958. *Arch. Rational Mech. Anal.* **2**: 197-226.
7. GREEN, A. E. & R. S. RIVLIN. 1957. *Arch. Rational Mech. Anal.* **1**: 1-21.
8. GREEN, A. E., R. S. RIVLIN & A. J. M. SPENCER. 1959. *Arch. Rational Mech. Anal.* **3**: 82-90.
9. GREEN, A. E. & R. S. RIVLIN. 1960. *Arch. Rational Mech. Anal.* **4**: 387-404.
10. COLEMAN, B. D. & W. NOLL. 1959. *Arch. Rational Mech. Anal.* **4**: 289-303.
11. COLEMAN, B. D. & W. NOLL. 1959. *J. Appl. Phys.* **30**: 1508-1512.
12. REINER, M. 1945. *Am. J. Math.* **67**: 350-362.
13. RIVLIN, R. S. 1948. *Proc. Roy. Soc. (London)*. **A193**: 260-281.
14. RIVLIN, R. S. & J. F. ERICKSEN. 1955. *J. Rational Mech. Anal.* **4**: 323-425.
15. RIVLIN, R. S. 1956. *J. Rational Mech. Anal.* **5**: 179-188.
16. ERICKSEN, J. E. *Rheol. Acta*. In press.
17. ERICKSEN, J. E. 1960. *Arch. Rational Mech. Anal.* **4**: 231-237.
18. WEISSENBERG, K. 1949. *Proc. 1st Intern. Rheol. Congr. Amsterdam*. **I**: 29-45.
19. LANGLOIS, W. E. 1957. Paper presented at Ann. Meeting Soc. Rheol. Princeton, N. J.
20. MARKOVITZ, H. & R. B. WILLIAMSON. 1957. *Trans. Soc. Rheol.* **1**: 25-36.
21. MARKOVITZ, H. 1957. *Trans. Soc. Rheol.* **1**: 37-52.
22. HERMANS, J. J. 1953. *Flow Properties of Disperse Systems*. Chap. 5. North-Holland. Amsterdam, Holland.
23. MOONEY, M. 1931. *J. Rheol.* **2**: 210-222.
24. PADDEN, F. J. & T. W. DEWITT. 1954. *J. Appl. Phys.* **25**: 1086-1091.
25. SERRIN, J. 1959. Mathematical principles of classical fluid mechanics. In *Encyclopedia of Physics*, S. Flügge, Ed. **VIII(I)**. (Fluid Mechanics I) : 125-263. Springer. Berlin, Germany.
26. HILLE, E. & R. S. PHILLIPS. 1957. *Functional analysis and semi-groups*. American Mathematical Society. Colloquium Publications. **XXXI**. New York, N. Y.
27. SPENCER, A. J. M. & R. S. RIVLIN. 1959. *Arch. Rational Mech. Anal.* **2**: 309-336; 435-446.
28. SPENCER, A. J. M. & R. S. RIVLIN. 1960. *Arch. Rational Mech. Anal.* **4**: 214-230.





MONOGRAPHIC PUBLICATIONS  
OF  
THE NEW YORK ACADEMY OF SCIENCES

(LYCEUM OF NATURAL HISTORY, 1817-1876)

(1) The ANNALS (octavo series), established in 1823, contain the scientific contributions and reports of researches, together with the records of meetings of the Academy. The articles that comprise each volume are printed separately, each in its own cover, and are distributed immediately upon publication. The prices of the separate articles depend upon their length and the number of illustrations, and may be ascertained upon application to the Executive Director of the Academy.

Current numbers of the ANNALS are sent free to all Members of the Academy desiring them.

(2) The SPECIAL PUBLICATIONS, established in 1939, are issued at irregular intervals as clothbound volumes. The price of each volume will be advertised at time of issue.

(3) The MEMOIRS (quarto series), established in 1895, are issued at irregular intervals. It is intended that each volume shall be devoted to monographs relating to some particular department of science. Volume I, Part 1 is devoted to Astronomical Memoirs, Volume II to Zoological Memoirs. No more parts of the Memoirs have been published to date. The price is one dollar per part.

(4) The SCIENTIFIC SURVEY OF PORTO RICO AND THE VIRGIN ISLANDS (octavo series), established in 1919, gives the detailed reports of the anthropological, botanical, geological, paleontological, zoological, and meteorological surveys of these islands.

Subscriptions and inquiries concerning current and back numbers of any of the publications of the Academy should be addressed to

EXECUTIVE DIRECTOR

*The New York Academy of Sciences*  
*2 East Sixty-third Street*  
*New York 21, N. Y.*

